Rhenium Mediated Formation of *N*-Containing Organic Compounds by Nitride Transfer

Dissertation

for the award of the degree

"Doctor Rerum Naturalium"

of the Georg-August-Universität Göttingen

within the doctoral program of the Georg-August University School of Science (GAUSS)

submitted by

Sesha Kisan, M. Sc.

from Bhubaneswar, India

Göttingen, 2022

Thesis Committee

Prof. Dr. Sven Schneider
Institute of Inorganic Chemistry, Georg-August University of Göttingen

Prof. Dr. Franc Meyer
Institute of Inorganic Chemistry, Georg-August University of Göttingen

Prof. Dr. Inke Siewert
Institute of Inorganic Chemistry, Georg-August University of Göttingen

Members of Examination Board

Reviewer: Prof. Dr. Sven Schneider
Institute of Inorganic Chemistry, Georg-August University of Göttingen

Reviewer: Prof. Dr. Franc Meyer
Institute of Inorganic Chemistry, Georg-August University of Göttingen

Other Members of the Examination Board

Prof. Dr. Inke Siewert
Institute of Inorganic Chemistry, Georg-August University of Göttingen

Dr. Michael John
Institute of Organic and Biomolecular Chemistry, Georg-August University of Göttingen

Dr. Daniel Janssen-Müller
Institute of Organic and Biomolecular Chemistry, Georg-August University of Göttingen

Dr. Alessandro Bismuto
Institute of Organic and Biomolecular Chemistry, Georg-August University of Göttingen

Date of oral examination: 08.08.2022

Acknowledgements

I am profoundly grateful to my supervisor Prof. Dr. Sven Schneider for providing me with a great opportunity to work on an interesting and crucial scientific topic. Thank you for your continuous support from the beginning with inspiring scientific discussions, excellent laboratory conditions and encouraging career guidance.

Furthermore, I would like to thank Prof. Dr. Franc Meyer for being my second supervisor and referee for this thesis. At the same time, I want to thank Prof. Dr. Inke Siewert for being my third supervisor. I admire your support.

The further examiners Dr. Michael John and Dr. Daniel Janssen-Müller and Dr. Alessandro Bismuto are acknowledged for their time, patience and uncomplicated communication in the entire examination process.

I would like to thank:

-Dr. Christian Würtele (x-ray), Dr. Markus Finger (DFT) and Dr. Claudia Stückl (EPR) for their scientific support and instructive discussion.

-The NMR department, especially Dr. Michael John, Martin Weitemeyer and Ralf Schöne for the numerous long-term measurements and the friendly and problem-oriented atmosphere.

-The analytical lab with Angelika Wraage, Diana Kumpart and Susanne Petrich for the numerous elemental analysis measurements.

My special thanks to the whole AK Schneider group which provided an enthusiastic working culture and great support. I would like to acknowledge my office colleagues Dr. Maximilian Fritz, Dr. Florian Wätjen, Dr. Richt Van Alten, Dr. Lukas Alig, Till Schmidt-Räntsch, Dr. Sebastian J. K. Forrest and Sebastian Kopp for the inspiring discussion and cooperative atmosphere.

Last but not least I would like to thank my family and friends for their continuous support and motivation over the last years.

Thank you everyone!

Content

I. Introduction

1. Nitrogenase and Haber-Bosch Process

N-containing organic compounds occur in all the organisms, such as in the form of amino acids (and thus proteins), nucleic acids (DNA and RNA) and in the form of energy transfer molecule adenosine triphosphate. The human body contains about 3% nitrogen by mass, the fourth most abundant element in the body after oxygen, carbon, and hydrogen. Therefore, N-containing organic compounds are a very crucial group of compounds which help to sustain life on earth. Ammonia is one of the most important raw materials in the synthesis of nitrogen-containing compounds such as amine, nitrile, and N-heterocyclic organic compounds. [1] Dinitrogen gas is occupying 78% of atmospheric gas, which makes it the most abundant unbound element available. Initially, ammonia was obtained from N_2 by biological enzymatic nitrogen fixation with the help of bacteria. To achieve ammonia, nitrogenases which is a [7Fe-9S-Mo-C-homocitrate] cluster, undergo successive protonation/ reduction ($6H^+$/ 6e-) of N_2 to ammonia by the process of N-atom hydrogenation. [2-5] In the alternative path way, the nitrogen atoms are hydrogenated simultaneously to provide hydrazine and then ammonia. [6]

$$N_2 + 8\ e^- + 8\ H^+ + 16\ MgATP \longrightarrow 2\ NH_3 + H_2\uparrow + 16\ MgADP + 16\ P_i$$

Enzymatic nitrogen fixation was the main pathway for the synthesis of ammonia until the early 20th century but in 1908, *Fritz Haber* developed a new process for ammonia production, which increased the production of ammonia significantly. In this industrial process, the dinitrogen gas is converted to ammonia through a process called the Haber-Bosch process upon reaction with hydrogen in the presence of iron or ruthenium at high pressures (50-200 atm) and temperatures (700-850 K). [7,8]

$$N_2 + 3\ H_2 \xrightarrow{[cat]} 2\ NH_3$$

The mechanism of the ammonia formation by this method is different from the enzyme-catalysed mechanism. In This process, the dinitrogen and dihydrogen initially undergo complete bond dissociation at the surface of the catalyst and further chemisorption of H and N atoms to form ammonia. The Haber-Bosch process currently provides a large scale of ammonia which is approximately 150 Mt per annum. [1] The increase in demand has influenced the development of bioinspired catalysts for nitrogen fixation at ambient conditions. [9] Remarkable work progressed by different groups [10–12] with a turn-over number up to 230, which is the most active catalyst till date. [13] About 20% of the industrially produced ammonia serves as feedstock for nitrogen-containing chemicals and the remaining major part is used for the production of fertilizer.

Alternative to this, ammonia and other nitrogen compounds can be synthesised directly from terminal metal nitrides by the *N*-transfer homogeneous pathway. [14–30] The chemistry of terminal transition metal nitride is very old. The first nitride complex i.e. $K[OsO_3N]$ was synthesised in 1847. [31] This field has been developed much more before than the transition metal dinitrogen chemistry. Till date, many terminal transition metal nitrides have been reported in the literature. [16] these nitrides can be synthesised from different nitrogen sources such as from dinitrogen gas, via ammonia deprotonation or decaying of azide, hydrazine and

its derivatives. [16,32] So synthesis of terminal rhenium nitride and its functionalization by organic electrophiles to get nitrogen-containing organic compounds will be discussed.

2. Preparative pathways for terminal nitrides

2.1 Dinitrogen splitting to terminal nitrides

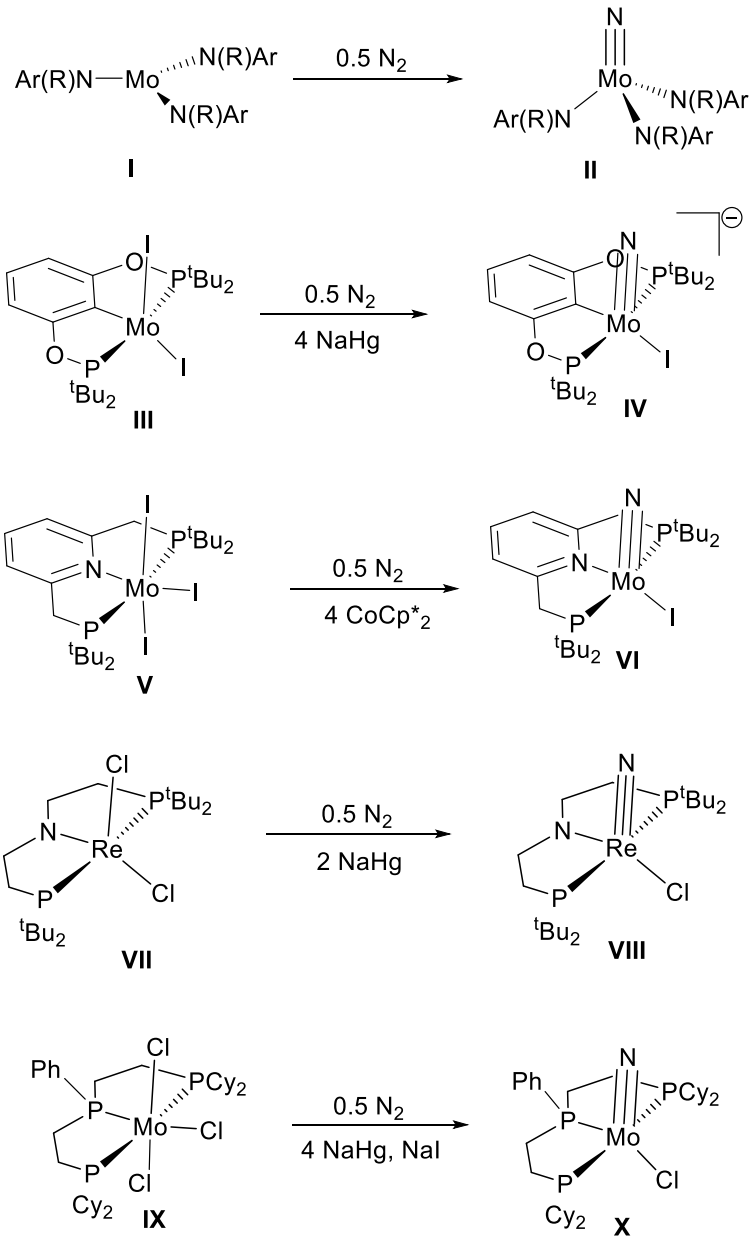

***Scheme 1**. Different routes for terminal nitride synthesis from N_2*

The formation of transition metal terminal nitride complex from dinitrogen was demonstrated by *Cummins* and co-workers for the very first time in 1995 (**Scheme 1**). They explained that their molybdenum complex **I** provides N_2 bridged complex dimolybdenum with N_2 which further undergoes N-N bond cleavage to form corresponding nitride complex $[Mo(N)(N(R)Ar)_3]$ (**II**). [33,34, 35] After the discovery of the N_2 splitting by the molecular metal

complex to terminal nitrides, many groups have reported the N-N bond cleavage in almost the next 3 decades. [17,36] *Nishibayashi* and co-workers demonstrated the initial full cleavage of the N-N triple bond which further catalysed to provided ammonia and here they explained the catalytic cycle has occurred through the formation of molybdenum terminal nitride. [37] In 2014, further, they reported the photochemical dinitrogen Splitting by a similar molybdenum complex. The Mo N_2 dimer complex undergoes photolytic N_2 cleavage into molybdenum terminal nitride (**VI**), which was further functionalized to N-containing compounds. [38] In 2012, *Schrock* and co-workers reported the cleavage of dinitrogen into terminal nitride with (t-BuPOCOP) molybdenum complex (**IV**). They proposed that the key intermediate is a bimetallic N_2 bridged Mo complex which is further reduced into a terminal Mo (IV) nitride complex. [39] *Schneider* and co-workers reported the well-defined N_2 splitting into terminal nitride in 2014. The formation of rhenium terminal nitride [Re(N)Cl(PNP)](**VIII**) occurs upon reduction of complex **VII** by Na/Hg under the N_2 atmosphere. Also, they observed the formation of identical complexes when they treated complex **VII** treated with $CoCp_2$* under an N_2 atmosphere. [40] In 2016, *Mezailles* and co-workers revealed the formation of Mo terminal nitride from N_2 with a tridentate phosphine molybdenum complex. Upon reduction of [($P^{Ph}P_2Cy$) $MoCl_3$] **IX** complex with NaHg in presence of NaI under N_2 atmosphere provides Mo (IV) nitride complex **X**. Further, they postulate that the identical complex could be obtained upon direct N_2 splitting by two unsaturated Mo(I) fragments, which generates in situ under N_2. [41]

2.2 Metal nitrides from other nitrogen sources

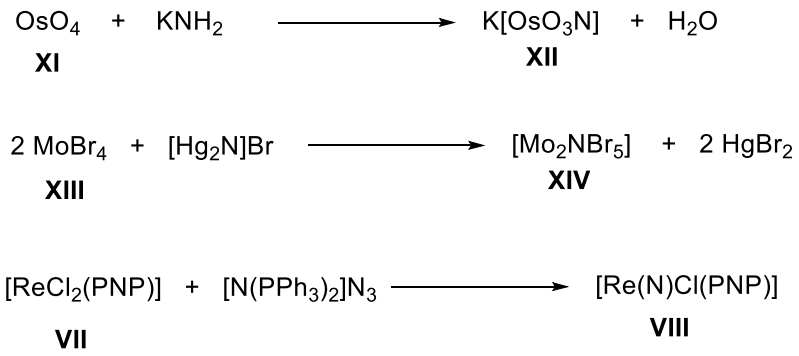

***Scheme 2**. Different routes for nitride synthesis from other nitrogen sources.*

Metal nitrides are prepared using a variety of nitrogen sources. The first transition metal nitride i.e. $K[OsO_3N]$ **XII** was prepared using potassium amide as the N_3^- source. [31] When osmium tetroxide **XI** is reacted with the potassium tetroxide it provides the $K[OsO_3N]$ and water as a byproduct. In 1988, *Godemeyer* and co-workers reported metal nitride which is synthesised by using the bromide of Millon's base. The reaction of molybdenum tetrabromide with $[Hg_2N]$ Br smoothly obtained the nitride complex of tetravalent molybdenum **XIV**. [42,43]

Most commonly the metal nitrides are synthesised from the decomposition of the azide sources, as the driving force of these reactions is the great stability of N_2. In 2014, *Schneider* and co-workers reported the facile synthesis of Re (V) nitride i.e. [Re(N)Cl(PNP)] **VIII** upon the reaction of $[N(PPh_3)_2]N_3$ with $[ReCl_2(PNP)]$ complex.[40] Besides this metal nitride can be synthesised from ammonia [44-48], nitrogen trichloride [49-51], azido complex [52-62] and trithiazyl chloride. [63-72]

3. Reactivity and functionalization of transition metal nitrides

3.1 Reactivity of transition metal nitrides

Metal nitrides can act as both a strong σ- and strong π-donor as they are restrained with a triple bond which consists of one σ and two π bonds. In general, metal nitrides are categorised as nucleophilic or electrophilic based upon the interaction with the external nucleophilic or electrophilic reagents. Moreover, they are determined as electrophilic or nucleophilic based on the relative energy of metal d-orbital and nitrogen p-orbital which are involved in the formation of π M-N bonds. In one scenario, when the energy level of metal d orbitals is higher than that of nitrogen p-orbitals, the MN π bond formed is more nitrogen centred and it facilitates the nitrogen to donate lone pairs of electrons, which makes the metal nitride more nucleophilic. In the other scenario, when the metal d orbitals are energetically lower than that of p orbitals, the MN pi bond results have mainly metal character and the corresponding antibonding π^*-orbital is more nitrogen centre, because of which it acts as the electrophilic nitride (**Figure 1**). [73] Based on this concept the electrophilicity of the transition metal increases when one moves right to the periodic table and it has been determined by DFT calculation and demonstrated the decreasing of the negative character of the metal nitride when moving toward the late transition metal nitride. [74]

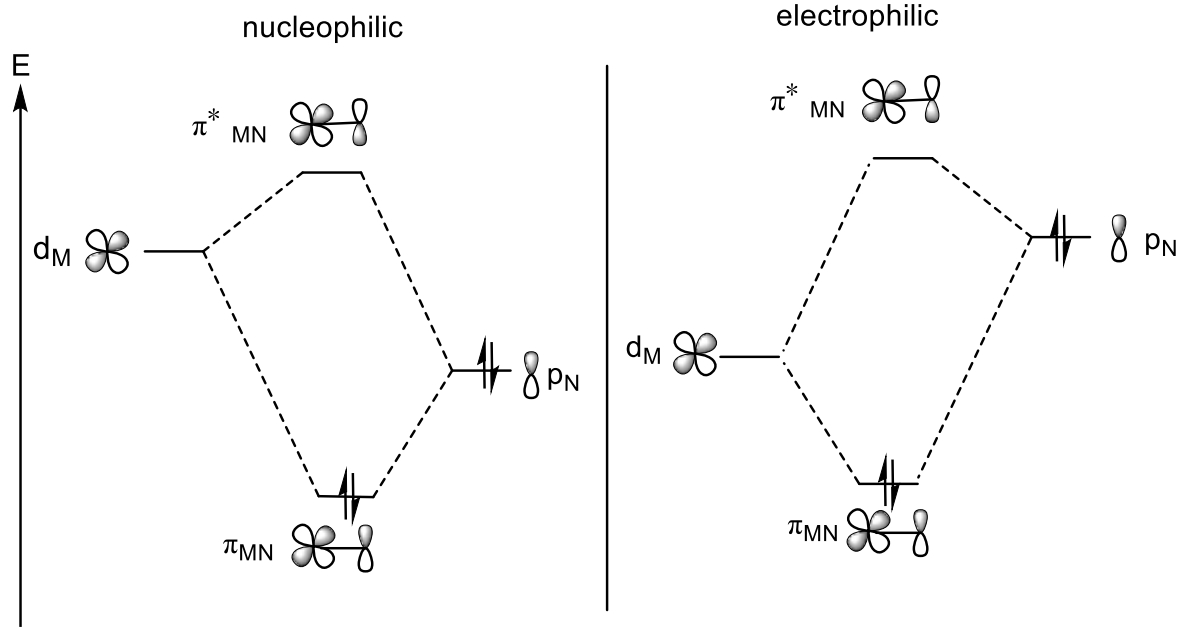

Figure 1. *Simplified MO scheme rationalizing the difference between a nucleophilic nitride (left)and an electrophilic nitride complex (right).*

The philicity of a metal nitride not only depends upon the metal but also the ancillary ligands around the metal centre which is explained by the Mayer and co-workers with a T_P (trispyrazolylborate) supported Os nitride complex [Os(N)R_2(Tp)] (R= Cl, Ph) **XV**. [75–77]

It was observed that when bis-chloro Os nitride [Os(N)Cl_2(Tp)] reacts quickly with Grignard's reagent such PhMgCl and undergoes N-C bond formation to provide respective imido complex shows the electrophilicity of the nitride. However, when the chloride ligand was changed to

phenyl, the bis-phenyl nitride complex reacts hardly with the Grignard's reagent PhMgCl showing a different reactivity. [75,76] Further, they demonstrated the reactivity of Os nitride **XV** using triarylborane (**Scheme 3)**. They observed the bis-phenyl Os nitride undergo nucleophilic attack with arylborane to form the N-B bond, [Os(NB(C_6F_5)$_3$)Ph_2(Tp)] **XVII**. In contradiction to that when the phenyl ligands were replaced with chloride ligands the bis-chloro Os nitride was inserted as an electrophile into the B-Ar bond into the respective borylimido complex **XVI**. [76,77] The amphiphilic nature of the Os nitride [Os(N)R_2(Tp)] was further demonstrated by DFT calculation where they explained LUMO and LUMO+1 of bis -chloro Os nitride [Os(N)Cl_2(Tp)] are low lying and M-N π-antibonding is found more nitrogen centred because of which it behaves as electrophilic. But when the chloride ligands were replaced with the better σ-donating phenyl ligand, the energy level of both the orbitals increased and now the M-N π-bonding is closer to the nitrogen centre because of which it shows nucleophilic behaviour.

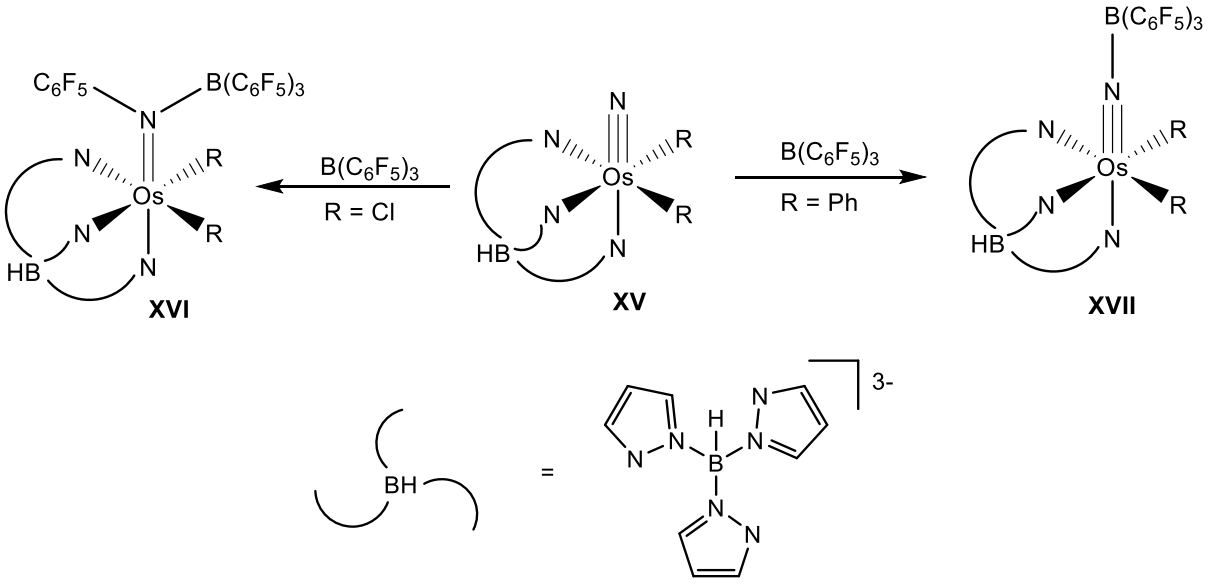

Scheme 3: *Ligand influence on the nucleophilicity of a Tp-supported Os nitride* ***XV****.*

3.2 Nitride functionalization to organic compounds

In 2003, *Vries* and co-workers reported the incorporation of dinitrogen into an organic molecule for the very first time where the terminal nitride plays an important role as an intermediate. Here they observed the direct release of trifluoroacetamide upon the reaction of Cummins's nitride **XVIII** with trifluoroacetic anhydride **(Scheme 4)**. The successful nitride transfer is possible upon partial degradation of amide to imide and 2 protons are donated from one of the tert-butyl groups by releasing isobutene. [78]

In 2016, *Mézailles* and co-workers demonstrated the synthesis of bis (silyl)amine from a tridentate phosphine ligated Mo nitride complex [Mo(N)I(PPP)] (PPP = PhP($CH_2CH_2PCy_2$)$_2$). [41, 79] When the nitride **XIX** was treated with substituted silanes the formation of Mo-H and N-Si bond was observed. They demonstrated that the reaction of substituted bis-silyl compound $HSiMe_2(CH_2CH_2)$ Me_2SiH with nitride provides a silylimido Mo intermediate by 1,2 insertion of

one of the Si-H group into the Mo-N moiety of the nitride. Further heating of the intermediate at 80 °C undergoes an intramolecular reaction with the second Si-H bond and successful N-transfer occurs to prove bis-silyl amine. They proposed the formation of [Mo(H)I(PPP)] **XX** but could not prove it. However, PMe_3 ligated complex [Mo(H)I(PMe_3) (PPP)] was isolated with bis-silyl amine upon a reaction of the adduct complex with phosphine. In this scenario, the reduction of metal centre to Mo (II) occurs by the reactant itself without using an external reducing reagent. Recently the author developed a similar reaction with Nitride and HBpin to give triborylamine $N(BPin)_3$ in high yields and the formation of the Mo hydride complex was observed. [80]

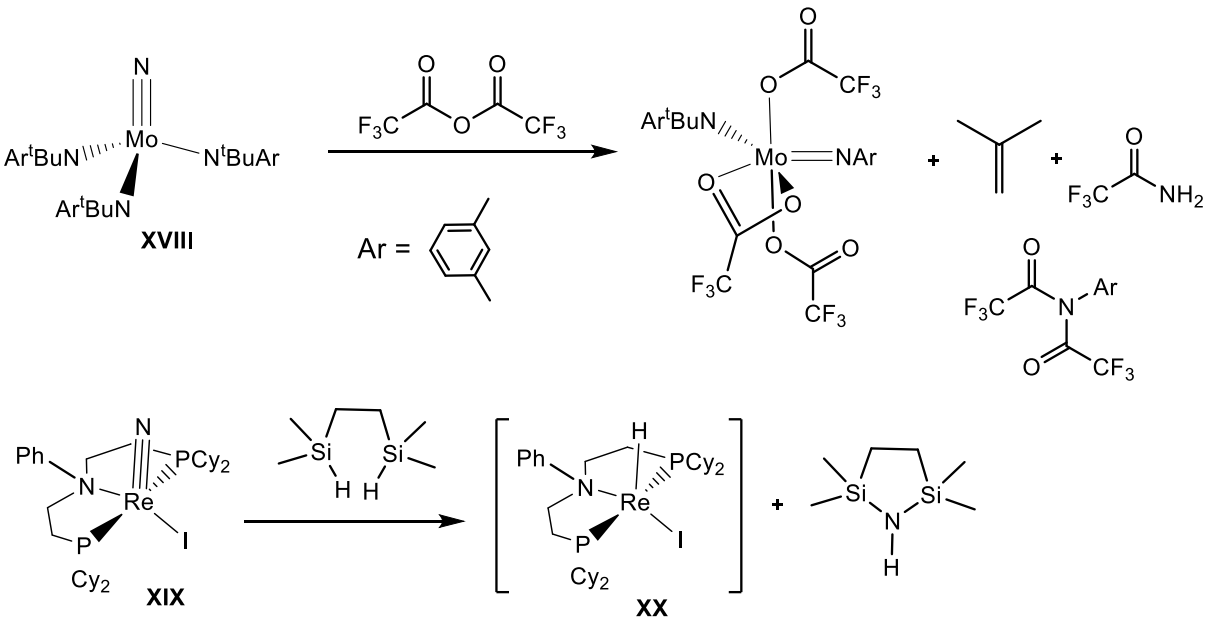

Scheme 4. *Top: Synthesis of amide from Cummins' nitride complex. Bottom: Conversion of a Mézailles nitride to a bis-silylamine.*

Cummins reported the synthesis of organic nitriles with the Mo terminal nitride, where he explained the generation of nitriles by a complete synthetic cycle **(Scheme 5).** [81] Mo terminal nitride **XVII** was activated using RC(O)OTf (R = Me. Ph, tBu) to corresponding acylamido complexes **XXI**. The acylated complexes are further reduced to the respective trimethylsiloxyketimides complexes **XXII** with Mg in presence of Me_3SiOTf. When the ketimido complexes were treated with $SnCl_2$ or $ZnCl_2$ resulted in the respective nitriles and Mo (IV) chloride complex **XXIII.** Further reduction of complex **XXIII** with Mg in presence of N_2 regenerates the nitride complex **XVII**. So, the synthesis of nitrogen-containing organic compounds was directly synthesized from the N_2-driven Mo terminal nitride for the first time.

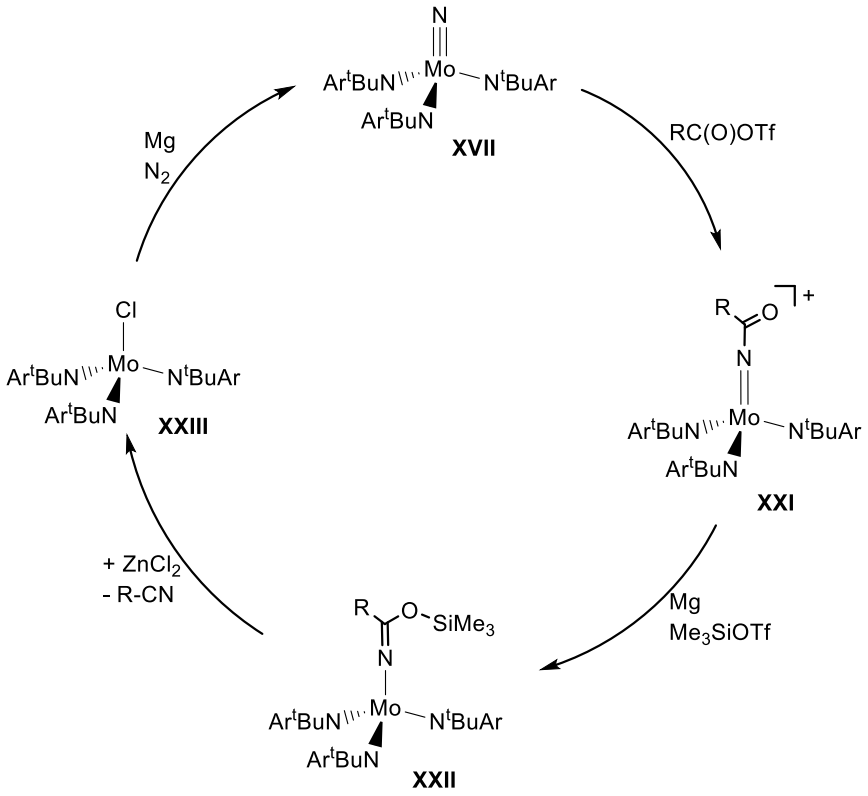

Scheme 5*: Cummins and co-workers synthetic cycle to generate organic nitriles (R = Me, Ph, ^{t}Bu).*

Schneider and co-workers design a synthetic cycle for the formation of acetonitrile by Re(V) nitride [Re(N)Cl(PNP^{t}Bu)] (**VIII**) functionalization with ethyl triflate **(Scheme 6).** Initially, when N_2-driven terminal Re (V) nitride was treated with EtOTf, it provided the Re(V)-ethylimido complex **XXIV** by nucleophilic N-C bond formation. Deprotonation of **XXIV** by KHMDS resulted in corresponding ketamide complex **XXV**. Here, the two-electron reduction was achieved from Re(V) to Re (III), where the two electrons came from the C-H bond of the α-carbon after deprotonation. Further deprotonation **XXV** with KHMDS and addition of isonitrile releases acetonitrile and two electrons reduced Re(I) complex **XXVI.** Complex **XXVI** formed requires strong acceptor ligands for its stabilization. It is also observed that the complex is unable to activate N_2. Addition of two equivalents of N- Chlorosuccinimide with **XXV** provides acetonitrile and Re (IV) trichloride complex **XXVII.** The terminal nitride **VIII** can be regenerated when **XXVII** is treated with NaHg in presence of N_2 and successfully closes the synthetic cycle**.** [24, a] Afterwards, they reported the synthesis of benzonitrile following an analogue mechanism where they prepared in situ $PhCH_2OTf$ instead of EtOTf. [24, b]

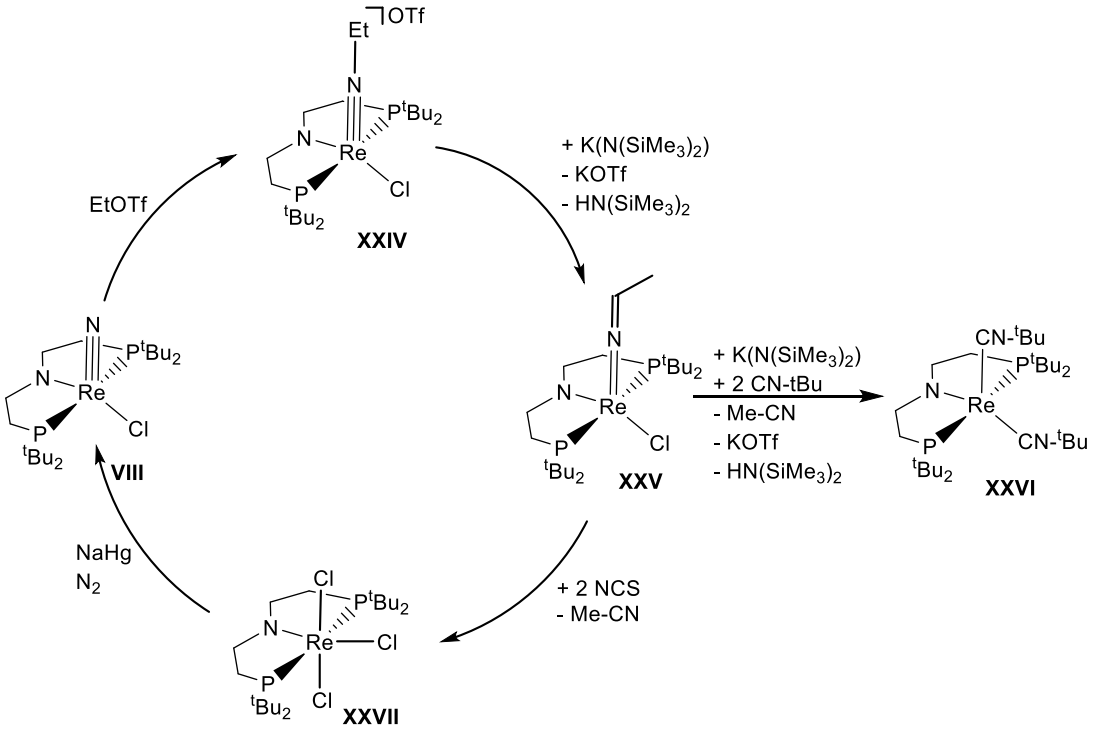

Scheme 6. *Synthetic cycle for acetonitrile by Schneider and co-workers.*

Later *Schneider* and co-workers published the metal-ligand cooperative synthesis of benzamide and benzo nitrile with an isopropyl-based Re(V) nitride complex [Re(N)Cl_2(HPNP^{iPr})] **XXX (Scheme 7).** When the nitride is treated with two equivalents of benzoyl chloride (PhC(O)Cl), it provides benzamide (PhC(O)NH_2), benzonitrile (PhCN) and benzoic acid ($PhCO_2H$) at 80 °C. The reaction is not so selective. The formation of benzoic acid and benzonitrile because of the reaction of benzoyl chloride with the immediately formed benzamide. Here the two electrons and two protons are donated by the ligand backbone to achieve the organic products and the reduced Re (III) imine trichloride complex **XXXI.** Stepwise addition of Li [$HBEt_3$] and [Ph_2NH_2]Cl with the imine complex **XXXI** provides Re(III) trichloride complex **XXVIII**. When Re trichloride complex **XXVIII** was treated with reductant NaHg in presence of dinitrogen it gives the N_2 bridged di nuclear complex **XXIX**, which can be obtained quantitatively upon electrochemical reduction (CPE, E = -1.65 V) of the imine complex xxx in presence of 2,6-dichlorophenol (acid). The dinuclear complex **XXIX** was further irradiated to cleave the N_2 bond successfully to regenerate the nitride. [82]

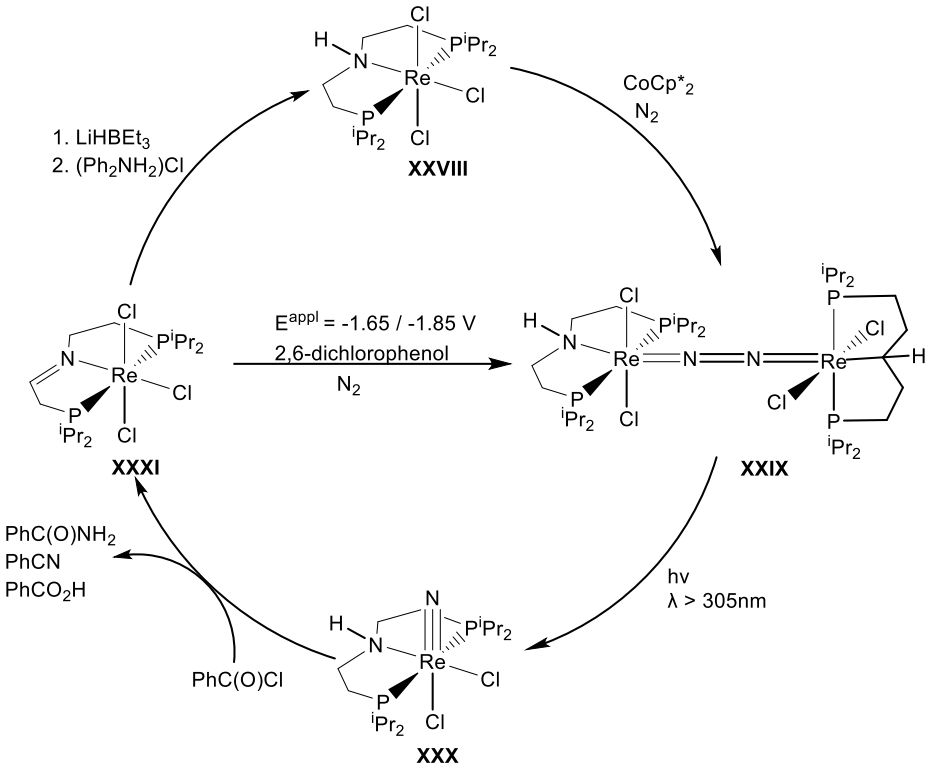

Scheme 7: *Synthetic cycle for the metal-ligand cooperative formation of benzamide, benzonitrile and benzoic acid from benzoyl chloride.*

4. Scope of this work

Numerous terminal nitrides have been reported till date which are employed in nitride functionalization to get the nitrogen-containing compounds. So here, Re(III) tribromide complex supported by the PNP ligand is designed which is further used for the synthesis of terminal rhenium nitride[(^{iPr}PNP)Re(N)Br_2] (**7**). Subsequently, the reactivity of terminal rhenium nitride is investigated with different organic electrophiles to get nitrogen-containing organic compounds. Hence, the nucleophilicity behaviour of the terminal rhenium nitride is examined.

Recently our group has reported the metal-ligand cooperative synthesis of benzamide and benzonitrile with [(^{iPr}PNP)Re(N)Cl_2] and benzoyl chloride, [82] but unfortunately selectivity of these nitrogen-containing organic compounds could not be achieved. Considering this work as inspiration, the metal-ligand cooperativity is demonstrated with [(^{iPr}PNP)Re(N)Br_2] (**7**) and benzoyl bromide. Importantly, the intermediates are investigated to get the resulting organic products selectively.

The key intermediate involved in the metal-ligand cooperativity i.e. [Re (PhC(O)N) Br_2(HPNP^{iPr})]Br (**11**) is isolated and characterized, and further metal-ligand cooperativity is demonstrated with it. The kinetics of the isolated intermediate is conducted to draw a plausible pathway of the metal-ligand cooperativity. The reactivity of the intermediate is further investigated by the PCET method using an external reductant and acid to get benzamide.

Para substituted benzoyl bromides are synthesized to systematically modify the electrophilicity of the benzoyl bromide to get stable benzoylimido adduct complexes. Reactivity in the formation of adduct complexes is further demonstrated by the Hammett plot. Metal-ligand cooperative reactions are examined with the substituted benzoylimido adduct complexes. Selective para-substituted benzamide formation is demonstrated by isolating the intermediate involved, using the PCET method. The substrate scope of synthesis of substituted benzonitriles is created.

II. Results and discussion

1. Re (III) Starting Platform

1.1. Precursor synthesis

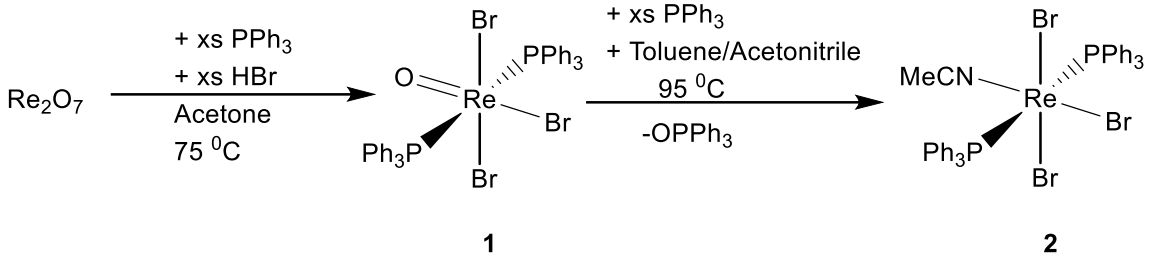

Scheme 8: *Synthesis of Re precursor **2**.*

The Re(III) complex $[ReBr_3(PPh_3)_2(MeCN)]$ **2** is used as the precursor for the synthesis of the Re(III)HPNP platform which can be easily synthesised from commercially available rhenium heptoxide (Re_2O_7) with a two-step process. Initially, the primary precursor rhenium heptoxide was reduced to oxo complex **1** by using an excess of triphenylphosphine (PPh_3) (18 eq) and an excess of hydrobromic acid (9 eq). Complex **1** was further reduced with an excess of PPh_3 (4 eq) in presence of acetonitrile at reflux conditions to get the required precursor **2** (**scheme 8**).

1.2 Synthesis and characterisation of $[(HPNP^{iPr})ReBr_3]$

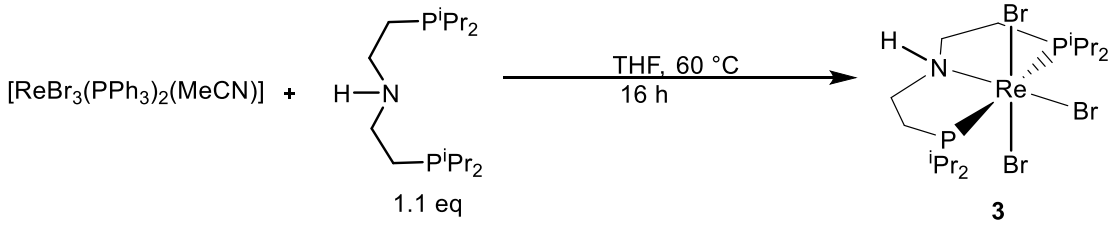

Scheme 9: *Synthesis of Re(III) platform $[(HPNP)ReBr_3]$.*[a, 86]

The precursor $[ReBr_3(PPh_3)_2(MeCN)]$ **2** treated with $HPNP^{iPr}$ ligand in THF at 60°C stirred for 16 h without base provided green complex $[(HPNP^{iPr})ReBr_3]$ (**3**)[a, 86] with 89 % yield (**Scheme 9**). The reaction indicates highly selective and no further reduction is observed. The Green complex is thermally stable even at 110°C for two days, however, the complex is sensitive toward the air and moisture. Complex **3** provided a strong shift $^{31}P\{^1H\}$ NMR shifted at δ_p = -1491.06 ppm. At the same time, it provided a strong shift ^1H-NMR with NH signal found at δ_H = 151.35 ppm. CH_2 backbone protons are found between δ_H = 6.42 ppm to -13.39 ppm, where isopropyl protons resonate between δ_H = 9.69 to 8.53 ppm. $^{13}C\{^1H\}$ NMR found between δ_C = 176.18ppm and 16.63 ppm. ^1H-^{15}N HSQC provided a peak at δ_N = -1250 ppm indicating the ^{15}N signal of backbone amine moiety (**Figure 2**).

---

[a] Synthetic route of complex **3** was initially designed and characterised (with NMR, IR, mass and CV) by Sesha Kisan. Later, Complex **3** was characterised with XRD by Niels Paul and elemental analysis by Dr. Maximilian Fritz (Alumnus, AK Schneider, Georg-August University, Gottingen) [86] using a similar procedure.

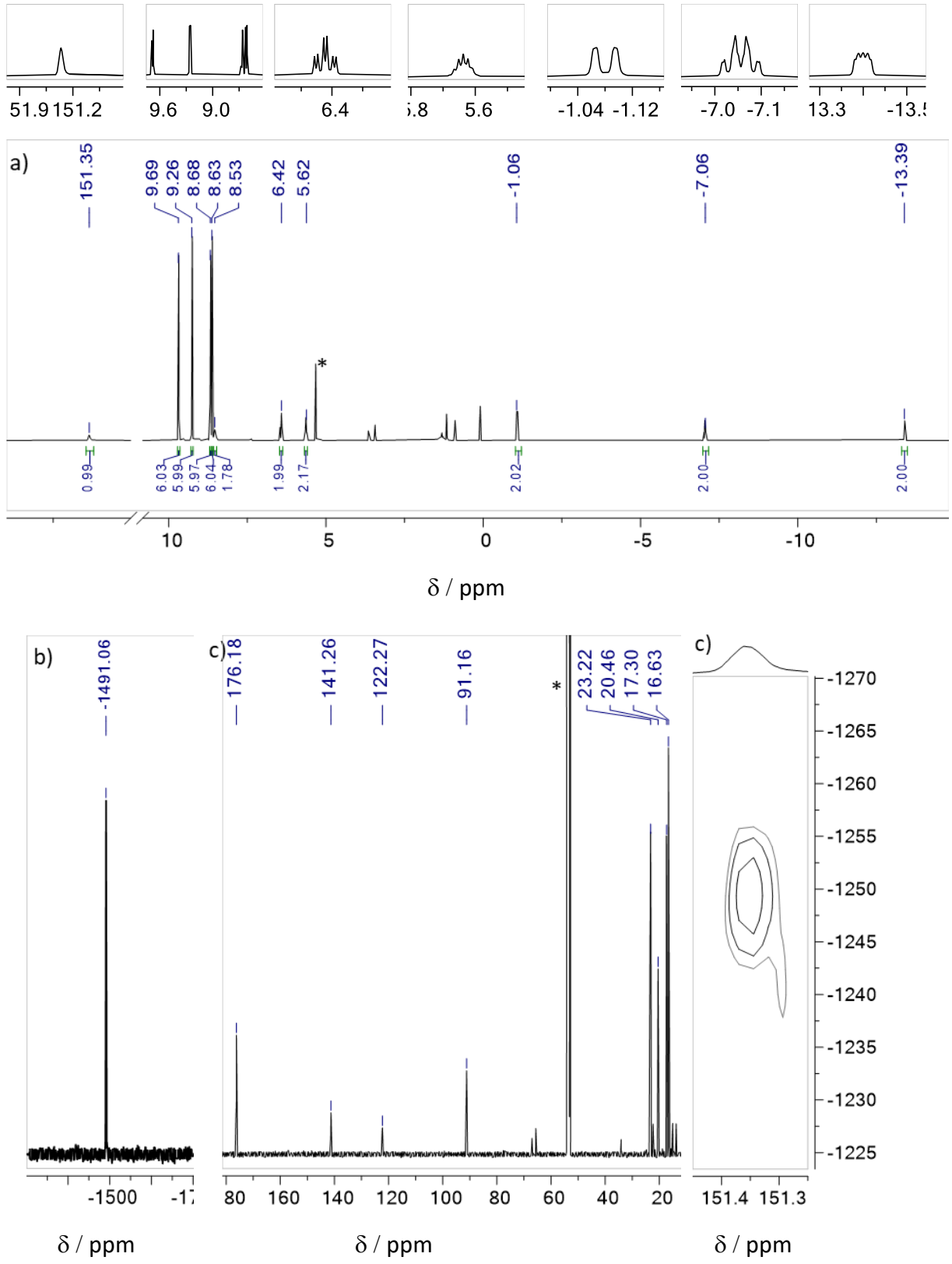

***Figure 2**. **a)** ^{1}H -NMR spectrum of **3** in CD_2Cl_2. **b)** $^{31}P\{^{1}H\}$ NMR spectrum. The solvent signal is marked with an asterisk. **c)** $^{13}C\{^{1}H\}$ NMR spectrum of **3** in CD_2Cl_2. **d)** ^{1}H-^{15}N-HSQC NMR spectrum.*

Further molecular structure of complex three is determined by x-ray diffraction measurement with 50% probability (**Figure 3**) indicating the molecule has an octahedral geometry, where the Re found at the centre and the HPNP and bromide ligands are octahedrally coordinated around it.

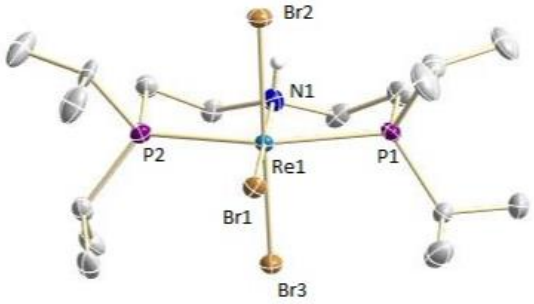

Figure 3. *Molecular structure of **3** obtained by single-crystal X-ray diffraction measurements. All H atoms but the NH proton are omitted for clarity. Anisotropic displacement parameters are set to 50 % probability. Selected bond lengths [Å] and angles [°]: Re1-N1 2.173(9), Re1-Br1 2.5433(13), Re1-Br2 2.5168(12), Re1- Br3 2.5121(12), P1-Re1-P2 161.26(10), N1-Re1-Br1 176.9(2), Br2-Re1-Br3 174.84(5).*[a, 86]

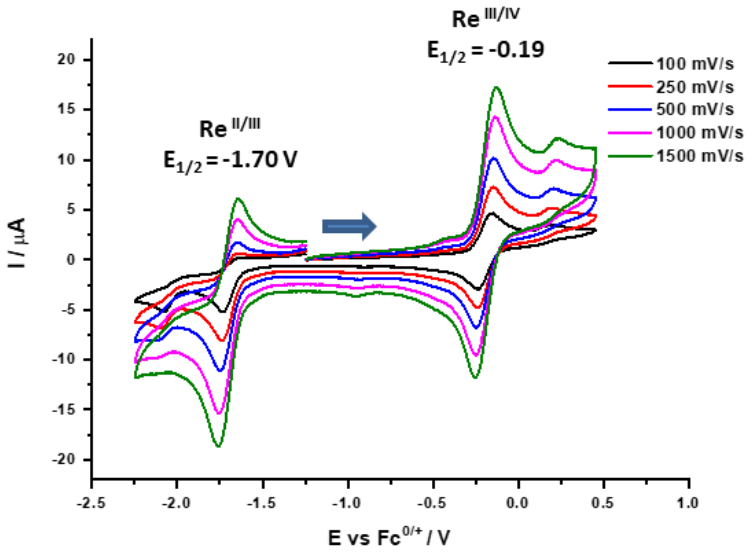

Figure 4. *CV of [$ReBr_3$(HPNP)] (3) (1 mM in THF with 0.1 M [nBu_4N][PF_6]) at different scan rates.* [a, 86]

The cyclic voltammetry of complex **3** was measured which provided a quasi-reversible wave at $E_{1/2}$ = -1.70 V and a reversible wave at $E_{1/2}$ = -0.19 V (**Figure 4**). Reduction of complex **3** anionic Re(ll) tribromide species which is not stable, due to bromide loss it provided Re(II) dibromide species because of which it gives a quasi-reversible wave at -1.70. To prove that the CV of complex **3** was repeated focusing at $Re^{II/III}$ coupling wave, titrating with 0-20 eq of tetrahexylammonium bromide [$N(C_6H_{13})_4$] Br (bromide source) at a constant scan rate of 100 mV/s, which indicates a there is a cathodic shift from $E_{1/2}$ = -1.70 V to -1.72 V (**Figure 5**) and the wave become more reversible indicates stabilization of Re(ll) anionic species in presence of bromide.

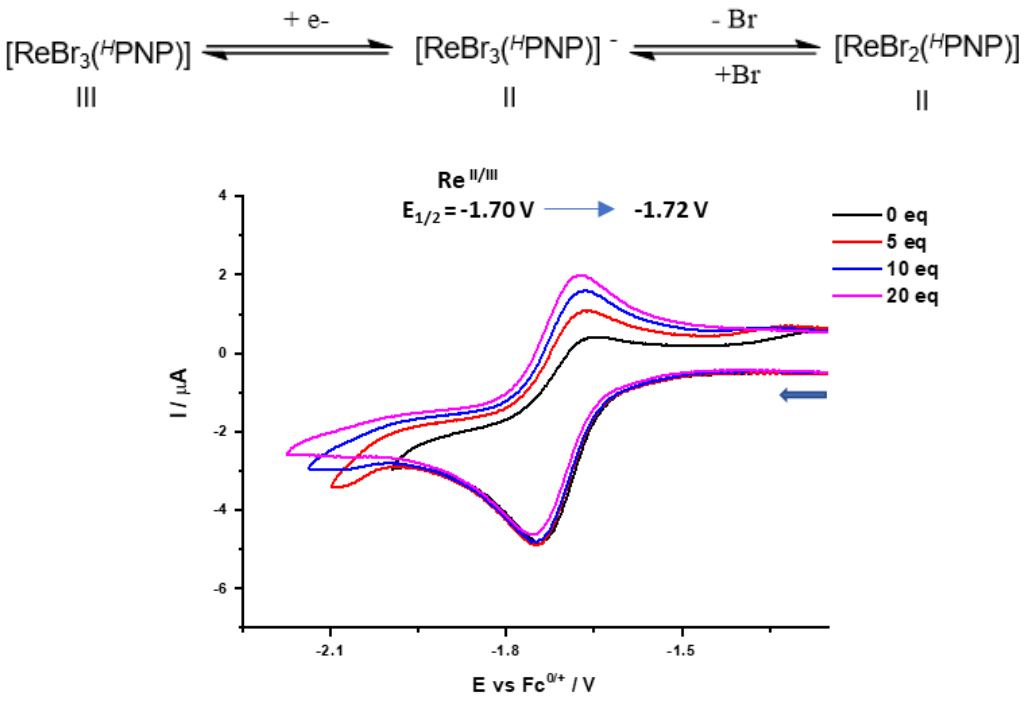

Figure 5 *CV of [ReBr$_3$(HPNP)] titrated with 0-20 eq of [N(C$_6$H$_{13}$)$_4$]Br at 100 mV/s.*

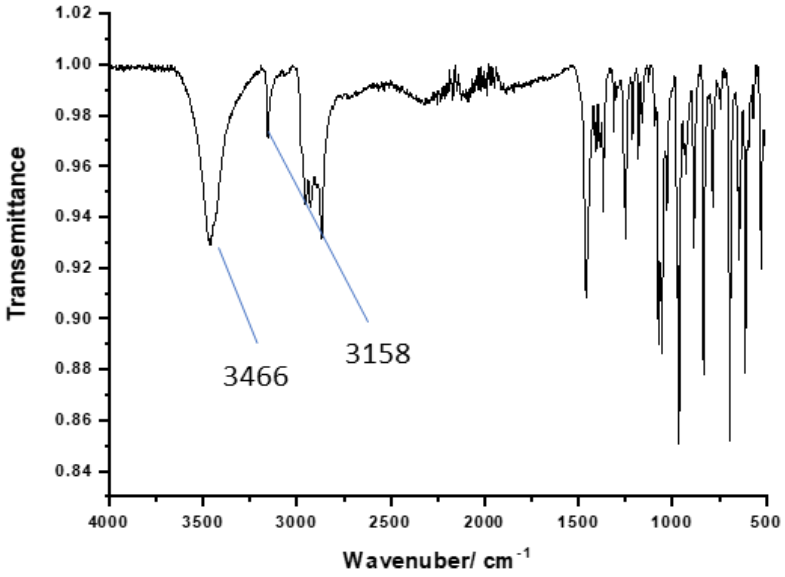

Figure 6. *IR spectrum of complex **3**.*

Further, complex **3** was characterised by IR spectroscopy. ATR-IR of the complex was measured by taking the solid sample with a regular transmittance IR measurement (**Figure 6**). The IR spectrum indicates a broad peak at υ = 3466 cm^{-1} arises because of the strong SOC effect [85], which is matching with calculated SOC stabilisation energy. Another prominent peak at $\upsilon_{N\text{-}H}$ = 3158 cm^{-1} corresponds to the N-H stretching vibration.

2. Other $ReBr_3$ complexes from parent complex 3

2.1. [(PNP^{iPr})$ReBr_3$] (4)

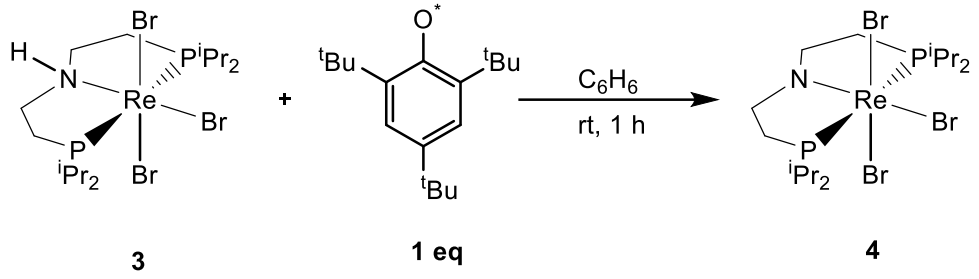

Scheme 10: *Synthesis of Re(IV) complex (PNP)$ReBr_3$.*

H-atom abstraction (from the NH moiety of the ligand) is tried with **3** by using TEMPO, but unfortunately, the complex **4** was unable to be isolated by this method. On the other hand, when complex **3** and 1 eq of 2,4,6-tri-tert-butylphenoxy radical (TTBP) are suspended in benzene and stirred at RT for 1 h, resulting in a deep red solution. All volatiles are removed in vacuo and the crude product is washed with pentane multiple times and extracted with benzene to obtain violet-coloured (PNP^{iPr})$ReBr_3$ (**4**), 63 % in yield.

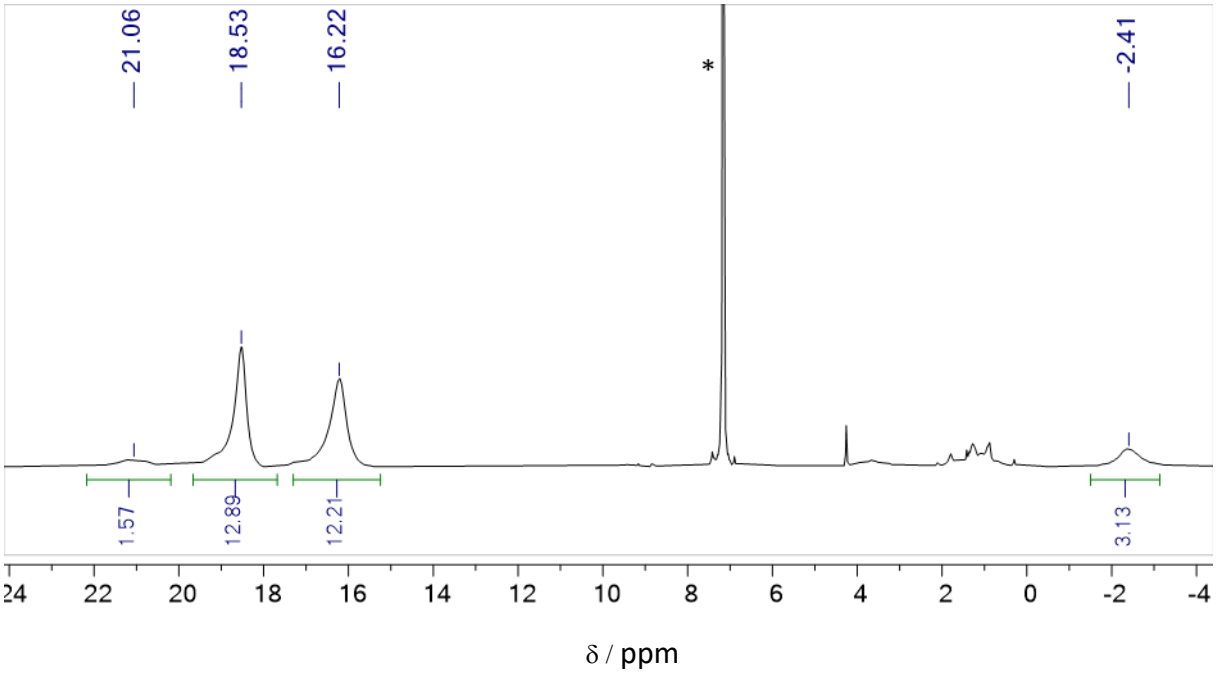

Figure 7. *^{1}H-NMR spectrum of **4** in C_6D_6. The solvent signal is marked with an asterisk.*

The complex provided no $^{31}P\{^1H\}$ NMR signals, whereas the ^1H NMR spectrum shows few broad, paramagnetically shifted signals in the range of δ_H = 16-21 ppm and at δ_H = -2 ppm (**Figure 7**). Two large signals at δ_H = 16 and 18 ppm can be assigned to CH_3 of the isopropyl group of the molecule which is because of a C_{2v} symmetry on the NMR time scale.

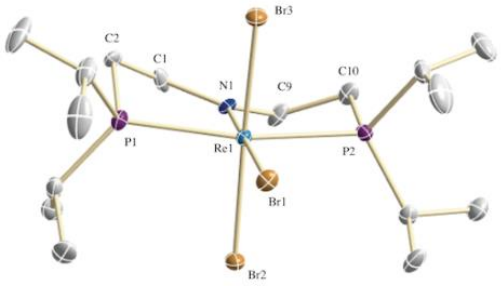

Figure 8. *Molecular structure of **4** obtained by single-crystal X-ray diffraction measurements. H atoms are omitted for clarity. Anisotropic displacement parameters are set to 50 % probability. Selected bond lengths [Å] and angles [°]: Re1-N1 1.908(6), Re1-Br1 2.5721(8), Re1-Br2 2.5222(7), Re1-Br3 2.5211(8), N1-Re1-Br2 91.17(17), P1-Re1-P2 163.56(6), Br1-Re1-Br3 175.47(3).*

Further, the molecular structure of complex **4** was obtained by X-ray diffraction measurement which indicates the Re atom is octahedrally coordinated by the PNP pincer and 3 bromide ligands (**Figure 8**). Moreover, H-atom abstraction from the amine moiety is confirmed by planar coordination of the pincer nitrogen atom (Σ(∡N1) = 359.5°), accompanied by a shortening of the Re-N distance (**3**: *d*(Re1-N1) = 2.173(9) Å; **4**: 1.908(6) Å), supporting the amide nature of the ligand. Moreover, IR, mass spectrometry and the elemental analysis confirm the H-atom abstraction. Complex **4** was investigated by CV measurement, which provided a quasi-reversible reduction at $E_{1/2}$ = -0.93 V vs. Fc^{+}/Fc (**Figure 9**). ATR-IR of the complex **4** (**Figure 10**) shows the absence of stretching frequency peak at $\upsilon_{N\text{-}H}$ = 3158 cm^{-1} indicating the H atom abstraction occurs successfully from the NH moiety.

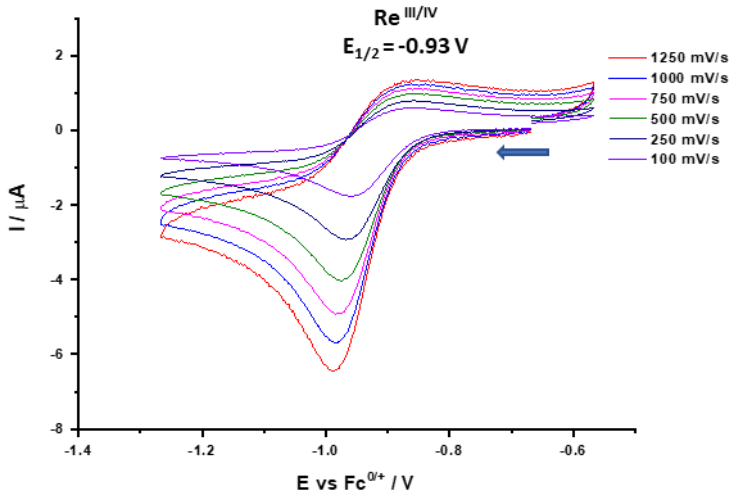

Figure 9. *CV of **4** (1 mM in THF with 0.1 M [nBu_4N][PF_6]) at different scan rates.*

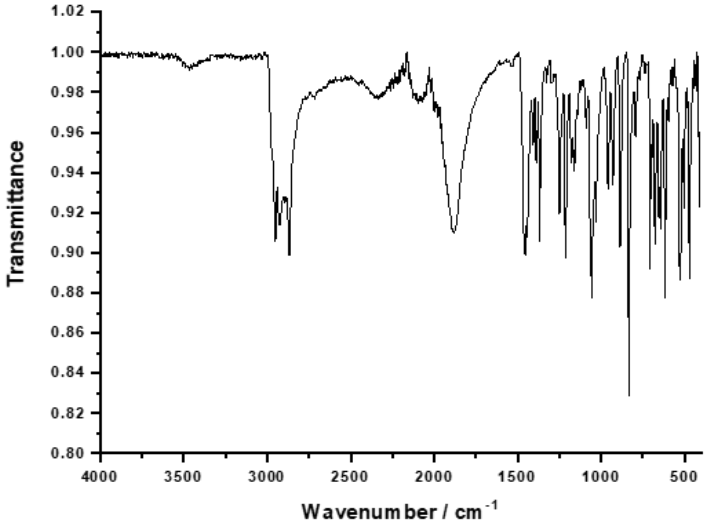

Figure 10. *IR spectrum of complex* ***4.***

2.2 [(P=N-P) $ReBr_3$] (5)

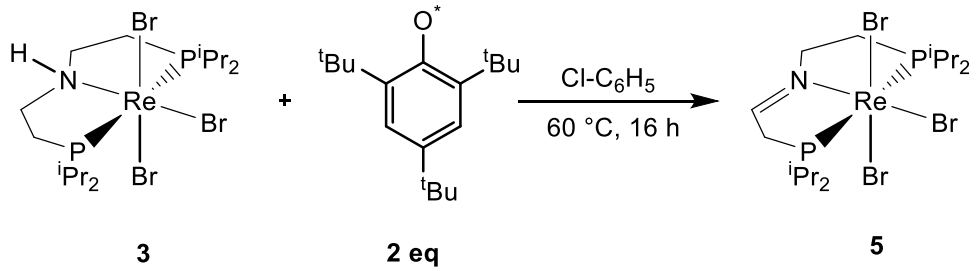

3 **2 eq** **5**

Scheme 11: *Synthesis of Re(III) complex* ***[****(P=N-P)*$ReBr_3$*].*

After successful synthesis of complex **4** by one H atom abstraction, here two H atom abstraction was performed to get complex **5**. Therefore, 2eq of TTBP was stirred with complex **3** in chlorobenzene at the elevated temperature of 60 °C overnight, which provided a yellowish-grey complex of 84% in yield after isolation. synthesised complex features two doublets $^{31}P\{^1H\}$ NMR at δ_P = -1501.19 and -1512.76 ppm with a coupling constant of $^2J_{PP}$ = 248 Hz (**Figure 11**). ^1H NMR provides all the signals in the range of δ_H = 59 ppm to -71 ppm. The four sets of large signals in the range of δ_H = 5-9 ppm belong to CH_3 of four isopropyl groups and it arises because of the Cs symmetry in the NMR time scale. In addition to that, 2 small signals at δ_H = 9 ppm and 5 ppm belong to CH peaks of isopropyl groups. Besides these signals, there are 4 more small signals which are integrated with the ratio 2:2:2:1 indicating the backbone signals of PNP. Though the $^{13}C\{^1H\}$ NMR have strongly shifted signals, some signals could not find but the four isopropyl signals are easily observed in the range of δ_C = 18-24 ppm and some backbone peaks are found in the range of δ_C = 131-156 ppm.

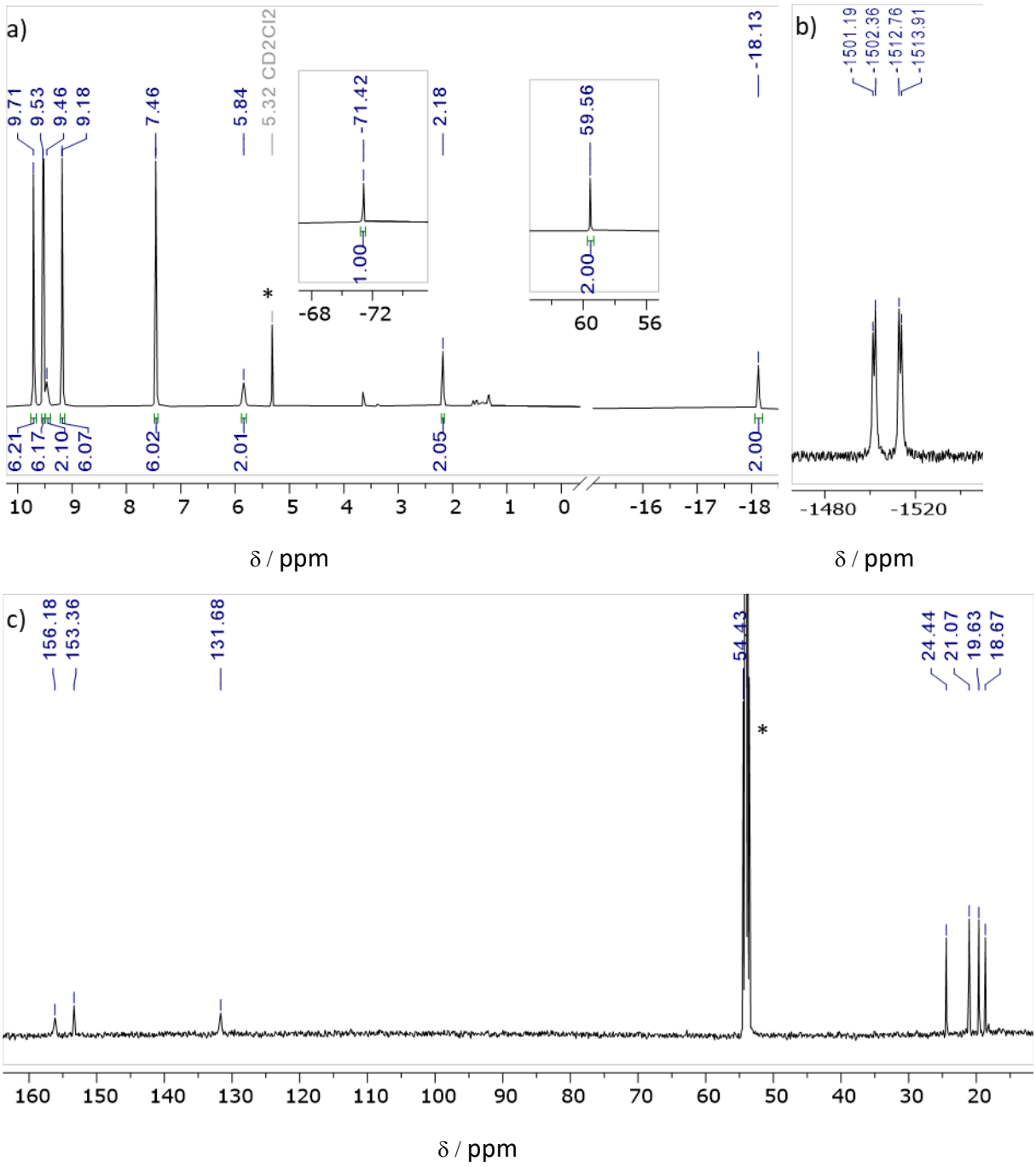

***Figure 11**. **a)** ^{1}H -NMR spectrum of **5** in CD_2Cl_2. **b)** $^{31}P\{^{1}H\}$ NMR spectrum. The solvent signal is marked with an asterisk. **c)** $^{13}C\{^{1}H\}$ NMR spectrum.*

A further X-ray crystal structure was obtained which indicates the complex has an octahedral geometry where the Re metal centre is octahedrally coordinated by PNP and three bromide ligands (**Figure 12**). Backbone oxidation to the imine is supported by one significantly shortened N-C bond (*d*(N1-C3) = 1.424(16) Å, *d*(N1-C1) = 1.304(15) Å), planar coordination of the nitrogen atom (Σ(∡N1) = 359.7°) and a Re-N bond distance which is too long for an amide ligand (*d*(Re1-N1) = 2.087(10) Å). The CV of the complex **5** provides two reversible Re (III/IV) oxidation waves and Re (III/II) reduction wave at $E_{1/2}$ = -0.14 V vs. Fc/Fc^{+} and $E_{1/2}$ = -1.53 V vs.

Fc/Fc^{+} respectively (**Figure 13**), which is a very similar electrochemical response with Re (III) complex **3**.

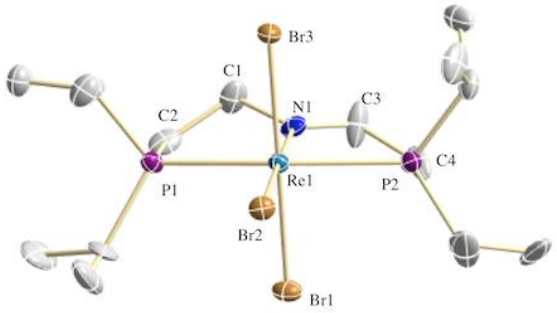

Figure 12. *Molecular structure of **5** obtained by single-crystal X-ray diffraction measurements. All H atoms but the backbone protons are omitted for clarity. Anisotropic displacement parameters are set to 50 % probability. Selected bond lengths [Å] and angles [°]: Re1-N1 2.087(10), Re1-Br1 2.5196(13), Re1-Br2 2.5369(13), Re1-Br3 2.5173(13), N1-C1 1.304(15), N1-C3 1.424(16), P1-Re1-P2 160.38(11), N1-Re1-Br2 179.2(3), Br1-Re1-Br3 177.16(5).*

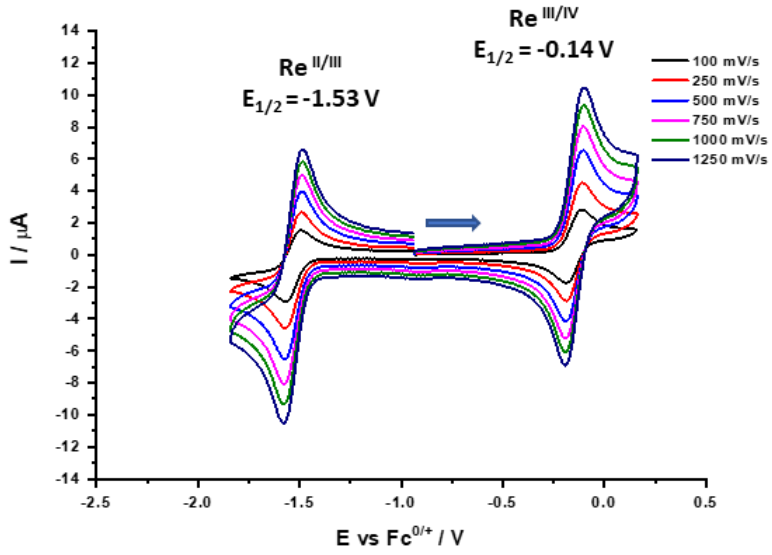

Figure 13. *CV of **5** (1 mM in THF with 0.1 M [nBu$_4$N][PF$_6$]) at different scan rates.*

Investigation of complex **5** with ATR-IR measurement indicates a broad peak at υ = 3418 cm^{-1} which is due to a strong SOC effect similar peak that could be observed in the IR spectrum of complex **3**. The most characteristic sign found is the absence of the N-H vibrational stretching signal indicates the loss of H from the NH moiety and a sharp peak arises at $\upsilon_{C=N}$ = 1603 cm^{-1} indicating the imine moiety confirms the formation of the complex **5** (**Figure 14**).

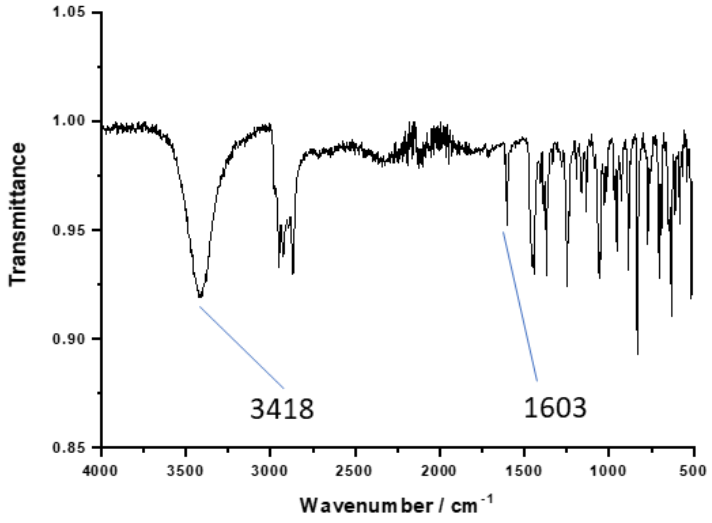

Figure 14. *IR spectrum of complex* ***5.***

2.3 [(P=N=P) $ReBr_3$] (6)

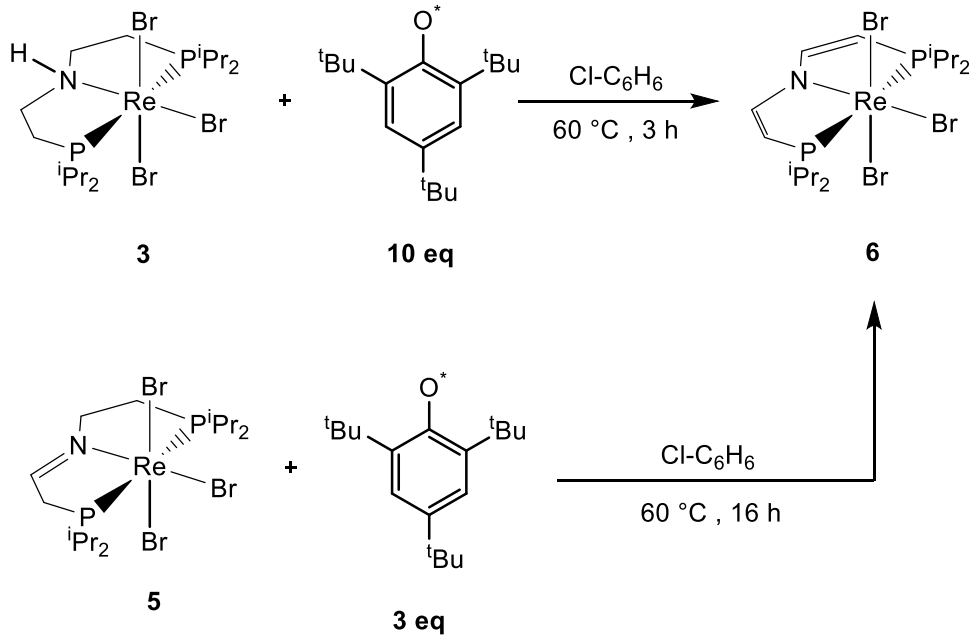

Scheme 11 (b): *Synthesis of Re(IV) complex [(P=N=P)*$ReBr_3$*].*

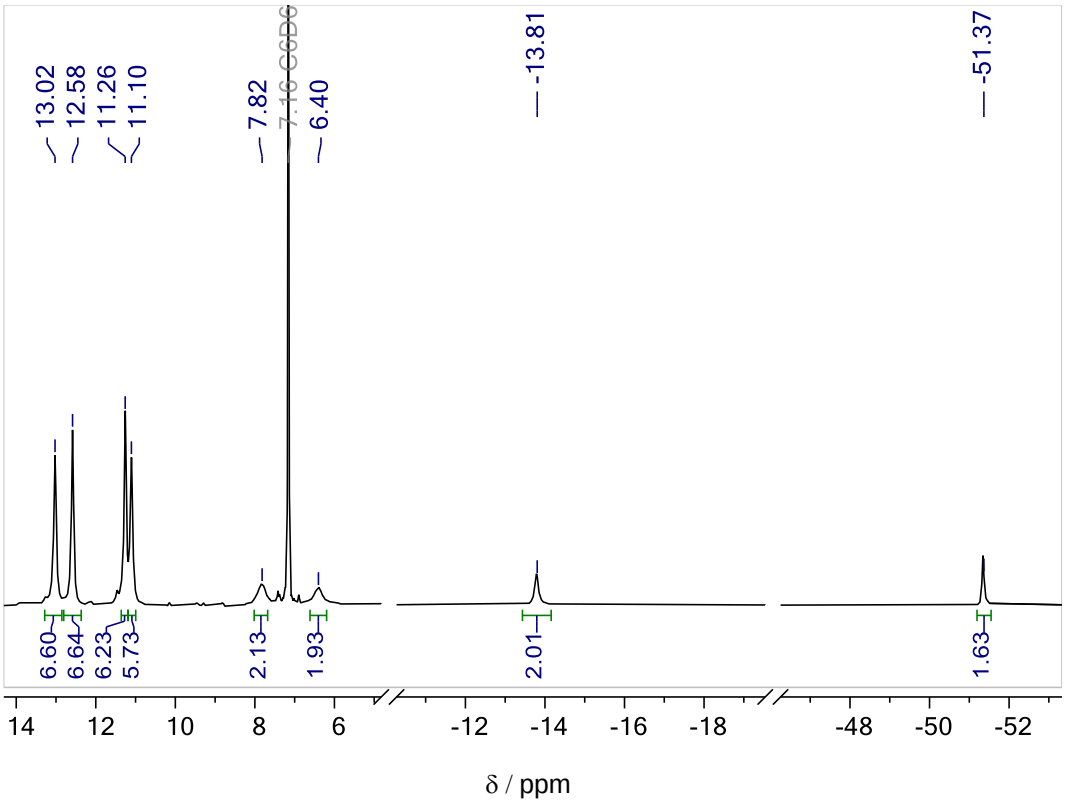

Figure 15. *The ^{1}H-NMR spectrum of **6** in C_6D_6.*

TTBP was found to be one of the most useful reagents in the process of H atom abstraction from Re pincer complexes which can be confirmed by a successful synthesis of complexes **4** and **5** which were synthesised by using 1 eq and 2 eq of TTBP respectively. Therefore 4 H atom abstraction was tried with complex **3** and TTBP. When **3** was stirred with excess (10 eq) of TTBP in chlorobenzene at 60 °C overnight, which provided complex **6** with 63 % in yield after sole isolation. The complex can be synthesized by a different route. When complex **5** was treated with 3eq TTBP and stirred at 60 °C for 3 h, complex **6** with 70% in yield. The complex provided no $^{31}P\{^{1}H\}$ NMR peaks but it exhibits sharpened ^{1}H NMR peaks. Unlike other Re (IV) complexes, **6** provided a sharpened peak in the range of δ_H = 13 to -51 ppm (**Figure 15**). Four sets of large peaks at δ_H = 13-11 ppm are the methyl peaks of 4 isopropyl groups of the PNP, which arise because of C_{2v} symmetry in the NMR time scale. two peaks at δ_H = 6 and 7 ppm are the CH peak of the isopropyl group. The other two highly shifted peaks at δ_H = -13 and -51 ppm indicate 4 backbone protons.

3. Nitride synthesis and characterization

3.1 [Re(N)Br$_2$(HPNP^{iPr})](7)

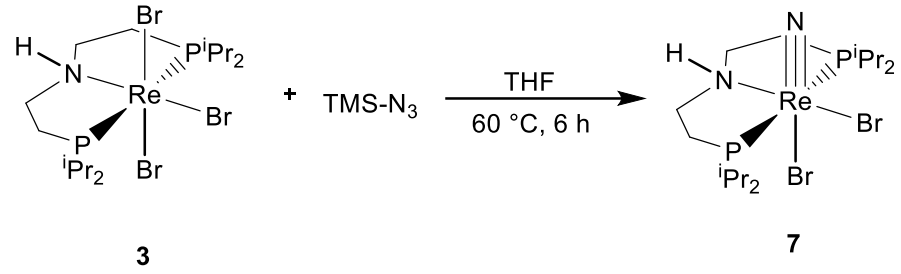

3 **7**

Scheme 12: *Synthesis of Re(V) nitride complex [(HPNP)(N)ReBr$_2$].*

When complex **3** was treated with TMS-N$_3$ and stirred at 60 °C for 6 h, it turned the solution green to brown. Evaporating the solvent in vacuo and washing with ether provided brown coloured complex *[(HPNP)(N)ReBr$_2$]* (**7**)[b, [86]] 93 % in yield (**Scheme 12**). In alternative to that complex **7** can be synthesised from **3** by electrochemical (CPE, *E* = -1.73 V) N$_2$ splitting, upon irradiating at 456 nm. [86]

Complex **7** exhibits ^{1}H NMR in the diamagnetic region i.e. δ_H = 5-1 ppm (**Figure 16**). The notable peak at δ_H = 5.18 ppm corresponds to the proton peak of NH moiety of HPNP. Besides that, the resonance at δ_H = 3.14 and 2.36ppm indicated the CH peaks of the isopropyl group which are in the ratio of 2:2. In addition to that, 4 other signals in the ratio of 2:2:2:2 belong to the HPNP backbone. Large 4 signals δ_H = 1.3 to 1.6 ppm are corresponding to the methyl signal of the isopropyl group and it shows the complex exhibits a C_{2V} symmetry in the NMR time scale. It provides a single resonance in ^{31}P{^{1}H} NMR at δ_P = 31.37 ppm. ^{13}C{^{1}H} NMR exhibits 8 prominent peaks. The 6 peaks between δ_C = 18 and 28 ppm correspond to the isopropyl group and the remaining two signals belong to the backbone carbons. To confirm the formation of terminal rhenium nitride ^{1}H-^{15}N-HSQC NMR was recorded which provided a singlet at $\delta_{N\text{-}H}$ -331.75 ppm.

[b] Synthetic route of complex **7** was initially designed and characterised (with NMR, IR, mass, CV and XRD) by Sesha Kisan. Later, Complex **7** was characterised by elemental analysis by Dr. Maximilian Fritz (Alumnus, AK Schneider, Georg-August University, Gottingen) using a similar procedure.

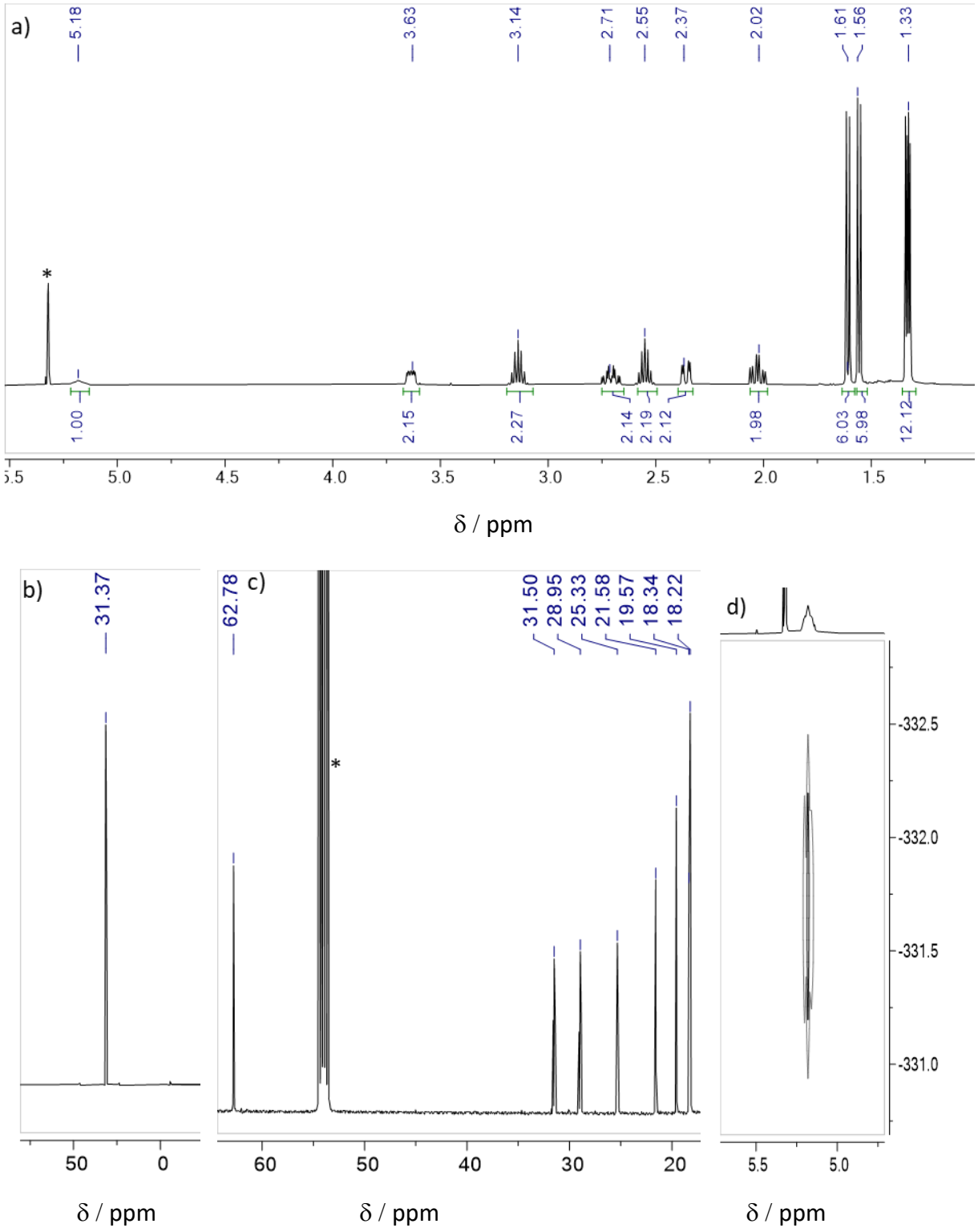

***Figure 16**. **a)** ^{1}H -NMR spectrum of **7** in CD_2Cl_2. **b)** $^{31}P\{^{1}H\}$ NMR spectrum. The solvent signal is marked with an asterisk. **c)** $^{13}C\{^{1}H\}$ NMR spectrum. **d)** ^{1}H-^{15}N-HSQC NMR spectrum.*

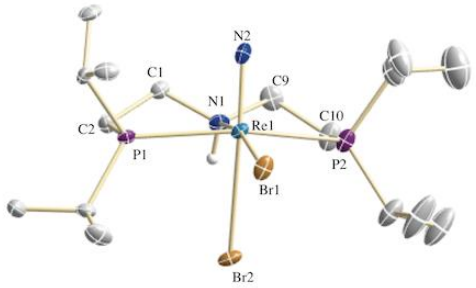

Figure 17. *Molecular structure of* ***7*** *obtained by single-crystal X-ray diffraction measurements. All H atoms but the NH proton, a second, disordered nitride molecule, cocrystallized in the unit cell are omitted for clarity. Anisotropic displacement parameters are set to 50 % probability. Selected bond lengths [Å] and angles [°]: Re1-N1 2.161(5), Re1-N2 1.663(5), Re1-Br1 2.5559(6), Re1-Br2 2.8644(6), N1-Re1-N2 93.7(2), P1-Re1-P2 160.54(5), Br1-Re1-Br2 88.781(19), N1-Re1-Br2 77.94(13)*

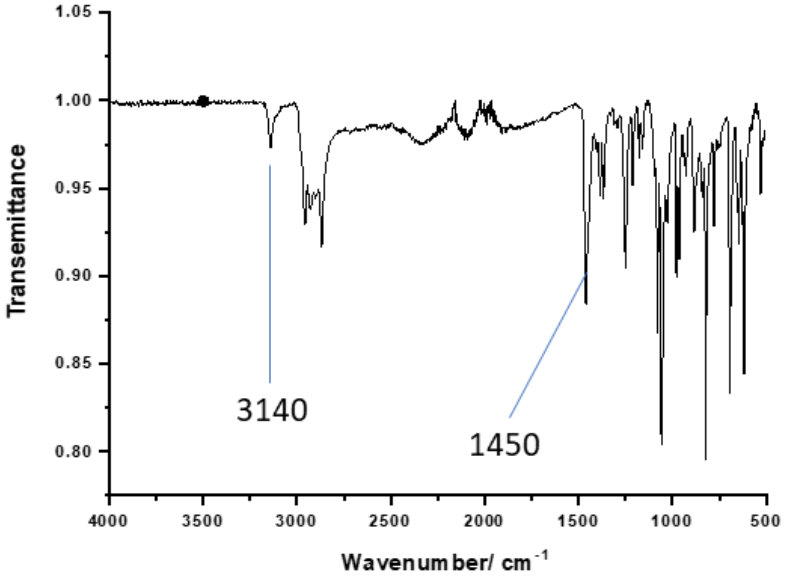

Figure 18. *IR spectrum of complex* ***7.***

Further, the molecular structure was detected by the X-ray diffraction methods which indicates Re metal is octahedrally coordinated with the nitride, HPNP and two Bromide ligands (**Figure 17**). The nitride ligand occupied the axial position and one of the bromides (Br2) ligand occupied trance to it with an elongated bond length of (*d*(Re1-Br2) = 2.8644(6) Å, *d*(Re1-Br1) = 2.5559(6)(Å). The bond length of Re and nitride ligand is too shorter than the rhenium amine moiety, indicating the triple bond character with the nitride ligands (*d*(Re1-N2) = 1.663(5) Å, *d*(Re1-N1) = 2.161(5) (Å). The small angle between the pincer backbone, the metal centre and the bromide (∡(N1-Re1-Br2) = 77.94(13) °) suggests some degree of intramolecular hydrogen bonding to stabilize the coordination of the bromide. Moreover, the complex 7 was characterised by CV measurement which provided a redox wave at $E_{1/2}$ = +0.06 V vs. Fc/Fc^{+}

and no reduction wave of complex **7** was observed within the CV window of the solvent (**Figure 19**). Further characterization of complex **7** with ATR-IR provided the most characteristic signal of N-H stretching frequency at $\upsilon_{N\text{-}H}$ = 3140 cm^{-1}. Moreover, the signal for Re-N was found at $\upsilon_{Re\text{-}N}$ = 1450 cm^{-1}(**Figure 18**).

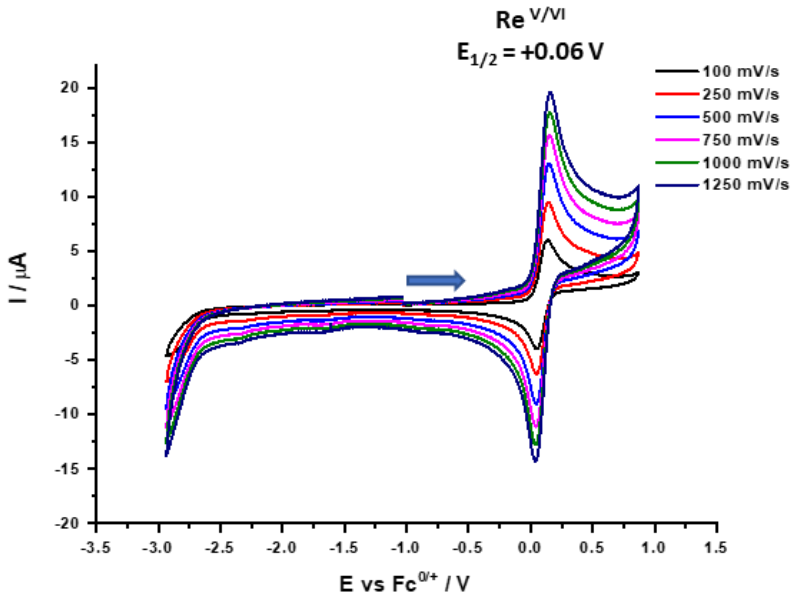

Figure 19. *CV of* ***7*** *(1 mM in THF with 0.1 M [nBu4N][PF6]) at different scan rates.*

3.2 Preparation of Re nitride from [(PNP)ReBr$_3$] (4)

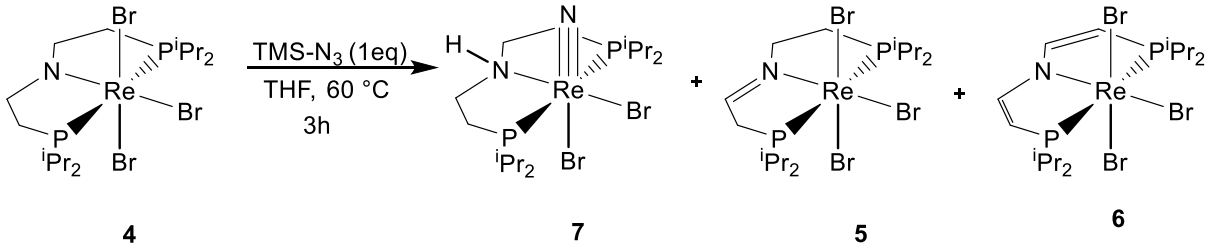

Scheme 13: *Synthesis of Re(V) nitride complex [(HPNP)(N)ReBr3] from complex* ***4****.*

When complex **4** was treated with TMS-N_3 and sat at a similar condition of 60 °C overnight, it provided complex **7** as a major product with complexes **5** and **6** as minor products which are the ratio **7**:**5**:**6** = 5:1:1 (**Figure 13**). It is because of the intermolecular H atom transformation by the PCET mechanism. The expectation of synthesis of Re (VI) nitride was unable to be accomplished by this method. After the solvent was evaporated in vacuo and further extraction in benzene and crystallization in toluene provides complex **7**, 50% in yield.

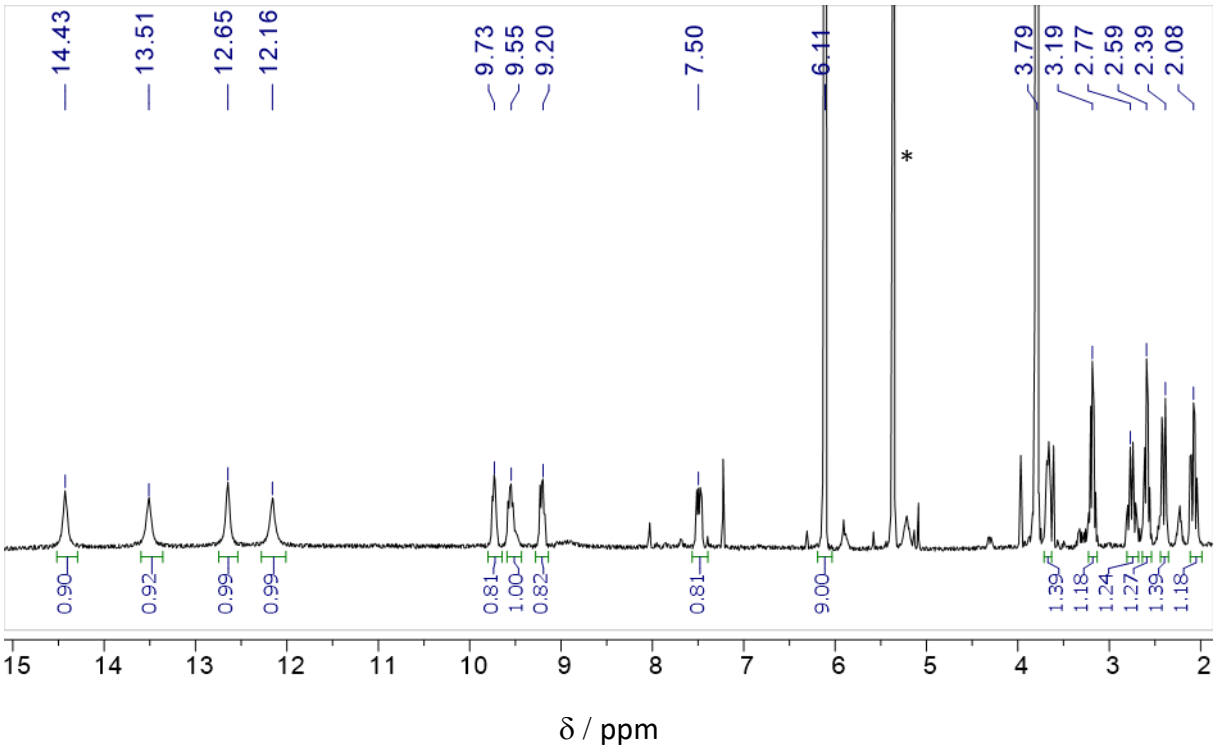

Figure 20. *^{1}H-NMR quantification of the reaction of **4** with 1eq of TMS-N_3 to **7**. 1,3,5-trimethoxybenzene (3 eq) was added and the product was quantified by ^{1}H NMR spectroscopy in CD_2Cl_2. Integration of the methyl groups of 3.8 (δ_H = 14.43 / 13.51 / 12.65/ 12.16, 24 H) indicates 16 % spectroscopic yield in **6**, methyl groups of 3.44 (δ_H = 9.73 / 9.55 / 9.20 / 7.50, 26 H) indicates 15 % spectroscopic yield in **5**, CH_2 signals of backbone and CH peaks of isopropyl group of 7.65 (δ_H = 3.79 / 3.19 / 2.77 / 2.59/ 2.39 / 2.08, 12 H) indicates 64 % spectroscopic yield in **7**.*

3.3 Preparation of [Re(N)Br$_2${N(CHCH$_2$P) (CH$_2$CH$_2$P)}] (9)

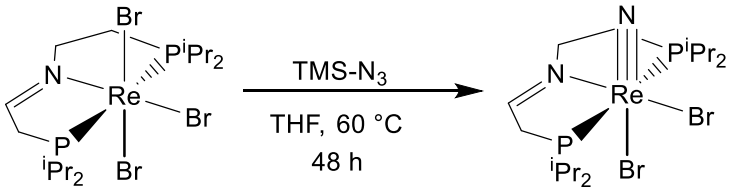

5 **9**

Scheme 14: *Synthesis of Re(V) nitride complex [(P=N-P)(N)ReBr$_3$]from complex **5**.*

Complex **5** and TMS-N_3 are stirred in THF at 60 °C for 2 days, then the solvent was removed in vacuo and the product was isolated by coulomb chromatography in benzene inside the glove box. Then the solvent was dried completely to obtain a reddish-brown product **9**, 60% in yield. ^{31}P{^{1}H} NMR exhibits two doublets at δ_P = 48.13 and 32.10 ppm indicating the C_S symmetry of the complex **9** (**Figure 21**). ^{1}H NMR provided a set of signals at the diamagnetic region from δ_H = 4.32-1.19 ppm. The large and broadened signals at δ_H = 1-2 ppm correspond to the methyl peaks of the isopropyl group and a set of 6 small signals indicates the CH peaks of the isopropyl

group and the backbone signals. The electrochemical response was recorded by the CV measurement which provided a single oxidation wave at $E_{1/2}$ = 0.11 V vs. Fc/Fc^+ (**Figure 22**) and no reduction wave was observed. Importantly, CV has a similar pattern as other Re(V) complexes.

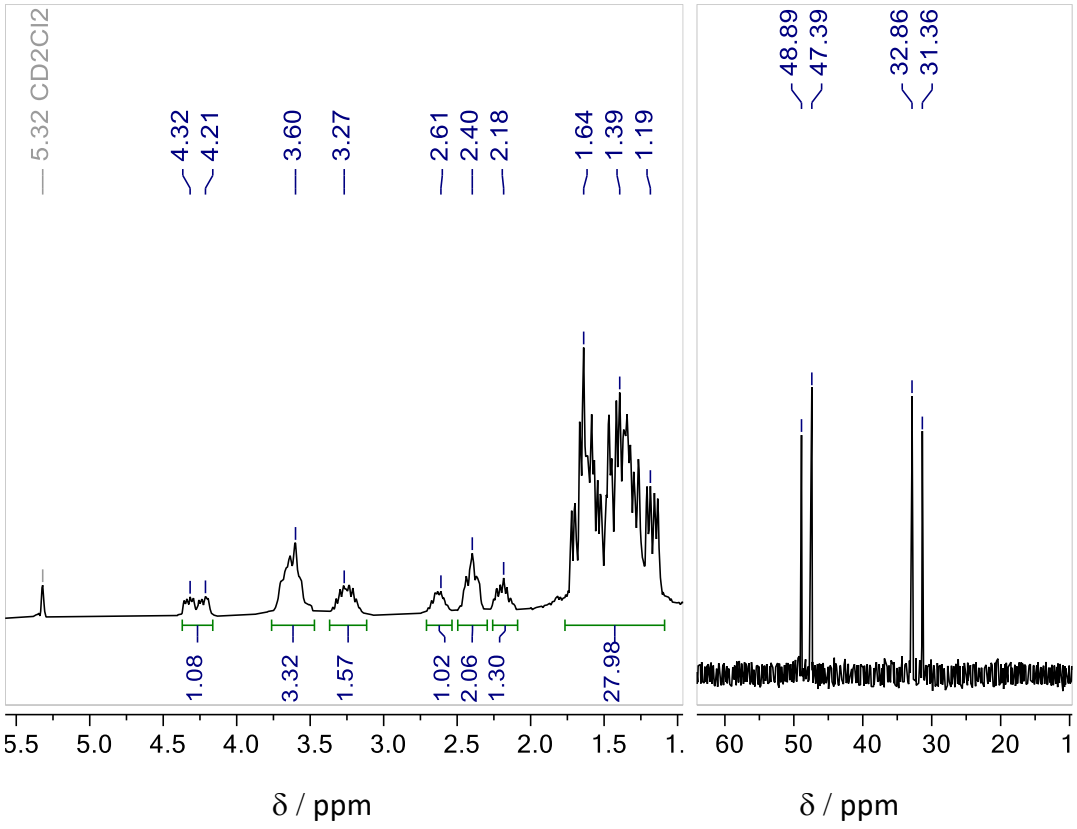

Figure 21. a) *(left) ^{1}H-NMR spectrum of **9** in CD_2Cl_2.* ***b)*** *(right) $^{31}P\{^1H\}$ NMR spectrum.*

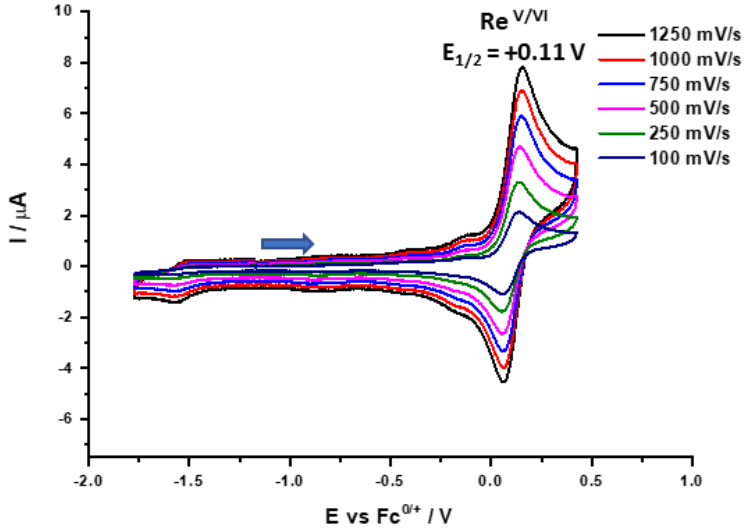

Figure 22. *CV of **9** (1 mM in THF with 0.1 M [nBu_4N][PF_6]) at different scan rates.*

4. Nitride functionalization with benzoyl bromide

After successful synthesis of terminal rhenium nitride **7**, it was employed in nitride functionalization by taking nucleophiles such as CO and HBpin but unfortunately, reactions were unable to proceed further. Therefore, here we tried to proceed toward the investigation of the nucleophilicity nature of the terminal nitride complex **7** with different electrophiles.

4.1 metal-ligand cooperative with complex 7

Previously our group has reported the nitride functionalization and the meta ligand cooperative synthesis of benzamide and benzonitrile with [Re(N)Cl_2(HPNP^{iPr})] and benzoyl chloride. [82] Similarly, here the metal-ligand cooperative synthesis of benzamide and benzonitrile was tried with complex **7** and the benzoyl bromide.

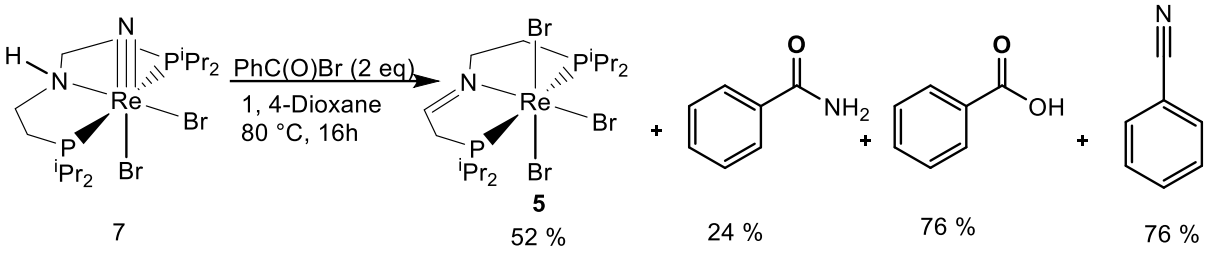

Scheme 15: *Synthesis of benzamide and benzonitrile by metal-ligand cooperation with* ***7***.

The reaction of complex **7** with 2eq of benzoyl bromide at 80 °C for 16 h provided complex **5** (52%), benzamide (24%), benzonitrile (76 %) and benzoic acid (76 %) (**Figure 23**). The solvent was evaporated in vacuo and TMB was used as an internal standard to calculate the yields by ^{1}H-NMR. 1.33 eq of TMB was added from the beginning of the reaction to get the accurate yield by getting the normalized value. Basically, in this reaction benzamide is the first product forming, which further reacts with benzoyl bromide to give rise the benzonitrile and benzoic acid. So, the sum of nitrogen-containing compounds is 100 %. Complex **5** was crystallised from the reaction mixture and was characterised with NMR and mass which was compared with complex **5** which was synthesized by using TTBP in section 2.2, indicating they are identical. Further, here the intermediates involved in the chemical reaction were tried to isolate to get a better explanation regarding the metal-ligand cooperativity. The equimolar formation of benzonitrile was observed when the reaction was carried out in toluene-d8 but was not suitable for quantification of **4** due to reduced yield and low solubility.

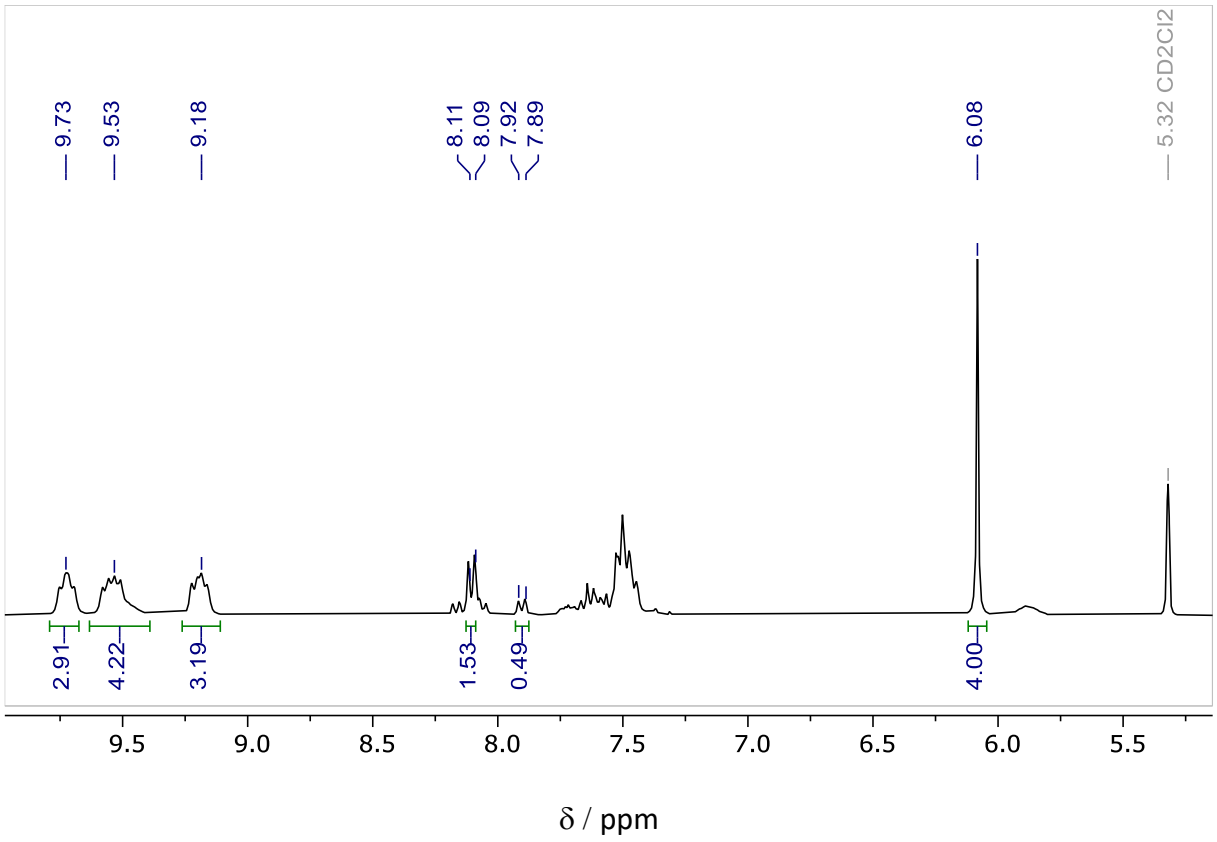

Figure 23. *^{1}H-NMR quantification of the reaction of **7** with 2 eq of benzoyl bromide to **5**. 1,3,5-trimethoxybenzene (1.33 eq) was added and the product was quantified by ^{1}H NMR spectroscopy. Integration of the methyl groups of 10.32 (δ_H = 9.73 / 9.53 / 9.18, 20H) indicates 52 % spectroscopic yield in **5**. Benzoic acid (δ_H = 8.11 ppm, 2H, H-ortho) and benzamide (δ_H = 7.92 ppm, 2H, H-ortho) are obtained in 76 % and 24 % respectively. The equimolar formation of benzonitrile was observed if the reaction was carried out in toluene-d8, but was not suitable for quantification of **5** due to reduced yields and low solubility.*

4.2 Synthesis and characterization of [Re(PhC(O)N) Br_2(HPNP^{iPr})] Br

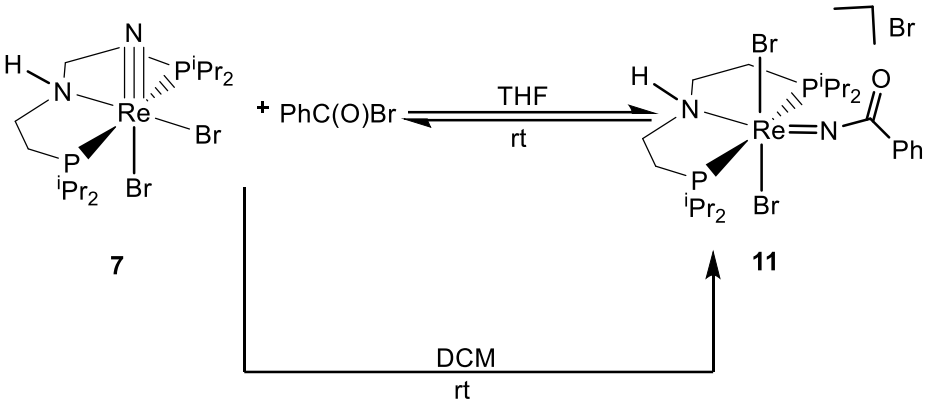

Scheme 16: *Synthesis of Re(V) complex* ***11*** *[Re(PhC(O)N) Br_2(HPNP^{iPr})] Br.*

Complex **7** and benzoyl bromide are mixed in DCM and stirred at rt overnight (16 h). Then the solvent was evaporated in vacuo. Further, the complex was washed with THF and extracted with DCM provided green coloured complex **11,** [c, 86] 86 % in yield. On the other hand, when the complex **7** is suspended in THF and further stirred with benzoyl bromide provided a green precipitate of complex **11** with a 72% in yield. Here, complex **7** found equilibrium with complex **11**. If the complex **7** dissolves completely before adding benzoyl bromide then the precipitate may not observe.

$^{31}P\{^1H\}$ NMR of complex **11** displays a single resonance at δ_P = 33.26 ppm which is in a very similar region as the other Re(V) complexes (**Figure 24**). ^1H NMR provided all the signals in the diamagnetic ranges from δ_H = 1.25 to 8.02 ppm. The prominent signals at δ_H = 7-8 ppm are corresponding to the aromatic signal of the benzoyl group. Another distinctive peak at δ_H = 5.55 ppm represents the signal for NH moiety. A set of larger peaks at δ_H = 1.25 to 1.53 ppm indicates the methyl signal of the isopropyl group, remaining set s of signals represents CH signals of the isopropyl group with the backbone signals. $^{13}C\{^1H\}$ NMR spectrum displays 12 prominent peaks from δ_C = 177.04 - 19.16 ppm. Further investigation by CV measurement provided an oxidative wave at $E_{1/2}$ (V) = - 0.5 (Re $^{V/VI}$) vs Fc/Fc^+ and an irreversible reductant wave at -1. 38 V. It has similar CV features as the other Re (V) complexes.

[c] Synthesis and characterization (NMR, IR, mass spectrometry, elemental analysis and CV) of complex **11** were carried out by Sesha Kisan. XRD sample (crystals) was prepared by Sesha Kisan and recorded by Dr. Maximilian Fritz. [86]

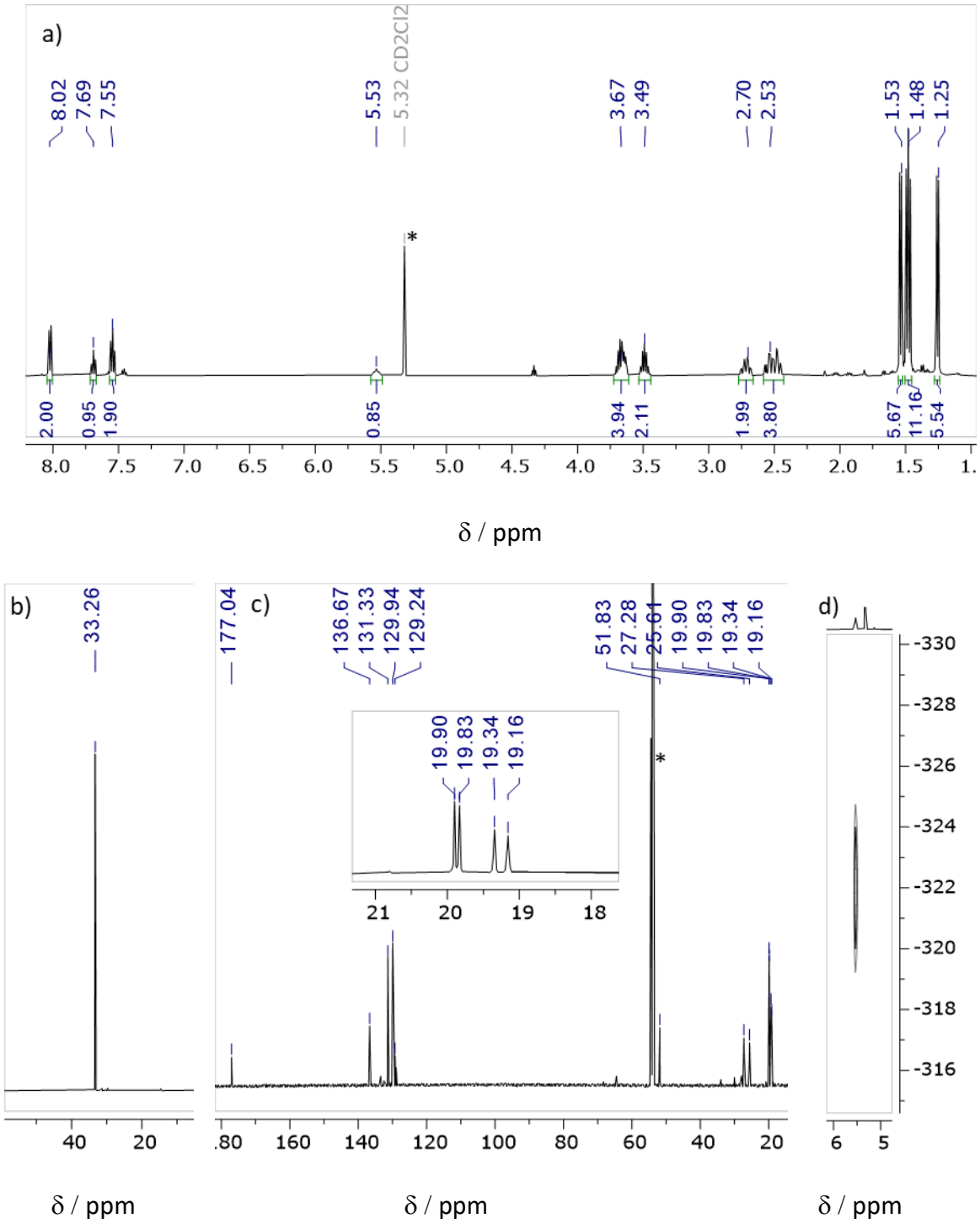

***Figure 24**. **a)** ^{1}H -NMR spectrum of **11** in CD_2Cl_2. **b)** $^{31}P\{^{1}H\}$ NMR spectrum. The solvent signal is marked with an asterisk. c) $^{13}C\{^{1}H\}$ NMR spectrum. d) ^{1}H-^{15}N-HSQC NMR spectrum.*

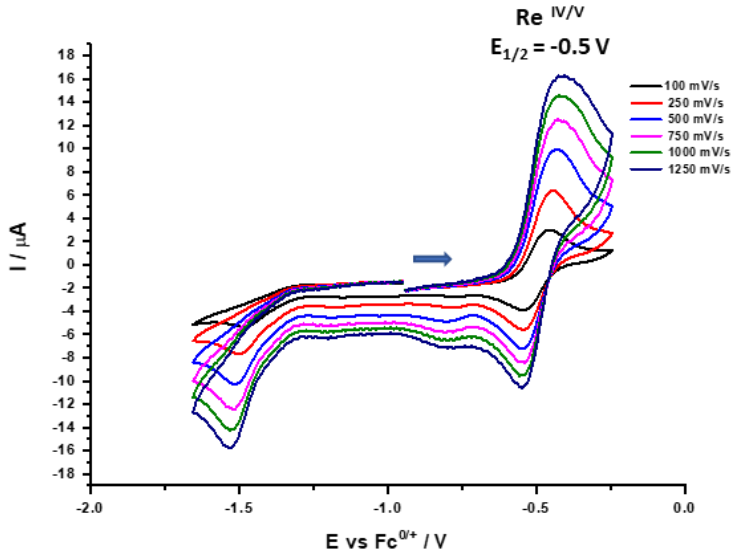

Figure 25. *CV of* ***11*** *(1 mM in DCM with 0.1 M [nBu$_4$N][PF$_6$]) at different scan rates.*

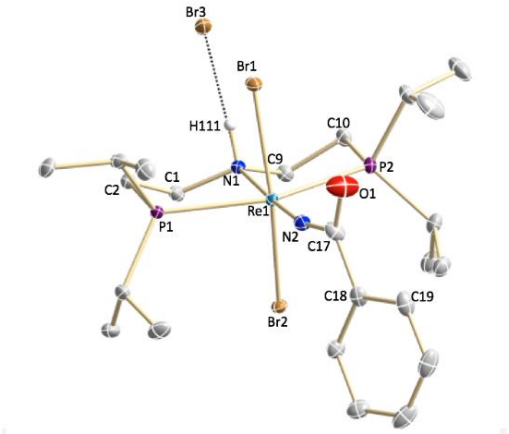

Figure 26. *Molecular structure of* ***11*** *obtained by single-crystal X-ray diffraction measurement. All H atoms but the NH proton and cocrystallized THF units are omitted for clarity. Anisotropic displacement parameters are set to 50 % probability. Selected bond lengths [Å] and angles [°]: Re1-N1 2.278(3), Re1-N2 1.724(3), Re1-Br1 2.5352(3), Re1-Br2 2.5427(3), N1-Re1-N2 176.37(12), P1-Re1-P2 154.66(3), Br1-Re1-Br2 165.462(12), N1-Re1-Br1 83.01(7).*[c, 86]

Molecular structure if complex **11** has a coordination environment around the central Re metal centre indicates an octahedral geometry, where the benzoyl group is situated at the equatorial position (**Figure 26**). The bond length of Re-N of complex **11**[Re (1)-N (2) = 1.72 Å] is longer than Re-N of complex **7** [Re (1)-N (2) = 1.66 Å] indicating the double bond character. Found shorter C-N bond [C (17)-N (2) = 1.42 Å] and almost linear coordination [Re (1)-N (2)-C (17) = 168.6] of the benzoyl moiety and it's coplanar with an aromatic ring. In the solid-state, it was found that the bromide [Br (3)] present in the outer sphere makes a hydrogen bond with the N-H proton [H (111)]. The IR spectrum of complex **11** provides a strong signal at $\upsilon_{C\text{-}O}$

=1693 cm^{-1} indicating the CO stretch of the imidobenzoyl group, which is one of the most characteristic peaks of this complex.

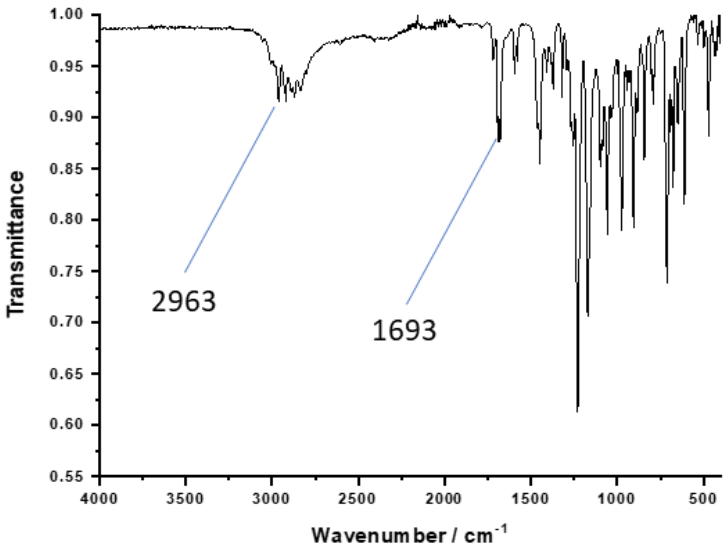

Figure 27. *IR spectrum of complex* ***11***

4.3 Independent synthesis of [Re(Ph(CO)N)Br_2(HPNP^{iPr})]Br (11)

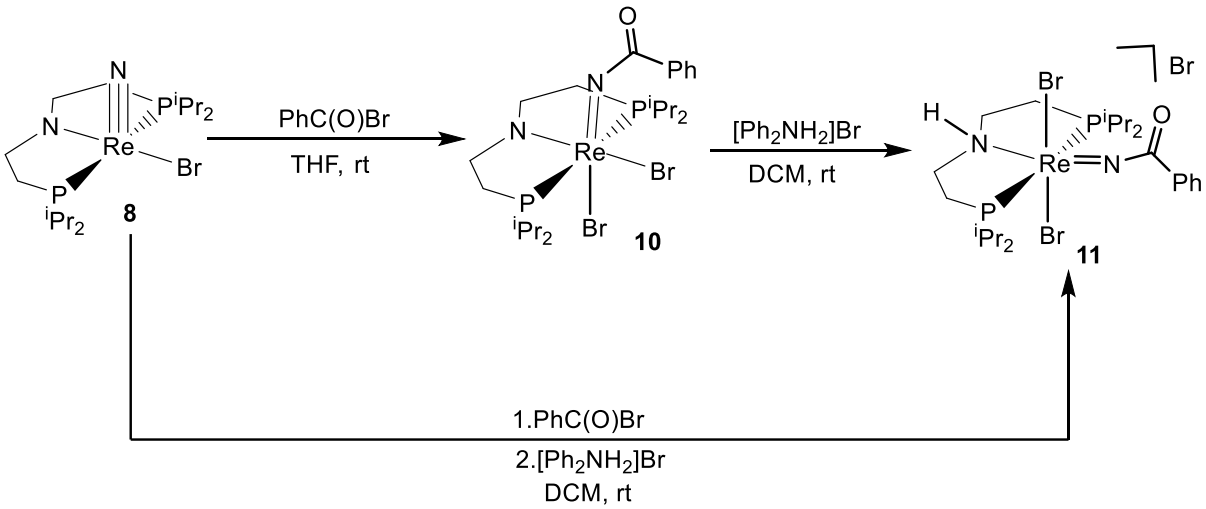

Scheme 17: *Synthesis of Re(V) complex* ***10*** *and independent synthesis of* ***11.***

Synthesis of Complex **10:** Complex **8**[d] can be synthesised from complex **7** upon reacting with a base such as KHMDS [86].

[d]Complex **8** is synthesised and characterised by Dr. Maximillian Fritz. [86]

When it is treated with 1eq of benzoyl bromide in THF it provides a dark violet colour solution. Evaporating the solvent and washing with pentane and extracting in Et_2O provided complex **10**, 86% in yield. $^{31}P\{^1H\}$ NMR provided a sharp peak at δ_P = -28.09 ppm which is only a prominent peak of the complex **10.** ^1H NMR provided all the peaks at the diamagnetic region from δ_H = 1.04 ppm to 8.17 ppm (**Figure 28**). The 3 larger and broad peaks at the region from δ_H = 1.04 ppm to 1.67 ppm corresponds to the methyl signals of the isopropyl group and the other 6 signals in the ratio 2:2:2:2:2:2 in the region from δ_H = 1.88 ppm to 4.68 ppm are the methine and backbone signals. The prominent peak at δ_H = 8.17 ppm is the ortho-proton of the benzoyl group and other signals integrated 3 are the remaining aromatic peaks. Further, the complex is characterised by X-ray measurement which indicates the complex has an octahedral geometry with Re at the centre coordinated by PNP and two bromide ligands (**Figure 29**). The benzoyl imido ligand obtained the axial position in a cis manner.

Dark purple coloured Complex **10** reacted with 1eq of diphenyl ammonium bromide in DCM stirred for 2h which provided green complex **11**, 84% in yield upon sole isolation. Complex **11** can be directly synthesised from complex **8** by step-wise addition of 1eq of benzoyl bromide and 1 eq of diphenyl ammonium bromide in DCM, which provided 80% in yield. Complex **10** can be regenerated from complex **11**. When 1eq of base (triethylamine) treated with complex **11** and solution provided a dark purple coloured complex **10**, after stirring in DCM for 1h. It is a simple reaction by a base which proceeds through the abstraction of protons and removal of hydrogen bromide**.** The ATR-IR of the complex **10** indicate the absence of NH moiety and provides a stretching frequency at $\upsilon_{C\text{-}O}$ = 1718 cm^{-1} indicating the carbonyl group of the benzoylimido ligand (**Figure 30**).

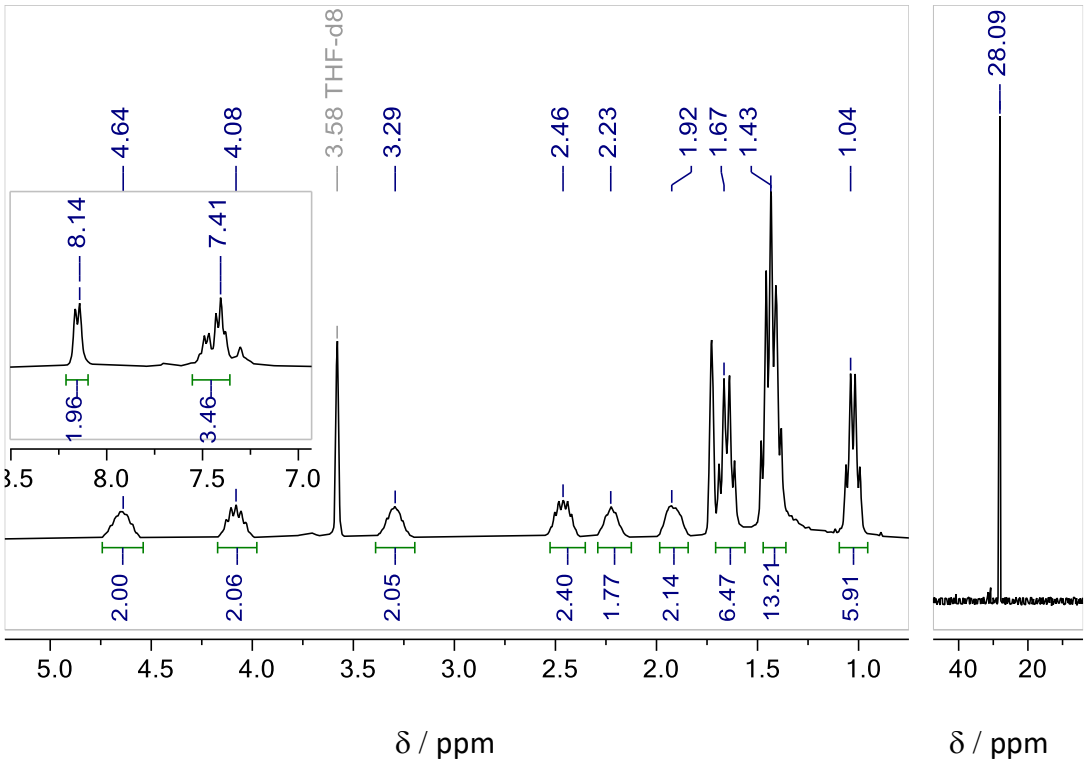

***Figure 28**. **a)** (left) ^{1}H -NMR spectrum of **10** in THF-d8. **b)** (right) $^{31}P\{^{1}H\}$ NMR spectrum.*

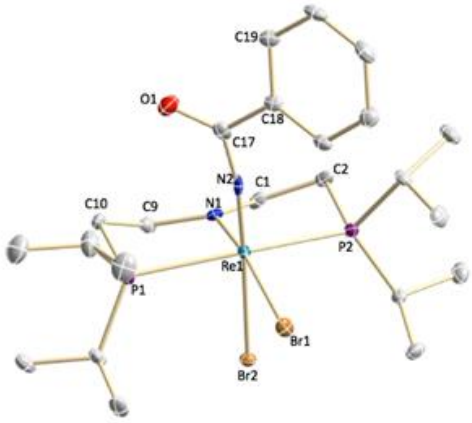

***Figure 29.** Molecular structure of **10** obtained by single-crystal X-ray diffraction measurements.*
All H atoms were omitted for clarity. Anisotropic displacement parameters are set to 50 % probability. Selected bond lengths [Å] and angles [°]: Re1-N1 1.948(3), Re1-N2 1.790(3), Re1-Br1 2.6251(4), Re1-Br2 2.6261(4), N1-Re1-N2 103.67(11), P1-Re1-P2 162.96(3), Br2-Re1-Br1 82.863(11), N1-Re1-Br1 166.07(8).

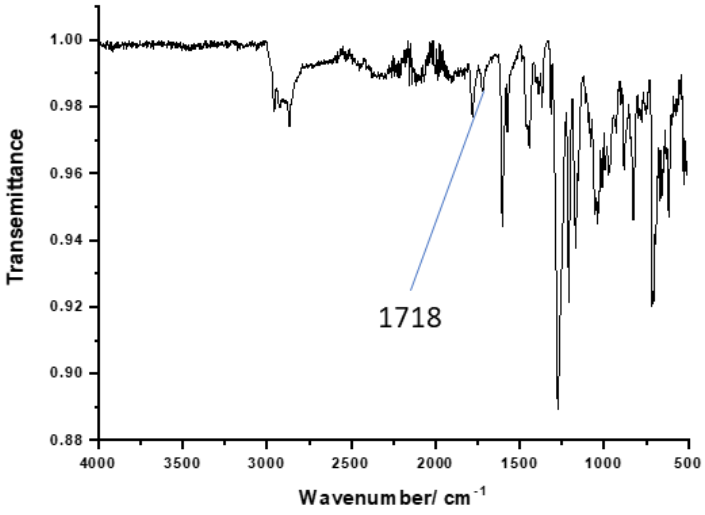

Figure 30. *IR spectrum of complex* ***10.***

5. Reactivity of [Re(Ph(CO)N)Br_2(HPNP^{iPr})]Br (11)

5.1 Metal-ligand cooperative reaction with complex 11

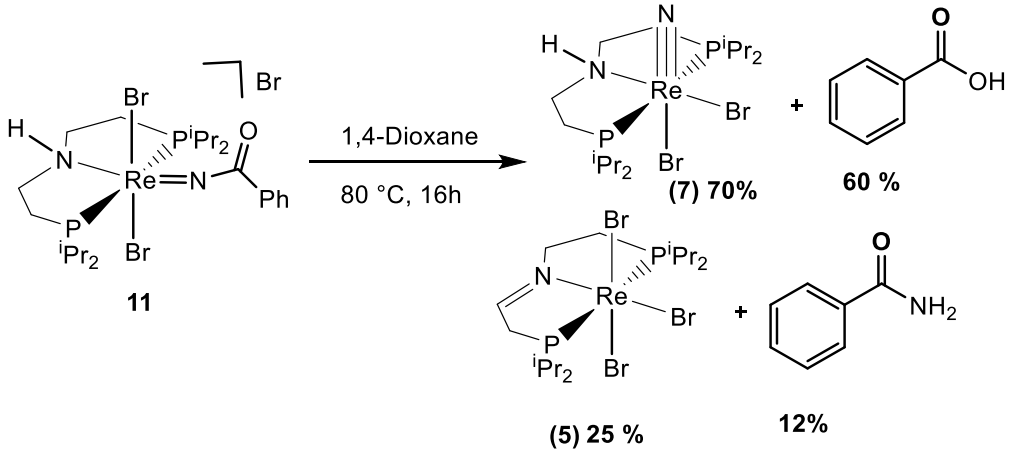

Scheme 18: *metal-ligand cooperative reaction with* ***11*** *in the absence of benzoyl bromide.*

Keeping the complex **11** in DCM solution is stable overnight but further keeping it started degrading to provide rhenium nitride. Heating of complex **11** at 80 °C overnight in 1,4-dioxane, degraded to provide 70% of complex **7**. A partial amount of rhenium nitride and benzoyl bromide undergo metal-ligand cooperative reaction provided 25% of complex **5** and 12% benzamide (**Figure 31**). Benzamide formed is subsequently reacts with benzoyl bromide to provide benzonitrile, benzoic acid, and HBr by a process called water-gas shift reaction. The

Formation of HBr might hydrolyse some of the benzoyl bromides to produce benzoic acid. So, overall 60% of benzoic acid is obtained by ^{1}H NMR.

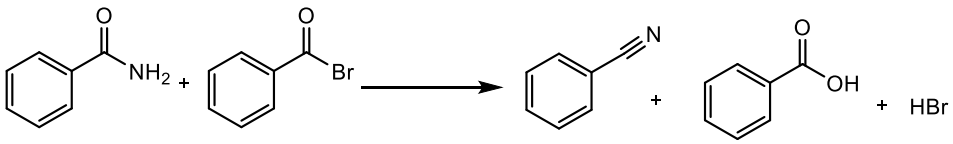

It was tried to explain the metal-ligand cooperative H atom transfer but unfortunately, it could not be explained clearly by this reaction.

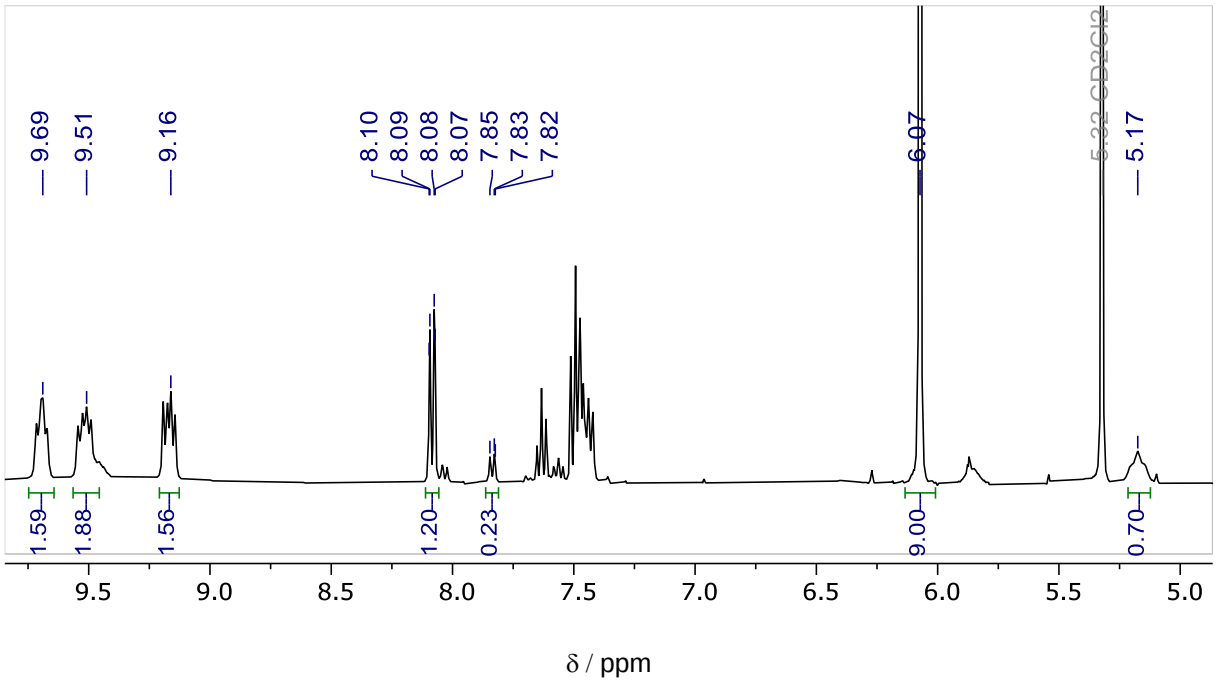

Figure 31. *^{1}H-NMR quantification of the reaction after heating complex **11** without benzoyl bromide to **7** and **5**. 1,3,5-trimethoxybenzene (3 eq) was added and the product was quantified by ^{1}H NMR spectroscopy. Integration of the methyl groups of 5.03 (δ_H = 9.69 / 9.51 / 9.16, 20H) indicates 25 % spectroscopic yield in **5** and Integration of the NH proton of 0.70 (δ_H = 5.17, 1H) indicates 70 % spectroscopic yield in **7.** Benzoic acid (δ = 8.11 ppm, 2H, H-ortho) and benzamide (δ_H = 7.92 ppm, 2H, H-ortho) are obtained in 60 % and 12 % respectively.*

Rhenium complex **11** and benzoyl bromide (1.0 eq) are mixed in 1,4-dioxane and heated to 80 °C for 16 h. All volatiles are subsequently removed in vacuo. 1,3,5-trimethoxybenzene was added as an internal standard and was added from the beginning of the reaction to get an accurate yield by finding its normalized value. NMR spectroscopic examination in CD_2Cl_2 reveals the formation of **5** in 56 % in yield. NMR spectroscopic features as well as the LIFDI mass spectrum are identical to those of **5** obtained from route **2.2**. The reaction is accompanied by the formation of benzamide (20 % spectroscopic yield) and equimolar amounts of benzoic acid and benzonitrile (73 % spectroscopic yield each) (**Figure 32**).

It was found the metal-ligand cooperative complex **11** with 1 eq of benzoyl bromide gives a similar and better result than when rhenium nitride **7** was reacted with **2** eq of benzoyl bromide, so it can be concluded that complex **11** is one of the key intermediates in the metal-

ligand cooperative synthesis of benzamide and benzonitrile. Even though we isolate one of the key intermediates complex **11** in the process of metal-ligand cooperation, selective benzamide could not be achieved from it. This arises because some amount of benzamide formed reacts with the benzoyl bromide to provide benzoic acid and the benzonitrile. As a metal-ligand cooperative reaction, the reaction benzamide with benzoyl bromide occurs simultaneously to provide a mixture of organic compounds. Further extra 2 eq of benzoyl bromide was added with complex **11** to get benzonitrile selectively.

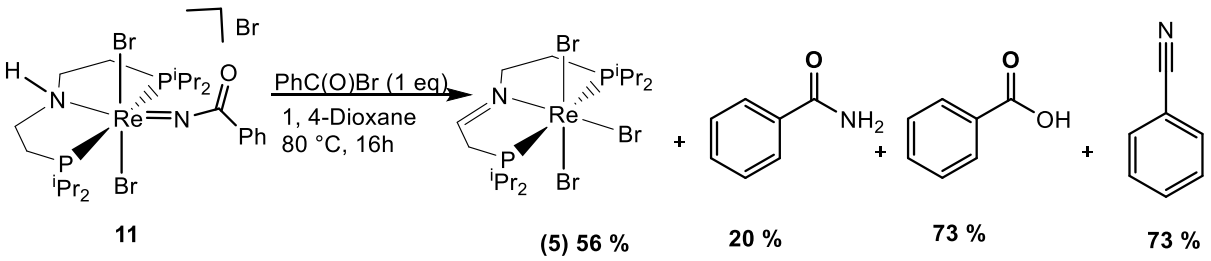

Scheme 19: *metal-ligand cooperative reaction with **11** in presence of 1eq of benzoyl bromide.*

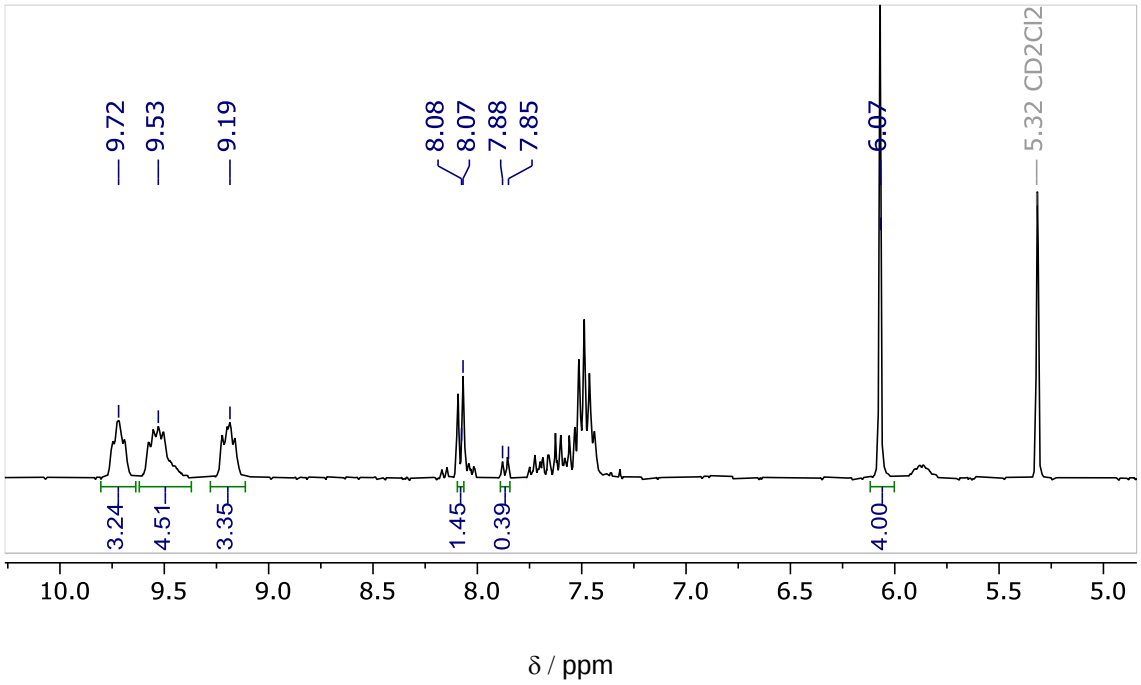

Figure 32. *^{1}H-NMR quantification of the reaction of **11** with 1eq of benzoyl bromide to **5**. 1,3,5-trimethoxybenzene (1.33 eq) was added and the product was quantified by ^{1}H NMR spectroscopy. Integration of the methyl groups of 11.1 (δ_H = 9.72 / 9.53 / 9.19, 20H) indicates 56 % spectroscopic yield in **5**. Benzoic acid (δ_H = 8.08 ppm, 2H, H-ortho) and benzamide (δ_H = 7.88 ppm, 2H, H-ortho) are obtained in 73 % and 20 % respectively. The equimolar formation of benzonitrile was observed if the reaction was carried out in toluene-d8, but was not suitable for quantification of **5** due to reduced yields and low solubility.*

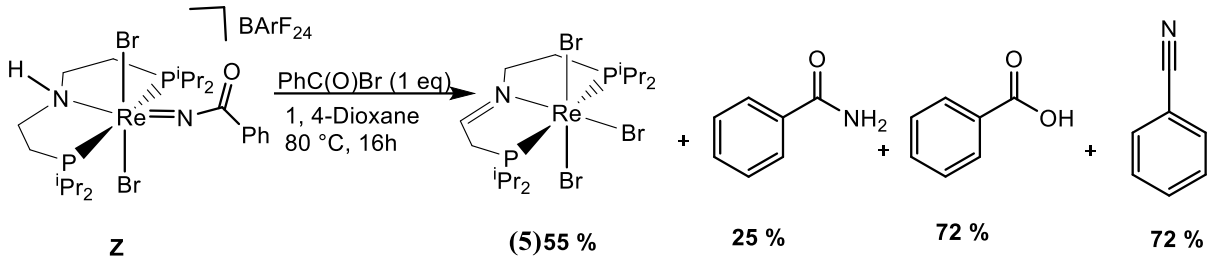

Scheme 20: *metal-ligand cooperative reaction with $BArF_{24}$ complex in presence of 1eq of benzoyl bromide.*

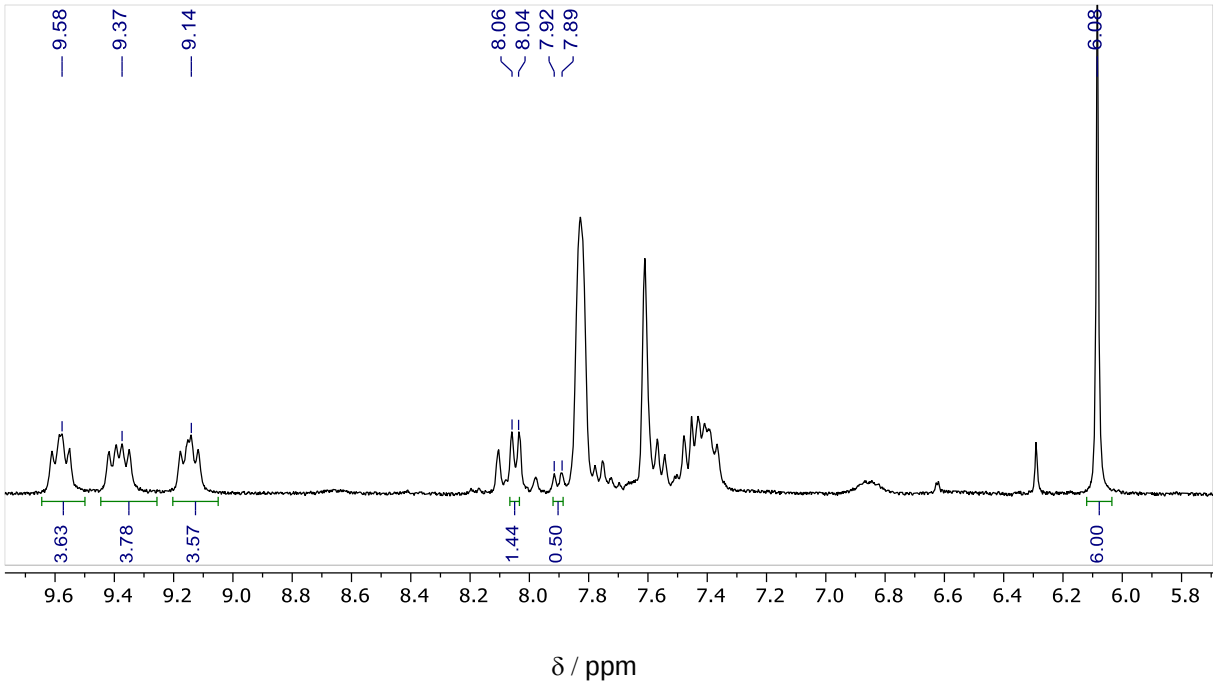

Figure 33. *^{1}H-NMR quantification of the reaction of $BArF_{24}$ complex **Z** with 1eq of benzoyl bromide to **5**. 1,3,5-trimethoxybenzene (2 eq) was added and the product was quantified by ^{1}H NMR spectroscopy in CD_2Cl_2. Integration of the methyl groups of 10.98 (δ_H = 9.58 / 9.37 / 9.14, 20H) indicates 55 % spectroscopic yield in **5**. Benzoic acid (δ_H = 8.06 ppm, 2H, H-ortho) and benzamide (δ_H = 7.92 ppm, 2H, H-ortho) are obtained in 72 % and 25 % respectively. The equimolar formation of benzonitrile was observed if the reaction was carried out in toluene-d8, but was not suitable for quantification of **5** due to reduced yields and low solubility.*

As complex **11** is not stable at elevated temperatures, the bromide ion was changed to $BArF_{24}$ to increase the stability. The $BArF_{24}$ complex **Z** [e] was synthesised and characterised by Dr. Maximilian Fritz [86]. When it is subjected to a similar condition of 80 °C for 16 h, which is found to be a stable compound under this condition. Further, the complex is treated with 1 eq of bromide source such as [nBu_4N][Br].

[e] The $BArF_{24}$ complex **Z** was synthesised and characterised by Dr. Maximilian Fritz. [86]

This result can be explained by the back attack, due to the back attack of the bromide it provided rhenium nitride and benzoyl bromide. But, heating the $BArF_{24}$ complex with 1 eq of benzoyl bromide at 80 °C for 16 h in dioxane. Evaporating the solvent and measuring NMR in CD_2Cl_2 provided 55 % of imine complex **5**, 25 % of benzamide and 72 % of benzonitrile and benzoic acid each. The yield was calculated spectroscopically using 1,3,5-trimethoxy benzene as the internal standard. It is observed that with the $BArF_{24}$ complex the production of benzamide is similar to the benzamide that was obtained with complex **11**, which can be explained because of increased stability with the $BArF_{24}$ complex.

5.2 Kinetic study

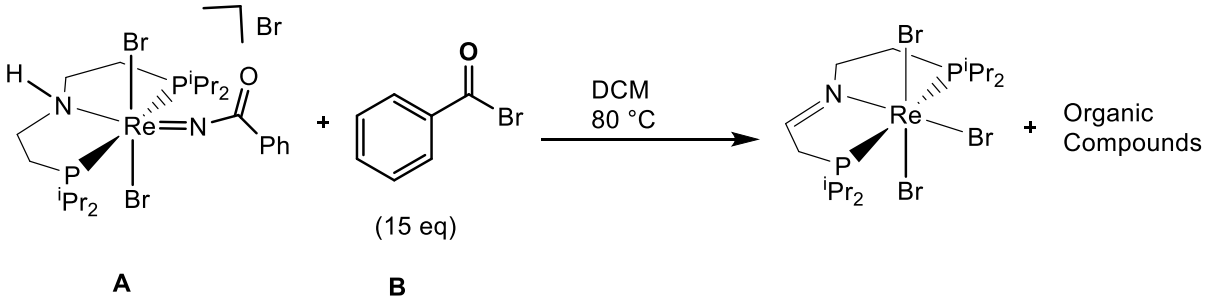

Scheme 21: *Kinetic study of Metal-ligand cooperative reaction*

To get more information regarding the mechanistic pathway for the metal-ligand cooperative formation of benzamide and benzonitrile from complex **11 (A)**, here kinetic study is done with complex **11**. At the initial state, excess (15 eq) of **B** w.r.t complex **11** (A) is taken and monitored the reaction by ^{1}H NMR in the interval of 1h, 2h, 3h, 4h, 6h, 7h, 8h, 9h, 10h at 80 °C. Here, DCM was used as solvent as the complex **11** does not exist equilibrium in this solvent only. All the NMR was measured at an increased relaxation time of 15s to get the accurate yields and monitored up to at least 3 half-lives (conversion > 92%) (**Figure 34**). At the same time1,3,5-trimethoxybenzene (4.12 eq) is used as an intern standard and is added from the beginning of the reaction to get the normalised integration value to get the most accurate conversion of the complex **11**. The conversion of the complex **A** was calculated with the signal at δ_H = 2.75 ppm (CH_2). Finally, concertation **A** vs time is plotted which provides a linear relationship with slope = -0.00164, (**Figure 35)** which indicates it's a zero-order to complex **11** (**A**) with a rate constant, k = 2.7* 10^{-5} M.s^{-1}.

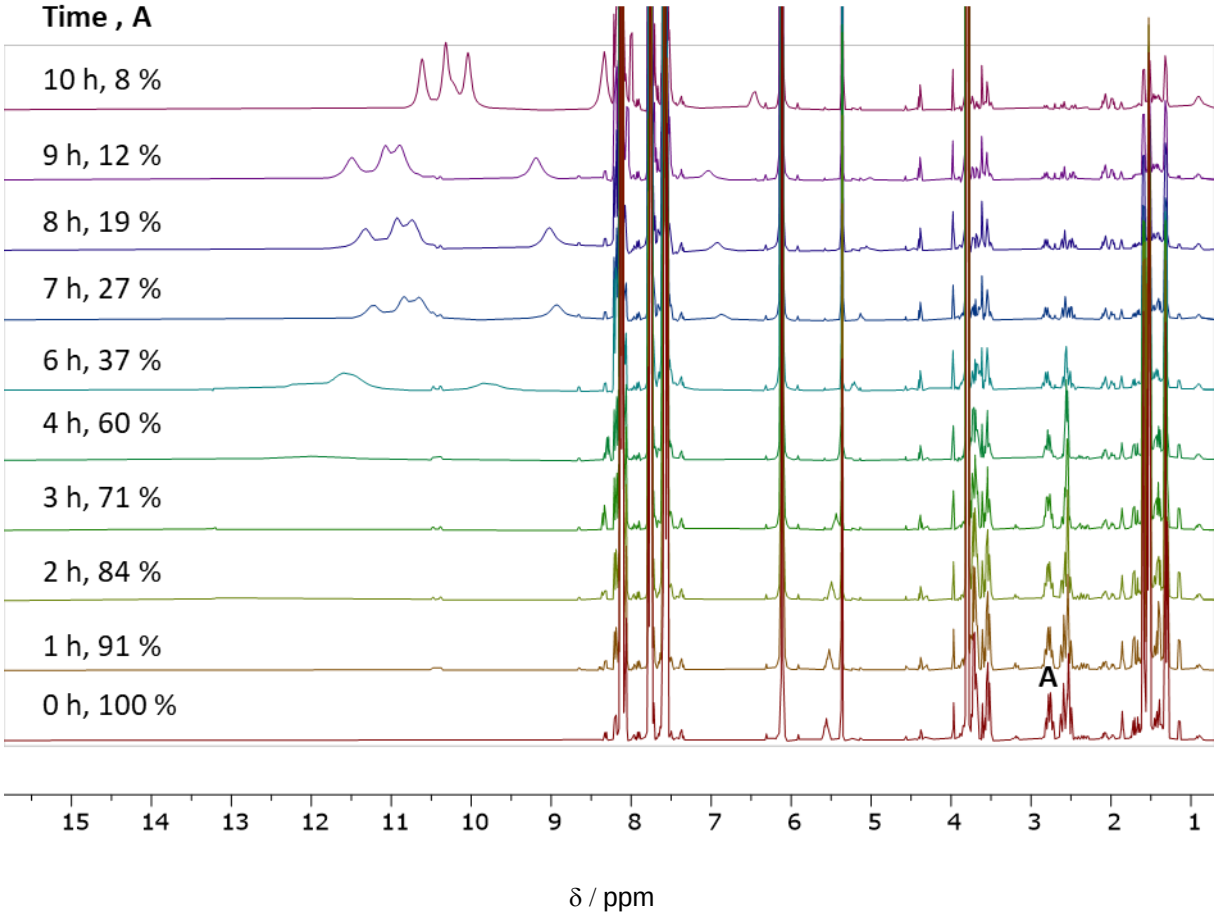

Figure 34. *Complex **11** (**A**) with 15 eq of benzoyl bromide to **5**. 1,3,5-trimethoxybenzene (4.12 eq) is added and the concentration of complex **11** are quantified by ^{1}H NMR at different time (0-10 h) in CD_2Cl_2. Conversion of complex A is calculated by integrating peak A.*

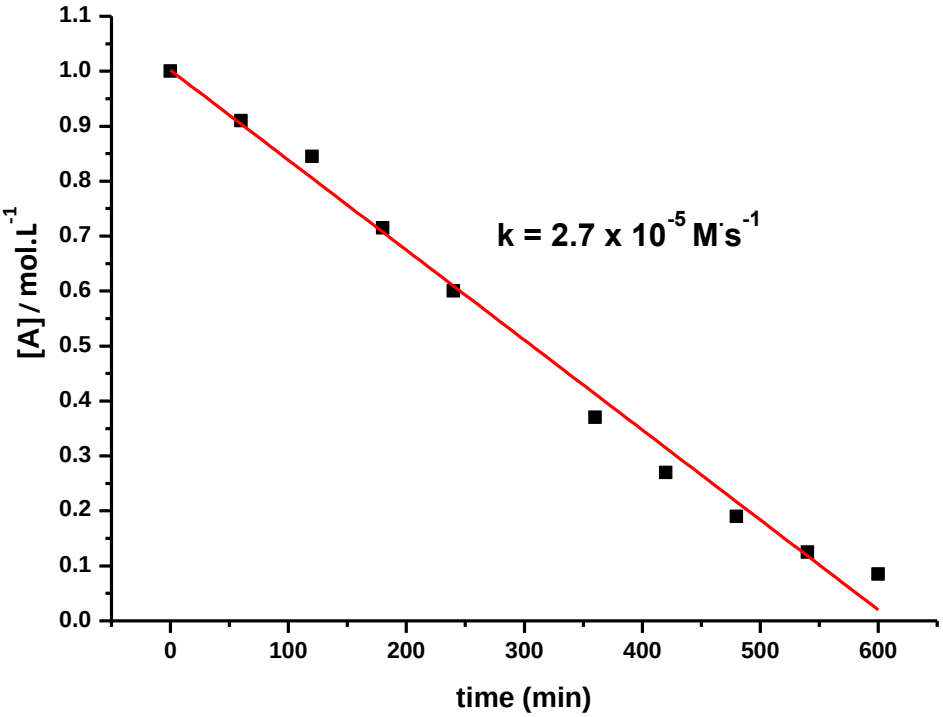

Figure 35. [**A**] vs time.

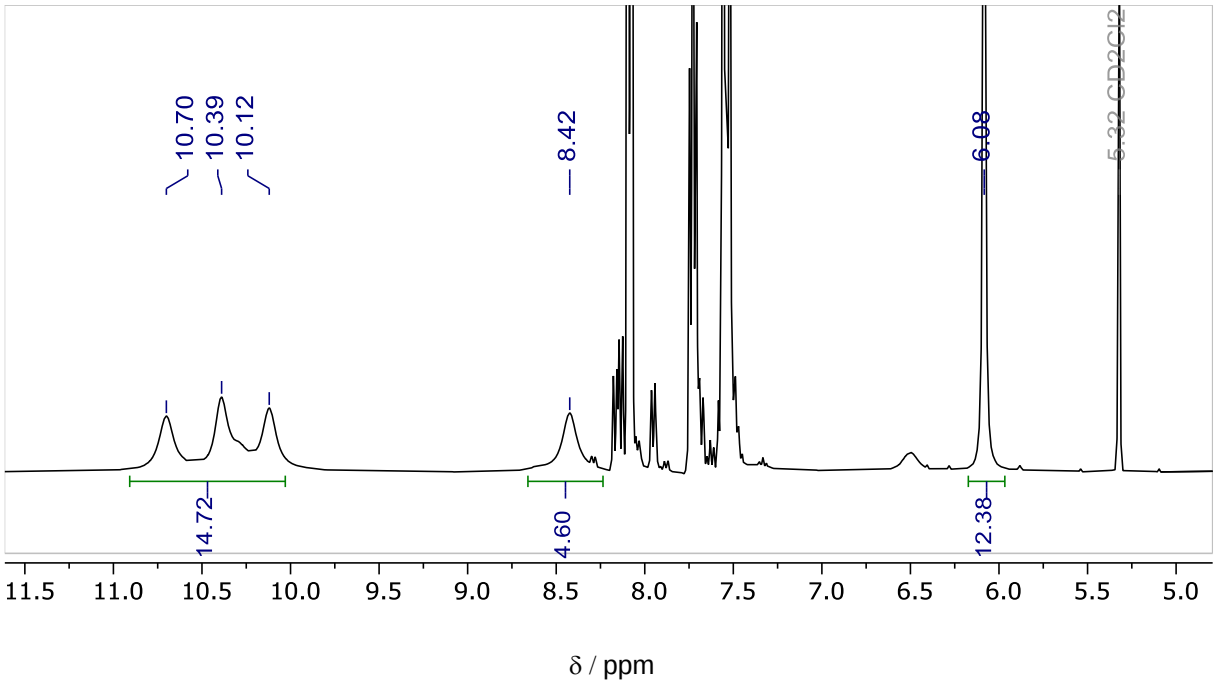

Figure 36. *Complex **11** with 15 eq of benzoyl bromide to **5**. 1,3,5-trimethoxybenzene (4.12 eq) is added and the complex **5** is quantified by ^1H NMR after 10h in CD_2Cl_2. Integration of the methyl groups of 19.32 (δ_H = 10.70 / 10.39 / 10.12/ 8.42, 26H) indicates 74 % spectroscopic yield in **5.***

On one hand, the degradation of the complex **11** is monitored by ^{1}H NMR and at the same time formation of the intermediates can be observed in it. After 10 h, the ^{1}H NMR indicates 74% formation of Imine complex **5** (**Figure 36**)**.** The signals of the complex **5** are confirmed by comparing with the characteristic signals of complex **5**, which was prepared by using TTBP phenoxy radical and it confirms they are identical. Moreover, the formation of benzamide and benzoic acid is also detected.

So, from all the above information, it has been obtained a zero order with respect to **A** in *scheme 21***.** It makes difficulties to explain the mechanism of hydrogen atom transfer takes place from ligand to metal in the process of metal-ligand cooperativity as it follows some unknown pathway. This phenomenon can be explained by hydrolysis. Benzoyl bromide is sensitive towards light, air, and moisture, because of which minor amount of it get hydrolysed to give benzoic acid and hydrogen bromide and these biproducts may act as catalyst and may take it to a different pathway to give zero order kinetics.

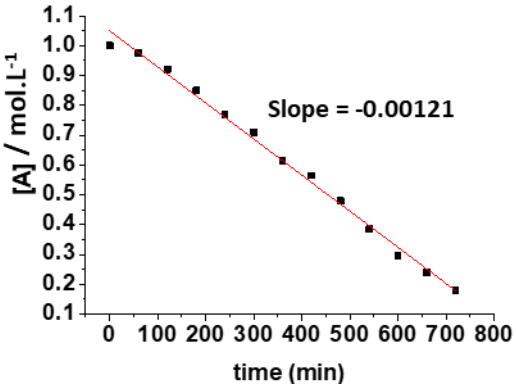

[B] (5 eq)

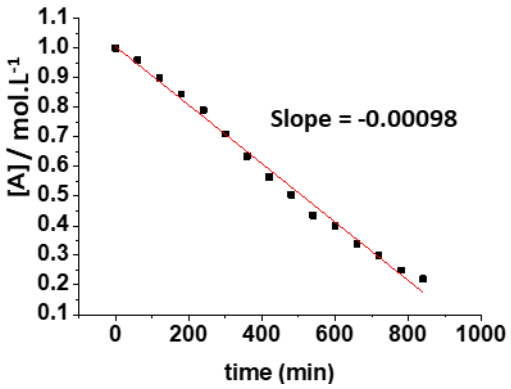

[B] (5 eq)

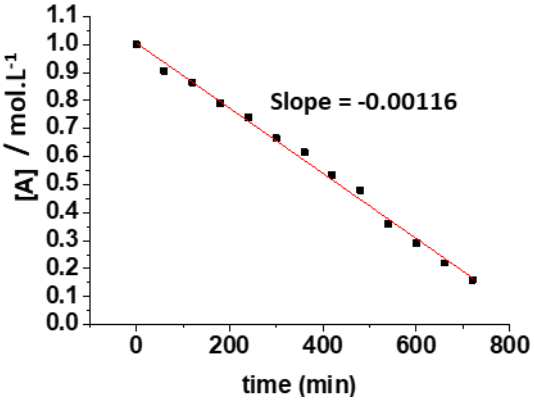

[B] (10 eq)

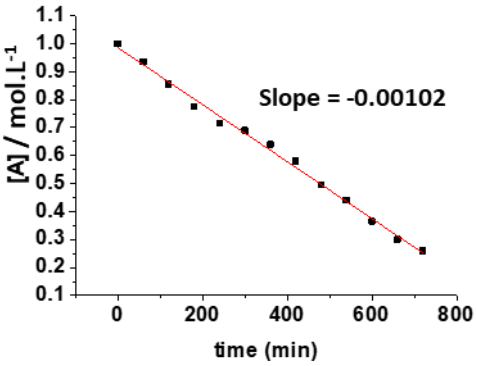

[B] (10 eq)

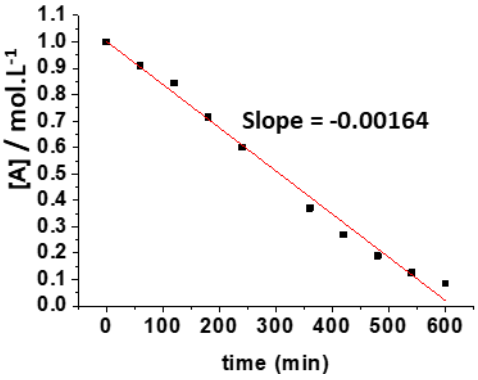

[B] (15 eq)

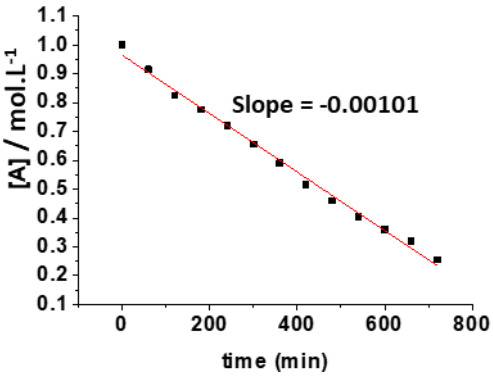

[B] (15 eq)

Fig 37. (a) *Kinetics with different concentrations of benzoyl bromide.*

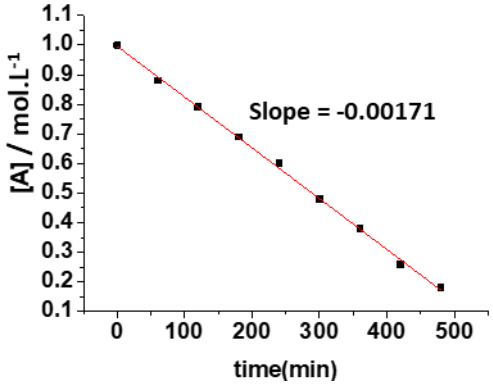

[B] (20 eq)

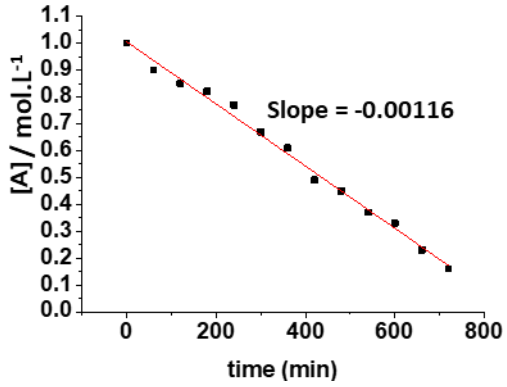

[B] (20 eq)

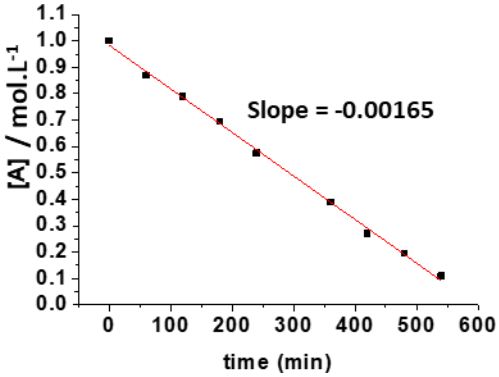

[B] (30 eq)

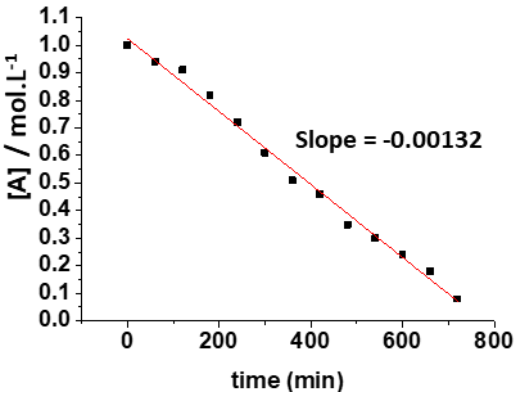

[B] (30 eq)

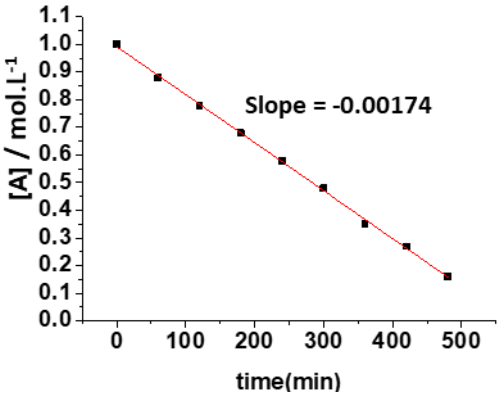

[B] (40 eq)

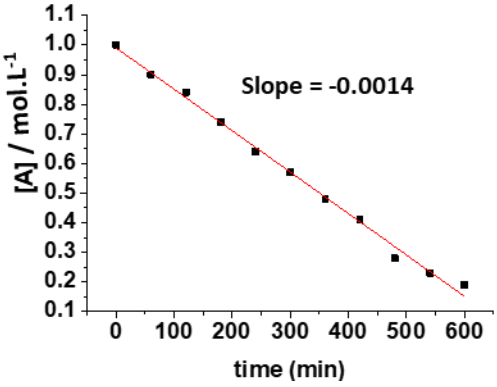

[B] (40 eq)

Fig 37. (b) *Kinetics with different concentrations of benzoyl bromide.*

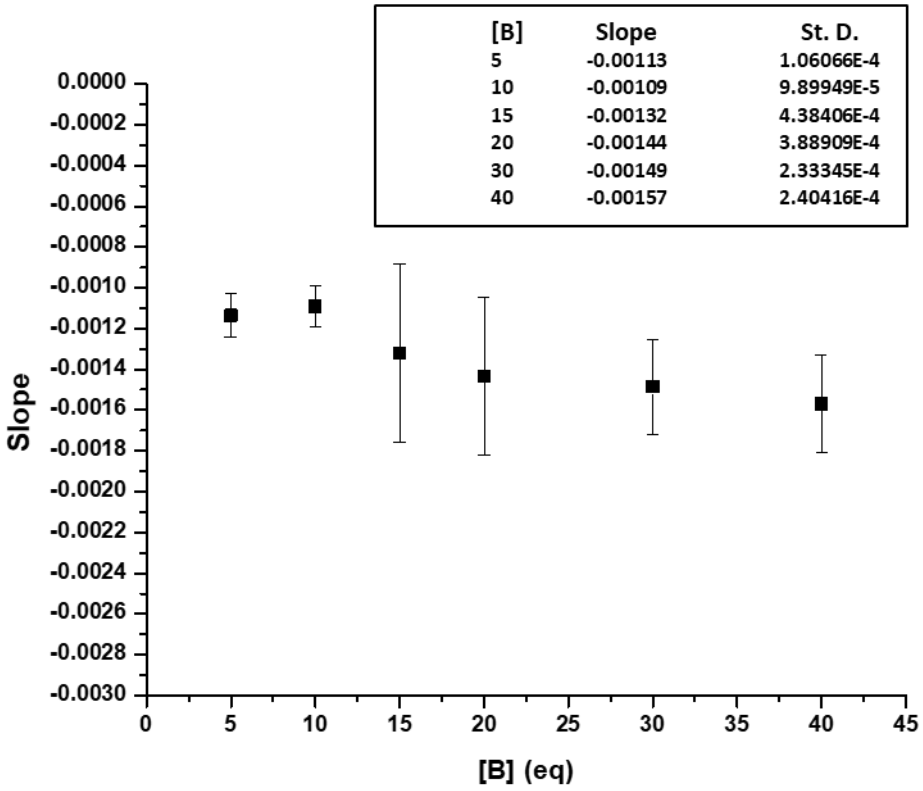

Figure 38. *Slope (-k) vs [B].*

Further, kinetic order with respect to **B** is investigated at different concentrations of **B** keeping other conditions constant. The concentration **B** is increased in the order of 5 eq, 10 eq, 15 eq, 20 eq, 30 eq and 40 eq with respect to a constant concentration **A** (3mg). Each kinetic experiment is performed twice to get the standard deviation (**Figure 37. a and 37. b**). All the experiments monitored up to at least three half-lives. Each reaction provided a different slope, but all the slopes found differed slightly from each other. Finally, different slopes found vs concentration of is plotted to find the order with respect to **B**, which seems to be constant slopes with different concentrations of **B**, which indicates it also has zero order with respect to **B** (**Figure 38**).

So, from the above information, we can conclude that the extra amount of benzoyl bromide does not involve in the metal-ligand cooperative formation of complex **5** and benzamide from complex **11**. Subsequently, benzamide formed is reacted with extra benzoyl bromide to provide benzonitrile, benzoic acid, and HBr.

6. Regeneration of starting complex from Imine complex 5

6.1 Ligand reduction of 5 with $LiHBEt_3$ and $[Ph_2NH_2]Br$ to obtain 3

The reaction of complex **5** with $LiHBEt_3$ (1.0 eq) and $[Ph_2NH_2]Br$ (1.0 eq) in THF was stirred overnight and trimethoxy benzene (1.0 eq) was added as the internal standard and products were quantified by ^1H NMR- spectroscopy was found in 51 % of complex **3** (methyl peak, 9.26 ppm, 6H) (**Figure 39**). Although no intermediates were able to isolate, the explanation may be the hydride and the proton from $LiHBEt_3$ and $[Ph_2NH_2]Br$ respectively reduce the imine backbone to amine to provide complex **3**.

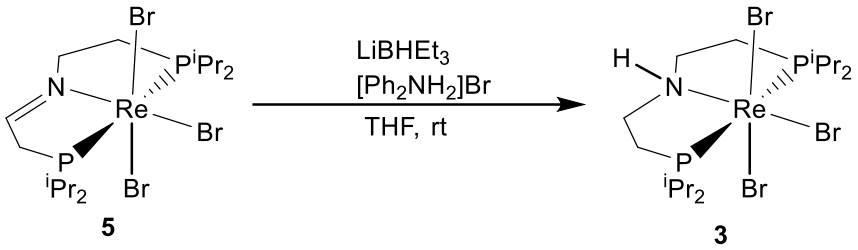

Scheme 22: *Regeneration of Re (III) complex **3** from complex **5**.*

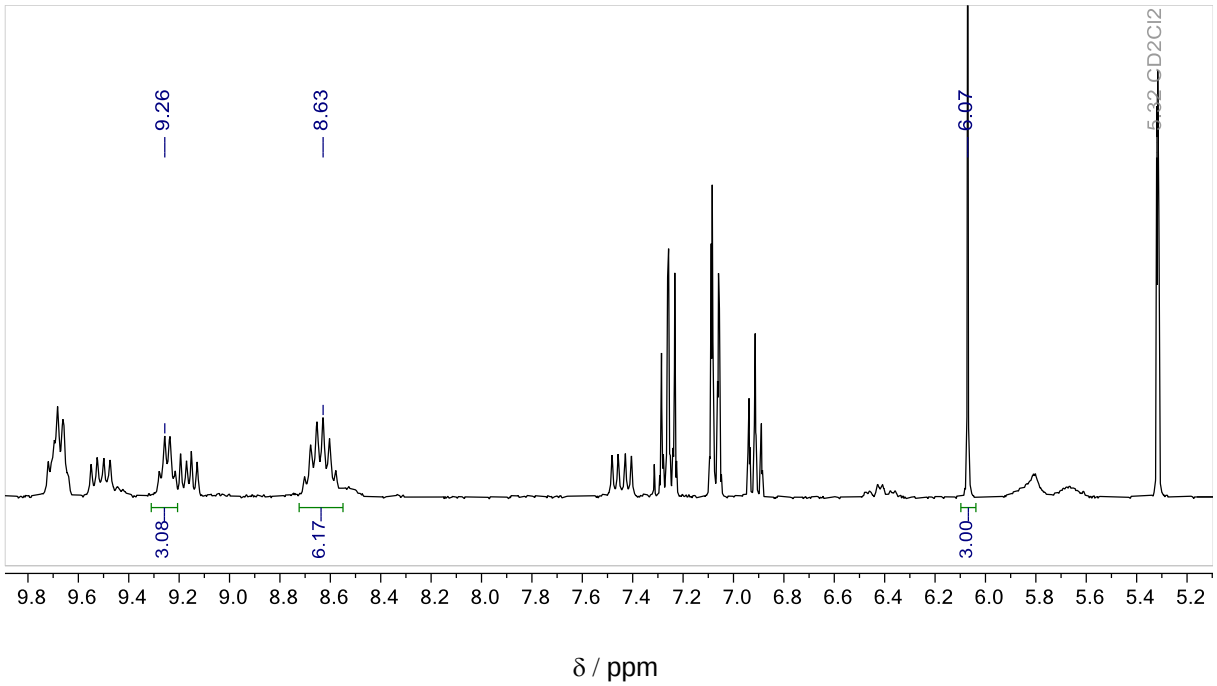

Figure 39. *^1H-NMR quantification of the reaction of **5** with 1eq of hydride ($LiHBEt_3$) and 1eq of a proton source ($[Ph_2NH_2]Br$) to **3**. 1,3,5-trimethoxybenzene (1 eq) was added and the product was quantified by ^1H NMR spectroscopy. Integration of the methyl groups of 9.25 (δ_H = 9.26 / 8.63, 18H) indicates 51 % spectroscopic yield in **3**.*

6.2 Titration of 5 with benzoic acid to 3

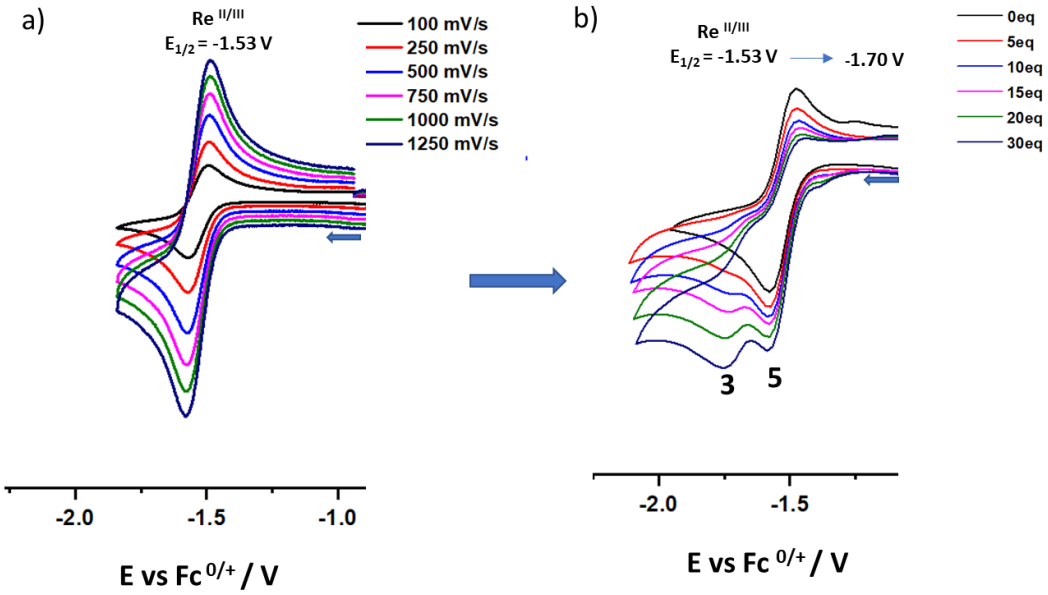

Figure 40. *(a)CV of complex **5** and (b) after titrated with 0-30 eq of benzoic acid (1 mM in THF with 0.1 M [nBu$_4$N] [PF$_6$], v = 100 mVs-1).*

The generation of complex **3** from complex **5** was also observed in electrochemical response in CV titration measurement. When complex **5** was titrated with 0-20 eq of benzoic acid in CV, it provided a new reductive wave at -1.72 V vs. Fc/Fc$^+$ and found a cathodic shift from -1.70 V to -1.72 V, which is the indicative reductive peak of the complex **3** (**Figure 40**).

7. 4-membered synthetic cycle for metal-ligand cooperative synthesis for the benzamide and benzonitrile

A 4- member synthetic cycle can be drawn from the above information for the metal-ligand cooperative synthesis of organic compounds (**Scheme 23**). The terminal nitride complex **7,** 93% can be achieved when TMS-N$_3$ is treated with complex **3** or complex **3** can be achieved by electrochemical N2 splitting. Complex **7** reacted with 2eq of benzoyl bromide in 1,4-dioxane at an elevated temperature of 80 °C providing benzamide and benzonitrile by metal-ligand cooperativity. Most importantly, the 2 electrons and 2 protons provided by the backbone to the organic compounds and hence, provided 52 % of imine complex **5** in this process. In search of intermediates, complex **11** is synthesized with complex **7** and benzoyl bromide. The intermediate is isolated and characterized. It has been explained that the complex exists as an equilibrium in a solvent like THF and 1,4-dioxane but there does not exist an equilibrium in DCM and stable enough in this solvent. Complex **11** is not stable at an elevated temperature and gets back to complex **7** but in presence of another 1eq of benzoyl bromide complex **11** undergoes a metal-ligand cooperative reaction and provides benzamide, benzonitrile and imine complex **5**. It provides the same result as the metal-ligand cooperative reaction with complex **7**, so it is demonstrated as the key intermediate in the metal-ligand cooperative

reaction. The imine complex **5** was treated with 1eq of super hydride and 1 eq of acid to regenerate starting complex **3**. Also, electrochemical reaeration of complex **5** from **3** is explained in presence of benzoic acid. Hence, a 4-membered synthetic cycle for benzamide and benzonitrile by metal-ligand cooperativity is demonstrated.

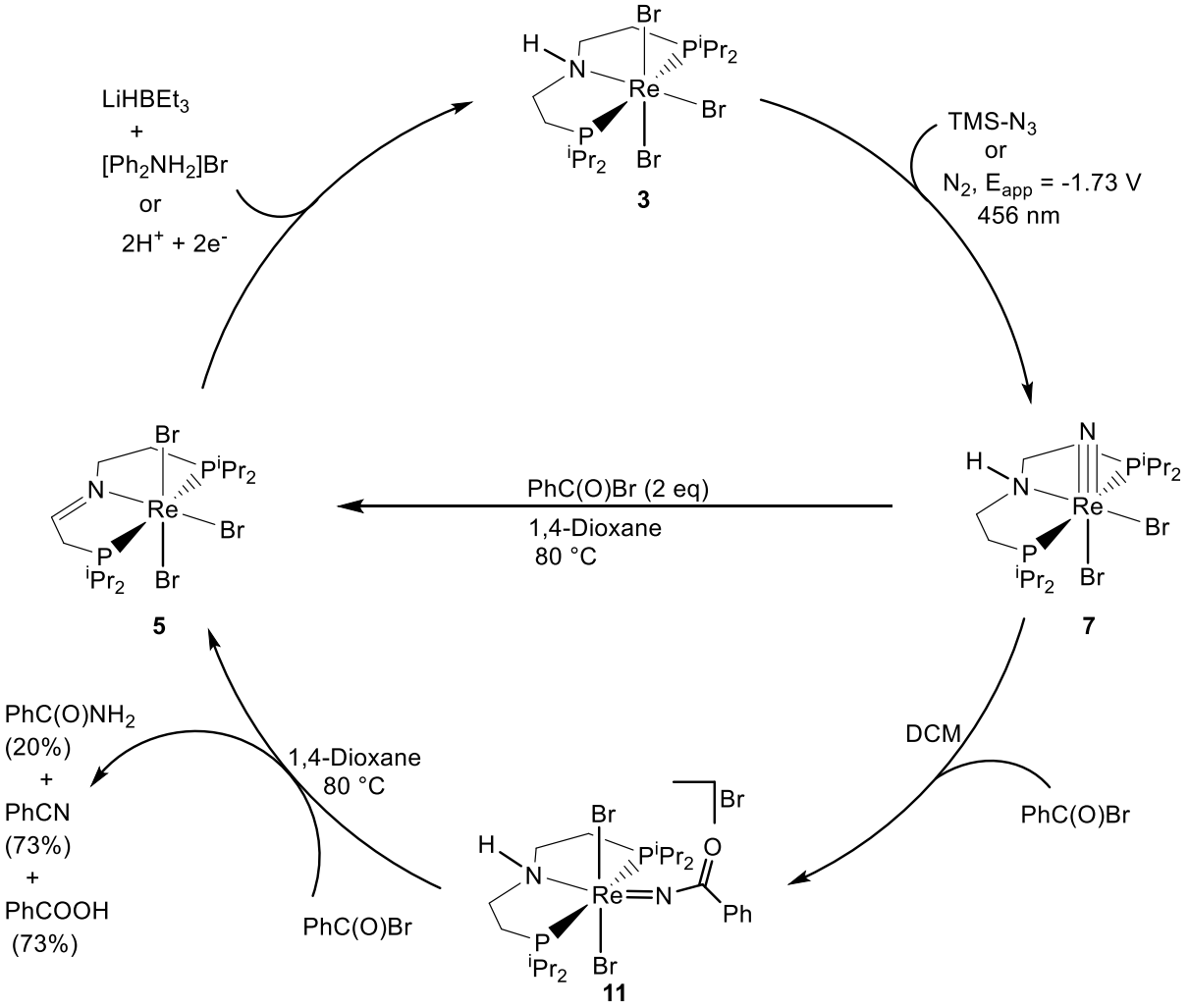

Scheme 23: *4-membered synthetic cycle for metal-ligand synthesis for the benzamide/ benzonitrile*

8. Synthesis of substituted benzoyl bromides

Different para-substituted benzoyl bromide was synthesised to modify the electrophilicity of carbonyl carbon of the benzoyl bromide to get more selective products. For that, some of the selective electron-withdrawing and electron-donating groups such as p-CF_3, p-Br, P-Me and p-OMe are selected. The main idea to increase or decrease the electrophilicity of benzoyl bromide is that it may help to synthesize benzamide or benzonitrile selectively.

8.1 Using DBI: Synthesis of p-$CF_3(C_6H_4)C(O)Br$

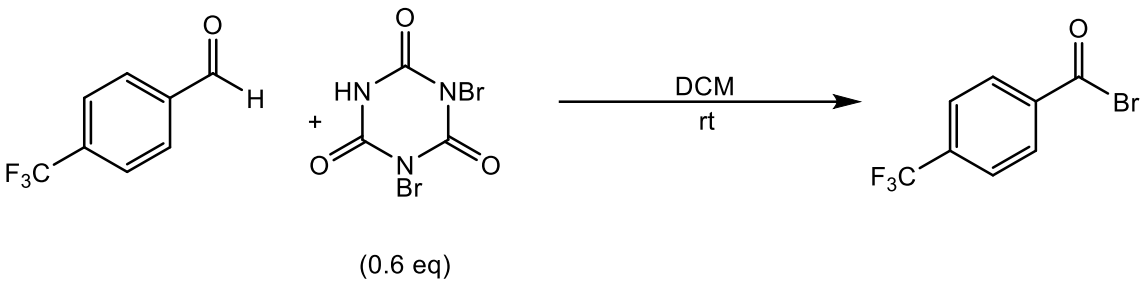

Scheme 24: *Synthesis of 4-trifluoromethyl benzoyl bromide.*

In 2018, *Kang* and co-workers reported the convenient mortal-free direct oxidative amidation of aldehyde using dibromoisocyanuric acid (DBI) under mild conditions. [83] Here, they demonstrated the in-situ formation of benzoyl bromide by TLC, however, they could not isolate any benzoyl bromide.

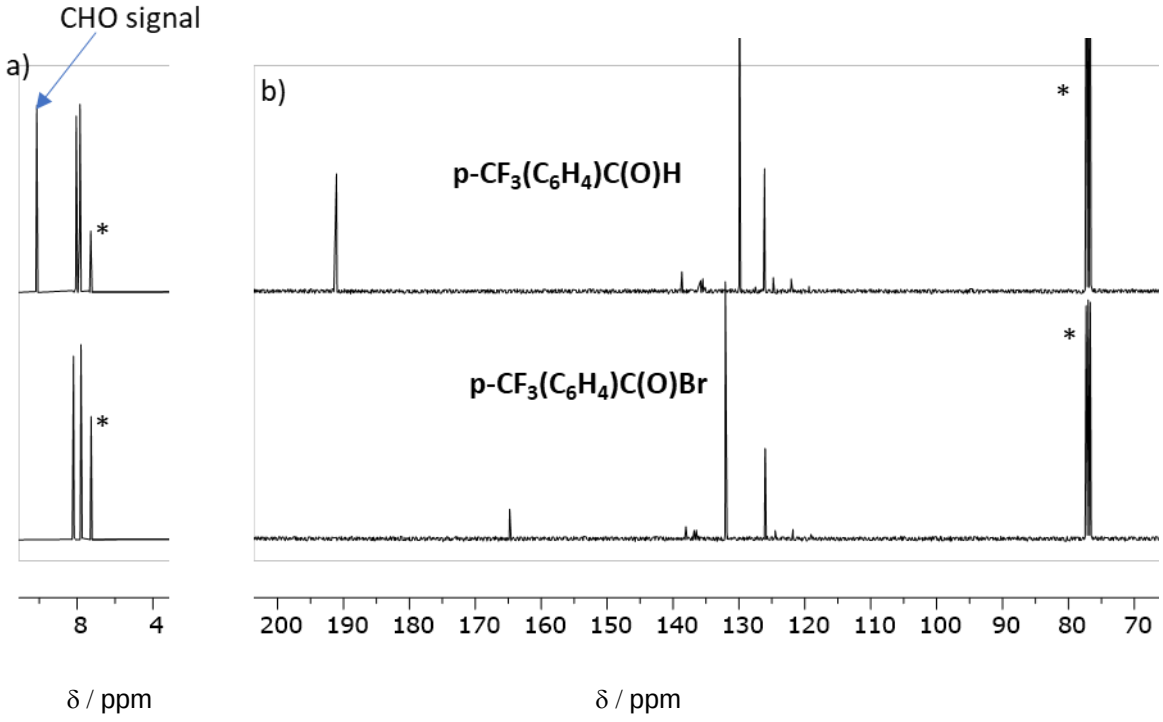

Figure 41. *Comparison* ***a)*** *^{1}H NMR &* ***b)*** *$^{13}C\{^{1}H\}$ NMR of isolated 4-triflouromethylbenzaldehyde & 4-triflouromethylbenzoylbromide. The solvent signal is marked with an asterisk.*

4-triflouromethylbenzaldehide is treated with 0.6 eq of dibromoisocyanuric acid in dry DCM and stirred for 24 h. Evaporating the solvent and after a vacuum distillation at 60 °C/ 0.1 mbar provided 4-trifluoro methylbenzoyl bromide 70% in yield. The isolated p-$CF_3(C_6H_4)(CO)Br$ was compared with starting material by NMR. ^1H NMR shows an absence of CHO peak and the up field shifted peak of carbonyl carbon at δ_C = -164.88 ppm in $^{13}C\{^1H\}$ NMR indicates the formation of benzoyl bromide (**Figure 41**). ^1H NMR provided two doublets at δ_H = 8.21 ppm and 7.80 ppm indicating ortho and meta protons respectively (**Figure 42**). $^{13}C\{^1H\}$ NMR δ_C = -164.88 ppm is corresponding to the carbonyl carbon. Besides that, peaks at δ_C = 138.02 ppm and 136.51 ppm denote the quaternary carbon. The remaining peaks at δ_C = 132.07 ppm and 126.08 ppm are the meta and ortho carbon peaks. Two quadrate peaks are because of fluorine coupling and the CF_3carbon at δ_C = 121.93 ppm. ^{19}F NMR indicates a single signal at δ_F = -63.43 ppm, which is a characteristic peak for p- (C_6H_4) (CO)Br.

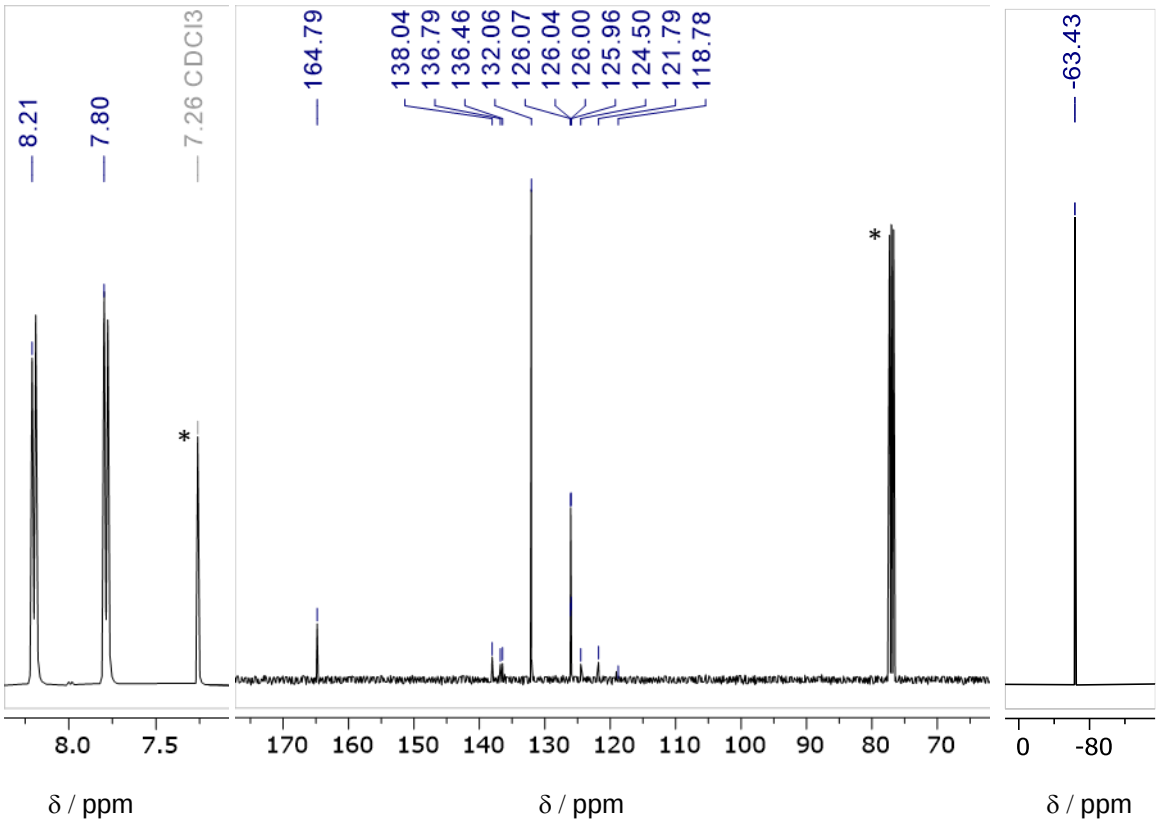

***Figure 42**. **a)** (left) ^1H -NMR spectrum of p-$CF_3(C_6H_4)C(O)Br$ in $CDCl_3$. **b)** (middle) $^{13}C\{^1H\}$ NMR spectrum. **c)** (right) ^{29}F NMR spectrum. The solvent signal is marked with an asterisk.*

8.2 Synthesis of substituted benzoyl bromides with $(COBr)_2$

Although the synthesis of benzoyl bromide using a DBI is one of the most attractive pathways, the yield reduces as the benzoyl bromides get hydrolysed in this method. So, an alternative pathway for the synthesis of benzoyl bromide is followed. In 1920, *Ulich* and *Adams* published "the use of oxalyl chloride and bromide for producing acid chlorides, acid bromides or acid anhydrides. iii." [84] where they explained the formation of substituted benzoyl bromides using oxalyl bromide and sodium benzoate. It is found to be one of the most efficient methods to prepare the substituted benzoyl bromide. Here they characterised the compounds with a very primitive analytical method. As no NMR data is available there, the compounds are characterised by NMR to check the purity and confirmation of the formation of substituted benzoyl bromides.

8.2.1 p-$CH_3(C_6H_4)C(O)Br$:

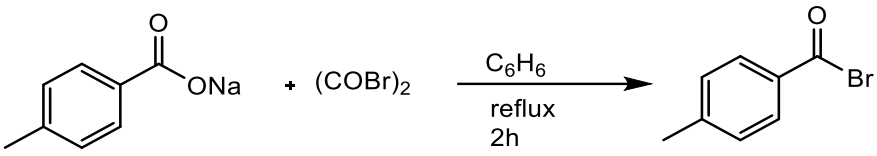

Scheme 25: *Synthesis of 4-methylbenzoyl bromide.*

Slow addition of p-$CH_3(C_6H_4)COONa$ to the solution of oxalyl bromide (1.5eq) and where CO_2 gas emission can be observed. Then the reaction mixture was stirred in reflux for 2h, which provided p-$CH_3(C_6H_4)COBr$ 80% in yield after a vacuum distillation at 90 °C/ 26 mbar.
^1H NMR provided two doublets at aromatic regions that correspond to the ortho and meta protons and a prominent peak at δ_H = 1.78 ppm assigned to signal for the substituted methyl group (**Figure 43**). $^{13}C\{^1H\}$ NMR provided six prominent peaks. The signals from δ_C = 164.86 – 129.28 ppm are the 5 aromatic signals and the peak at δ_C = 20.91 ppm corresponds to the methyl group.

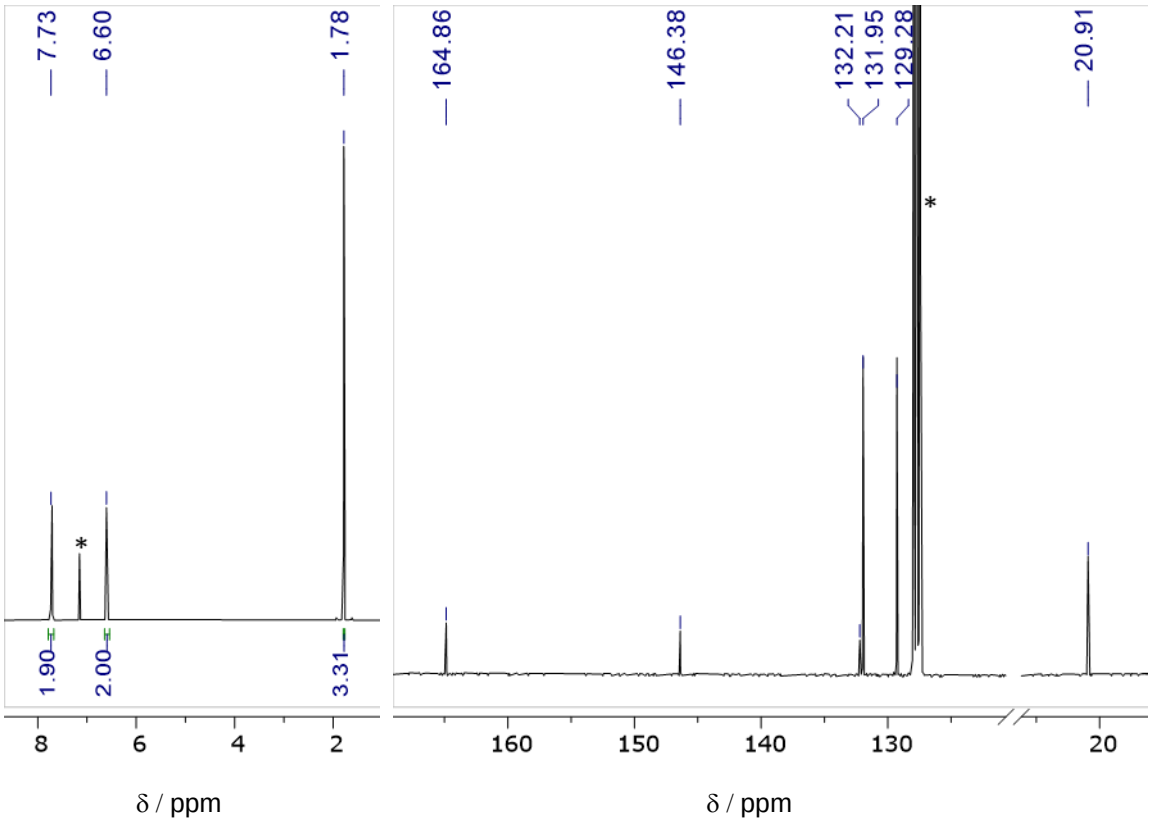

***Figure 43**. **a)** (left) ^{1}H -NMR spectrum of p-$CH_3(C_6H_4)C(O)Br$ in C_6D_6. **B)** (right) $^{13}C\{^{1}H\}$ NMR spectrum. The solvent signal is marked with an asterisk.*

8.2.2 p-$OCH_3(C_6H_4)C(O)Br$:

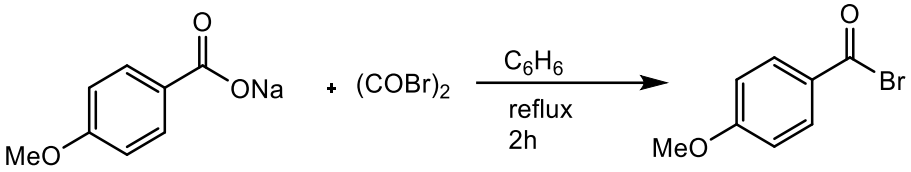

***Scheme 26:** Synthesis of 4-methoxylbenzoyl bromide.*

Using the same procedure with oxalyl bromide p-OMe substituted benzoyl bromide is synthesized, which obtained 4-methoxy benzoyl bromide 92% in yield upon a vacuum distillation at 70 °C/ 0.001 mbar. ^{1}H NMR of p-$OCH_3(C_6H_4)COBr$ provided a prominent signal at δ_H = 3.01 ppm signal for the methoxy group. Besides that, the other two doublets in the aromatic range are aromatic protons (**Figure 44**). $^{13}C\{^{1}H\}$ NMR provides 6 sets of signals. A prominent peak display at δ_C = 54.69 ppm corresponds to the carbon signal for the methoxy group. From δ_C = 113.88-163.72 ppm are the aromatic peaks and the remaining peak at δ_C = 165.26 ppm is the carbonyl carbon signal.

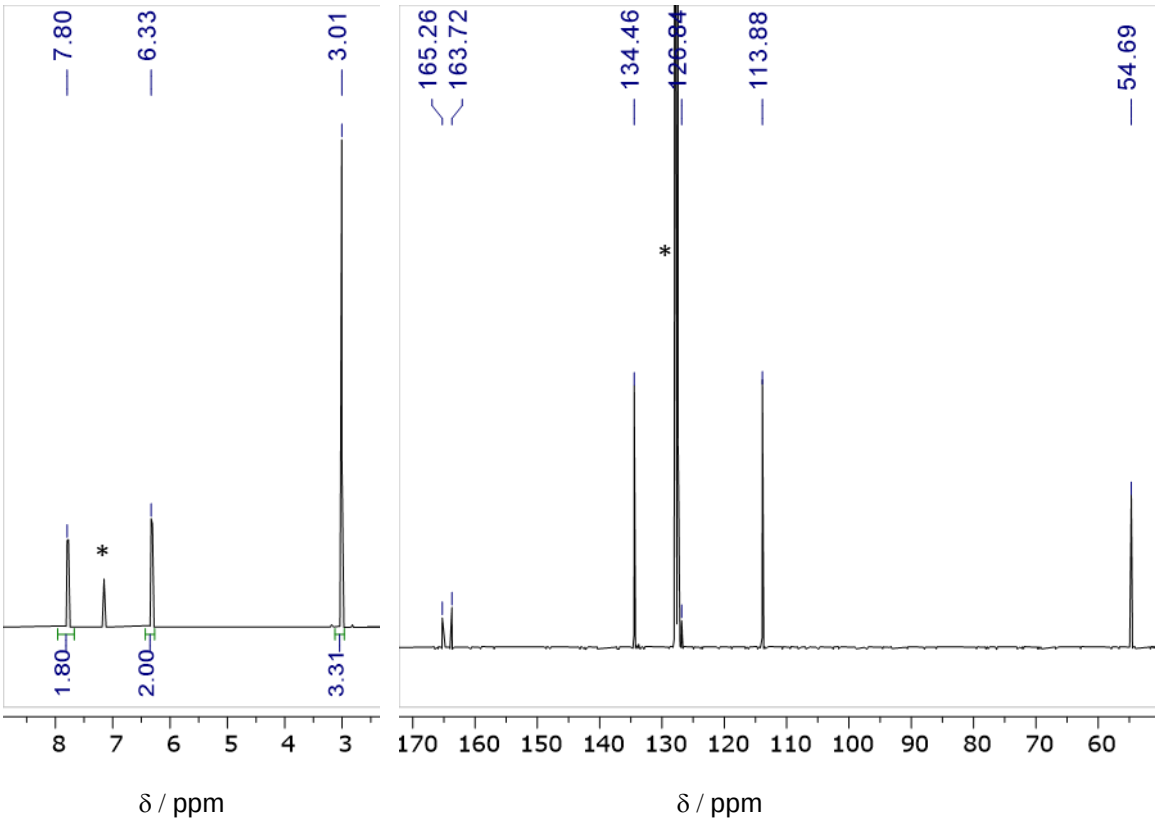

***Figure 44**. **a)** (left) ^{1}H -NMR spectrum of p-$OCH_3(C_6H_4)C(O)Br$ in C_6D_6. **b)** (right) $^{13}C\{^{1}H\}$ NMR spectrum. The solvent signal is marked with an asterisk.*

8.2.3 p-Br(C_6H_4)C(O)Br:

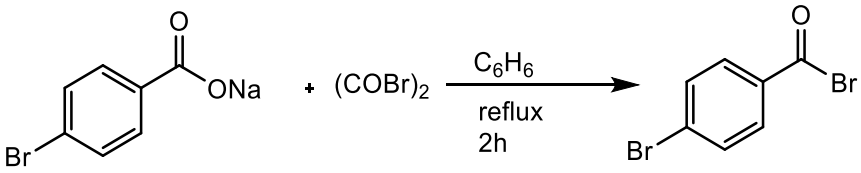

***Scheme 27:** Synthesis of 4-bromobenzoyl bromide.*

Another electron-withdrawing group substituted benzoyl bromide i.e. 4-bromobenzoyl bromide is synthesised using the same procedure which provided a yield of 90 % after a vacuum distillation at 0.021 mbar at 100 °C. ^{1}H NMR provided two doublets of the aromatic signals δ_H = 7.30 and 6.87 ppm (**Figure 45**). $^{13}C\{^{1}H\}$ NMR provides 4 signals at δ_C = 133.81-131.12 ppm indicating the 4 sets of aromatic carbon. A downfield shifted peak at δ_C = 164.53 ppm is the carbonyl carbon.

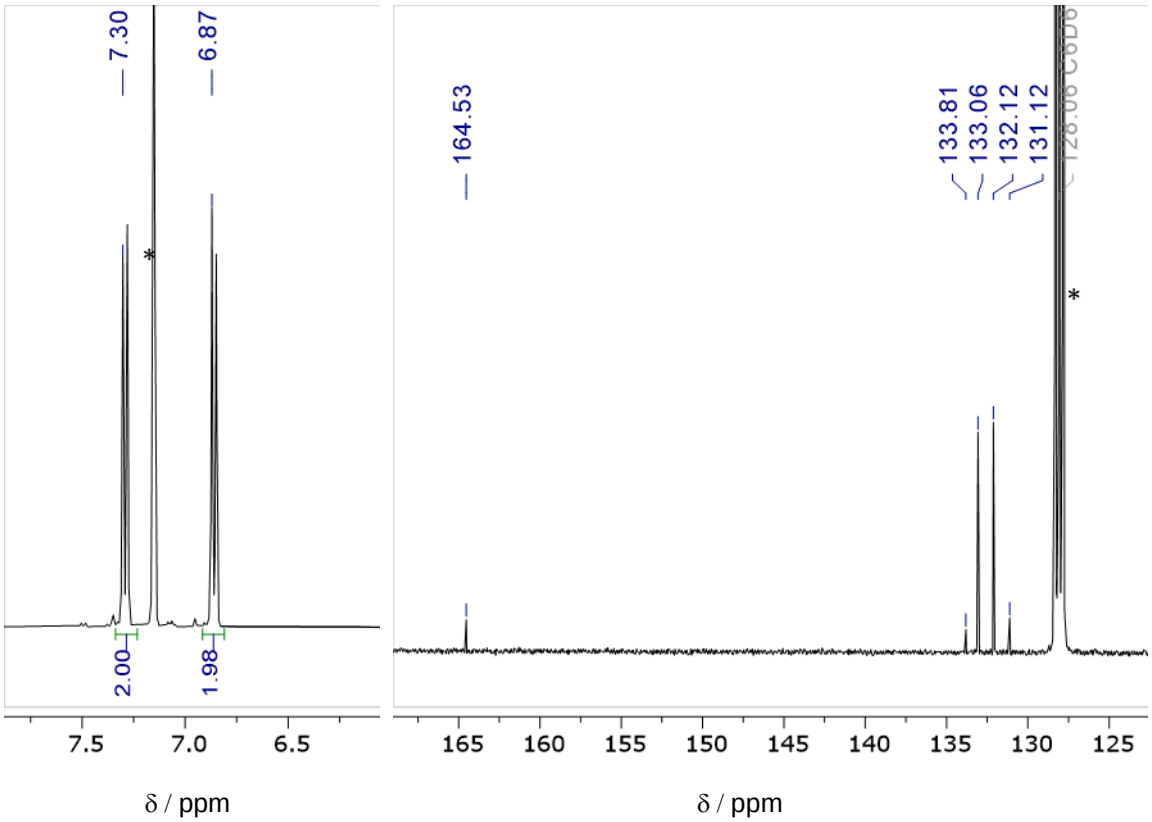

***Figure 45**. **a)** (left) ^{1}H -NMR spectrum of p-Br(C_6H_4)C(O)Br in C_6D_6. **b)** (right) $^{13}C\{^{1}H\}$ NMR spectrum. The solvent signal is marked with an asterisk.*

9. Synthesis of substituted benzoylimido adduct complexes

9.1 [Re(p-$CF_3C_4H_4C(O)N)Br_2(HPNP^{iPr})$]Br (12)

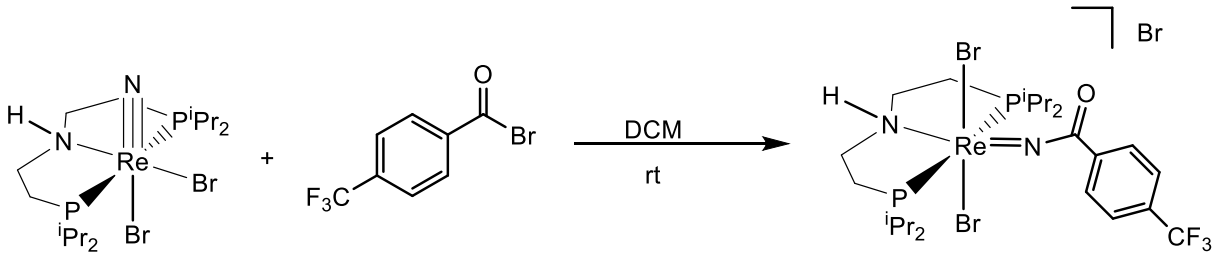

***Scheme 28:** Synthesis of complex **12**.*

Complex **12** can be synthesised in the same procedure as the synthesis of complex **11**. When complex **7** was treated with p-$CF_3(C_6H_4)(CO)Br$ in DCM and stirred at room temperature provided complex **12**, 88% in yield (**Scheme 28**). ^{1}H NMR provided all the signals at the diamagnetic range from δ_H = 8.15- 1.24 ppm. A distinguished peak at δ_H = 5.68 ppm indicates the NH peak. The most characteristic signals at δ_H = 8.15 and 7.82 ppm are the signals of the aromatic protons (**Figure 46**). The set of larger signals from δ_H = 1.24 - 1.55 ppm is the methyl signal of the isopropyl group and the remaining signals are the CH signals and the backbone signals. $^{31}P\{^{1}H\}$ NMR provides a single peak at δ_P = 33.29 ppm and $^{19}F\{^{1}H\}$ NMR provides a prominent characteristic signal at δ_F = -63. 83 ppm. Further, the electrochemical response was

recorded by a CV which provided a very similar oxidative wave at $E_{1/2}$ = -0.44 V vs. Fc/Fc^+ (**Figure 48**).

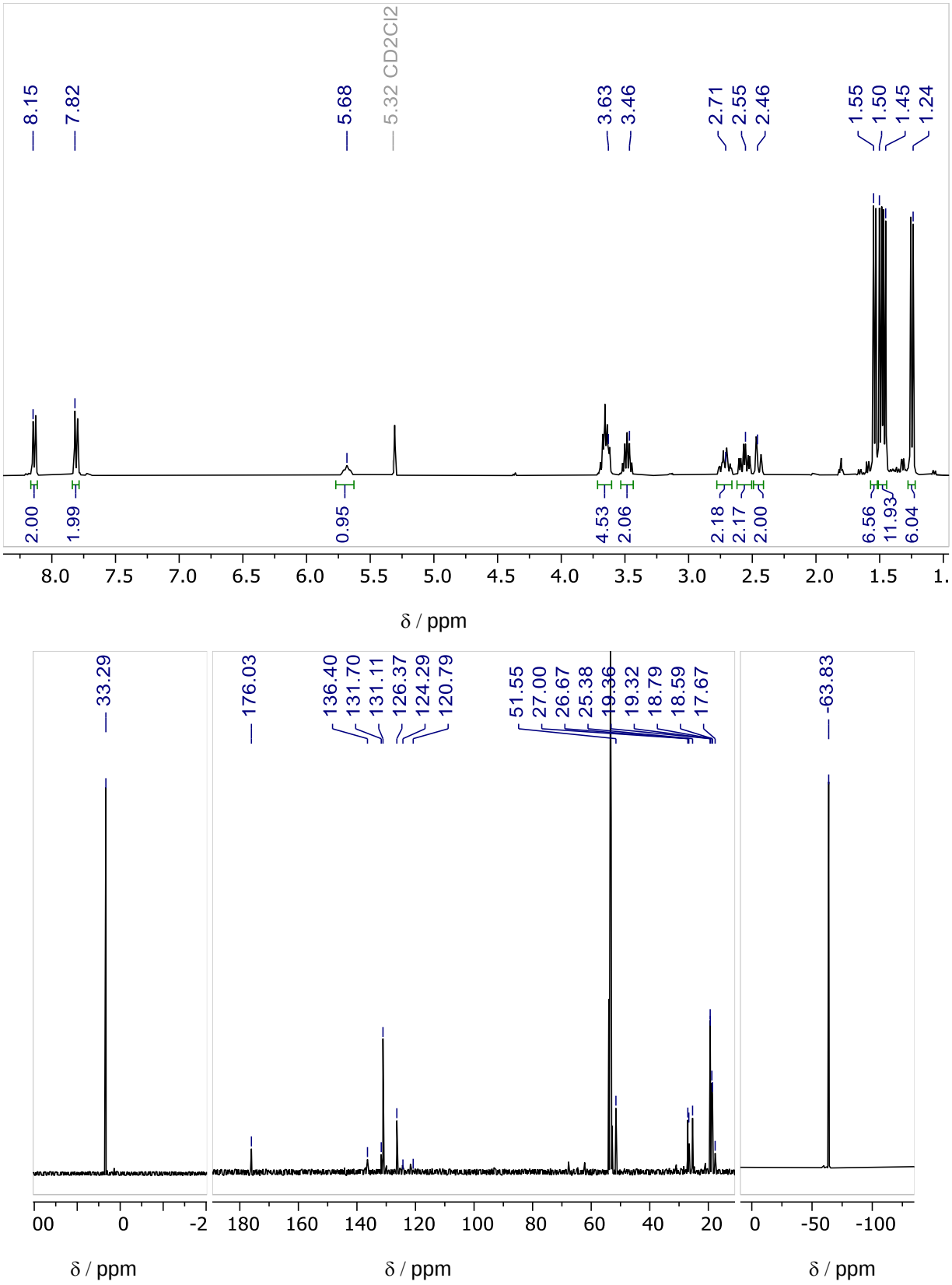

***Figure 46**. **a**) ^{1}H -NMR spectrum of **12** in CD_2Cl_2 (top). **b**) (bottom left) $^{31}P\{^{1}H\}$ NMR spectrum. **c**) (bottom middle) $^{13}C\{^{1}H\}$ NMR spectrum. **d**) (bottom right) ^{19}F NMR spectrum.*

The ATR-IR spectrum of complex **12** provides a prominent peak at $\upsilon_{C\text{-}O}$ = 1680 cm^{-1} indicating the C-O stretching of the carbonyl carbon (**Figure 47**).

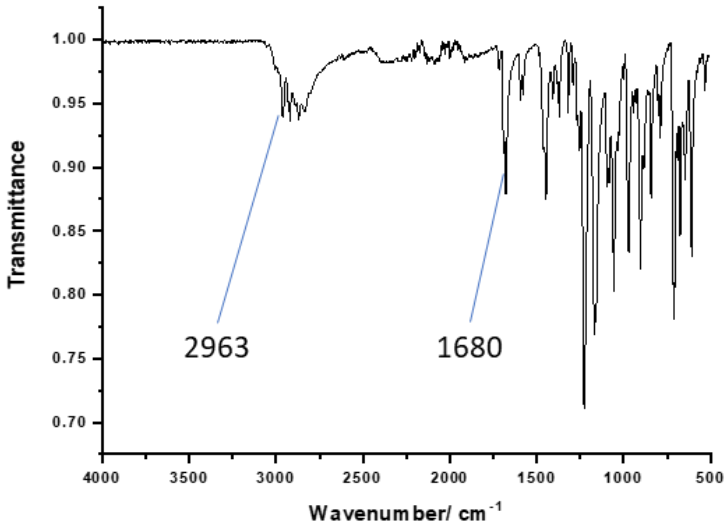

Figure 47. *IR spectrum of complex* ***12.***

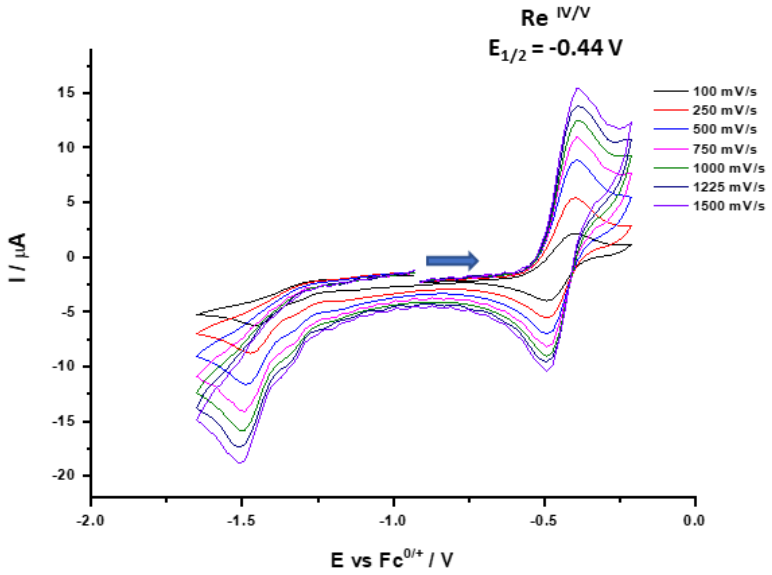

Figure 48. *CV of* ***12*** *(1 mM in DCM with 0.1 M [nBu$_4$N][PF$_6$]) at different scan rates.*

9.2 [Re(p-MeC$_4$H$_4$C(O)N)Br$_2$(HPNP^{iPr})]Br (13)

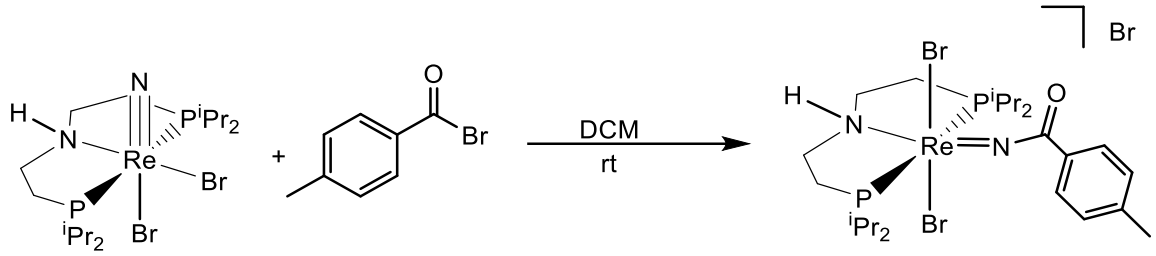

Scheme 29: *Synthesis of complex **13**.*

Complex **13** can be synthesised by using a similar procedure as the synthesis of complexes **11** and **12**, which provided complex **13**, with 87% in yield. $^{31}P\{^1H\}$ NMR delivers a single signal at δ_P = 33.45 ppm and the ^1H NMR provides all the signals in the diamagnetic range (**Figure 50**), which is very similar to the NMR of complex **11** and complex **12**. The most characteristic peak found at δ_H = 2.50 ppm corresponds to the substituted methyl group. The CV measurement provides a very similar pattern of results as complex **11** and **12** which provided an oxidative wave at $E_{1/2}$ = -0.56 V vs. Fc/Fc$^+$ (**Figure 49**).

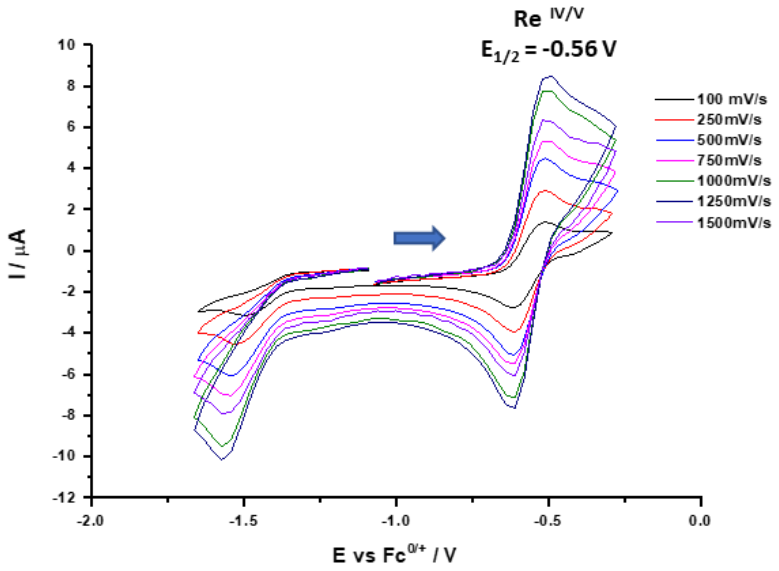

Figure 49. *CV of **13** (1 mM in DCM with 0.1 M [nBu$_4$N][PF$_6$]) at different scan rates.*

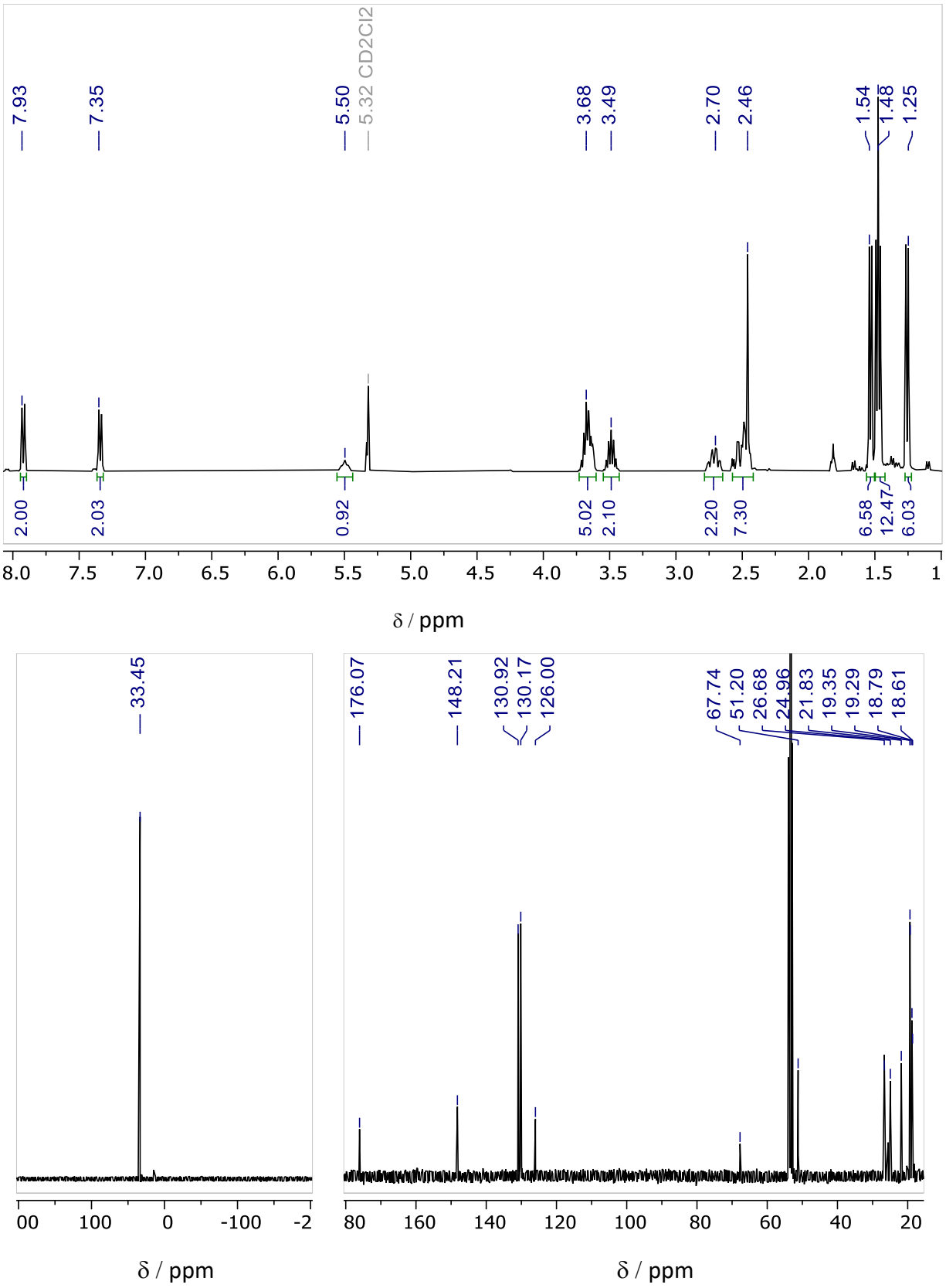

***Figure 50**. **a)** (top) ^{1}H -NMR spectrum of **13** in CD_2Cl_2. **b)** (bottom left) $^{31}P\{^{1}H\}$ NMR spectrum. **c)** (bottom right) $^{13}C\{^{1}H\}$ NMR spectrum.*

9.3 [Re(p-OMeC$_4$H$_4$C(O)N)Br$_2$(HPNP^{iPr})]Br (14)

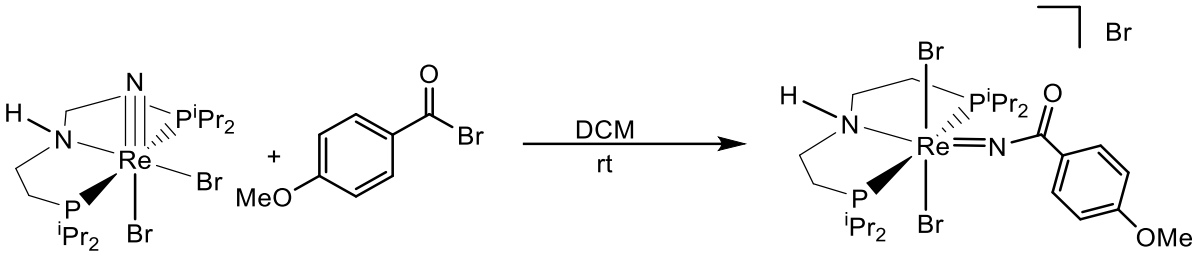

Scheme 30: *Synthesis of complex **14**.*

4-methoxybenzyl bromide was synthesized and employed in the reaction with complex **7** using a similar procedure as complex **11** syntheses, to get complex **14**, 85% in yield. The most important characteristic signal of this complex in ^{1}H NMR is at δ_H = 3.94 ppm which corresponds to the OC*H*$_3$ signal and a doublet at δ_H = 8.04 ppm indicates the ortho aromatic signals and a peak at δ_H = 7.05 ppm indicates the meta aromatic protons (**Figure 51**). ^{31}P{^{1}H} NMR provides the most characteristic single at δ_P = 33.63 ppm. ^{13}C{^{1}H} NMR provides a set of 14 signals. The 6 signals from δ_C = 175.11 to 67.74 ppm belong to the 4-methoxy benzoylimido ligands. And 4 prominent signals from δ_C = 19.37 ppm to 18.62 ppm indicate the CH$_3$ of isopropyl signals and the remaining are the backbone signals.

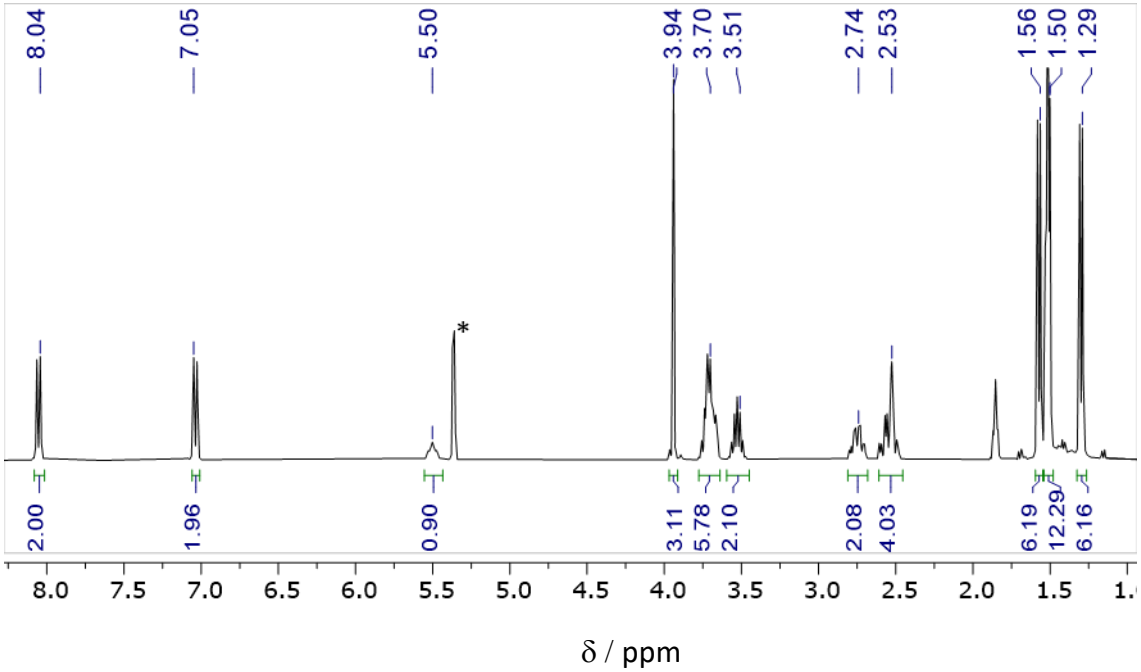

Figure 51. a) *^{1}H -NMR spectrum of **14** in CD$_2$Cl$_2$. The solvent signal is marked with an asterisk.*

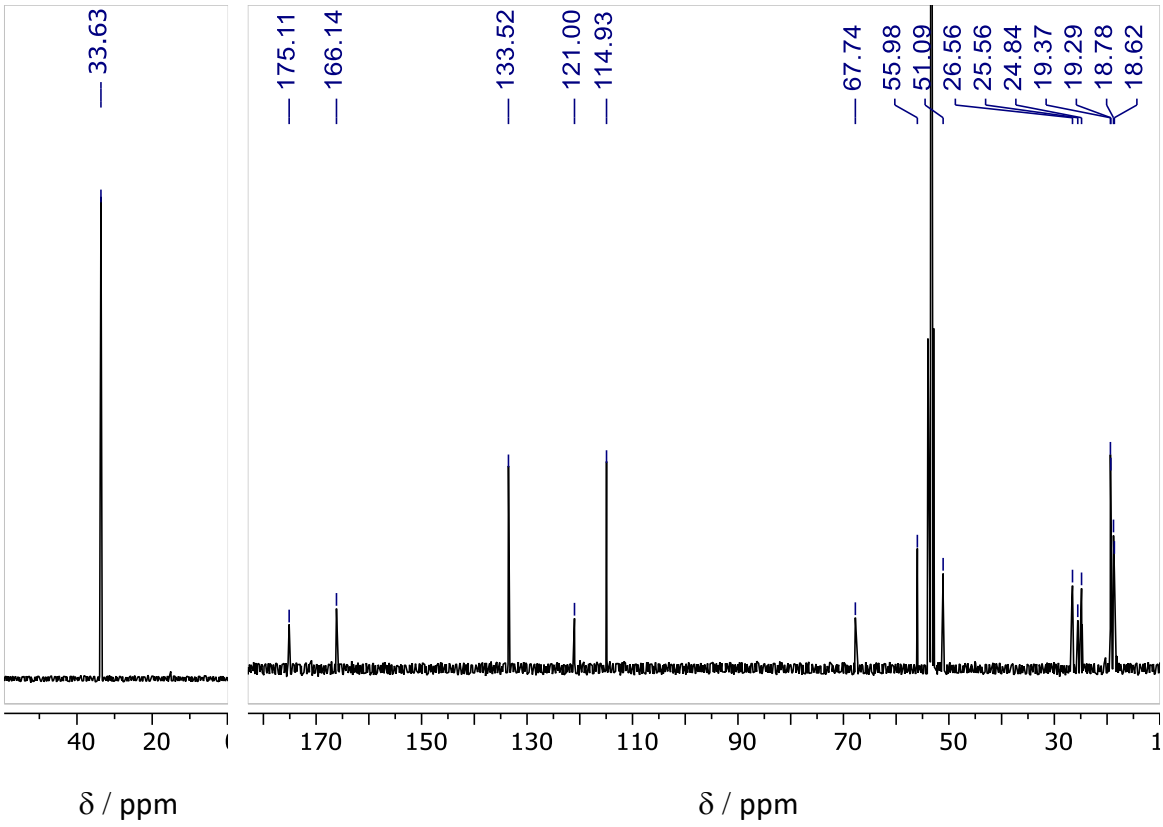

***Figure 51**. **b**) (left) $^{31}P\{^{1}H\}$ NMR spectrum of **14** in CD_2Cl_2. **c**) (right) $^{13}C\{^{1}H\}$ NMR spectrum.*

9.4 [Re(p-BrC$_4$H$_4$C(O)N)Br$_2$(HPNP^{iPr})]Br (16)

Complex **16** can be synthesised using a similar procedure as the synthesis of other benzoyl adduct complexes, which obtained complex **16**, 82% in yield after sole isolation. $^{31}P\{^{1}H\}$ NMR provides a sharp and single signal at δ_P = 33.56 ppm, which indicates a cs symmetry in the NMR time scale. The most characteristic peaks in $^{31}P\{^{1}H\}$ NMR are at δ_H = 7.90 ppm and 7.72 ppm which are the ortho meta signal of the aromatic ligand (**Figure 52**). The set of 5 signals from δ_C = 176.03 ppm to 67.74 ppm in $^{13}C\{^{1}H\}$ NMR is the aromatic carbon signals and the remaining are the PNP^{ipr} signals.

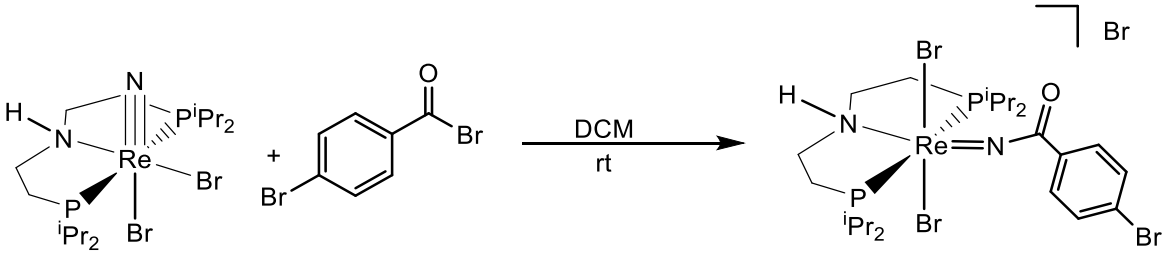

***Scheme 31:** Synthesis of complex **16**.*

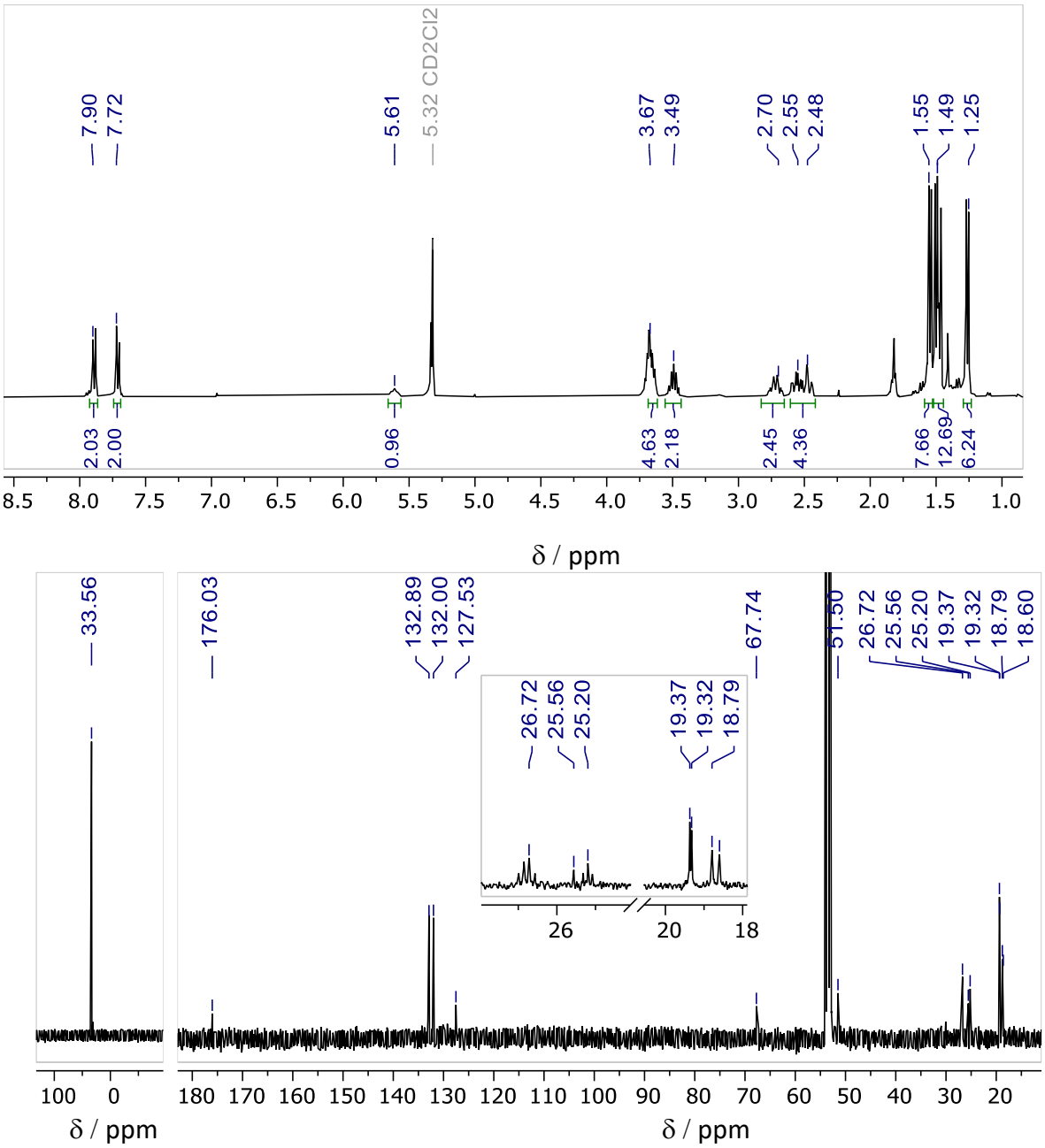

***Figure 52**. **a)** (top) ^{1}H -NMR spectrum of **14** in CD_2Cl_2. **b)** (bottom left) $^{31}P\{^{1}H\}$ NMR spectrum. **c)** (bottom right) $^{13}C\{^{1}H\}$ NMR spectrum.*

10. Hammett plots

9.1 Hammett plot in DCM

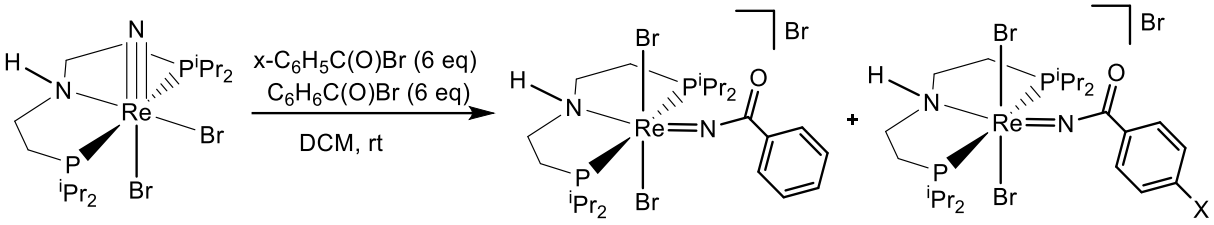

k_x/k_H= B/A X = OMe, Me, Br, CF_3 **A** **B**

Scheme 32: *Reaction of complex **7** with substituted and non-substituted benzoyl bromide in DCM.*

After successful synthesis of different para-substituted benzo bromides and the respective substituted benzoylimido rhenium complexes, here a Hammett plot was plotted with the completive reaction of substituted and the non-substituted benzoyl bromides and rhenium nitride (**scheme 32**). The adduct complex **A** and **B** were synthesised and characterised before which makes it easier to detect them in the competitive reactions. It has been observed that the reaction of rhenium nitride with substituted and non-substituted benzoyl bromides provide respective benzoyl imido adduct complexes such as **A** and **B** selectively in DCM and here, equilibrium does not exist. Therefore, the nitride complex is treated with excess and equimolar amounts of substituted and the non-substituted benzoyl bromides in the competitive reaction. Excess amounts substituted and unsubstituted are used to reduce the reaction time. Once the competitive reactions are completed, the $^{31}P\{^1H\}$ NMR are measured with increased relaxation time to 15s to get the accurate integration ratio of complex **A** and **B**. Next, substituted and the non-substituted rate constants **k_x and k_H** were calculated. It is observed that the ratio of rate constants **k_x/k_H** with p-OMe, p-Me, p-Br and p-CF_3 provides a gradually increasing value i.e 0.25, 0.38, 2.66, 5.87 respectively (**Figure 53**). Finally, the $\log(k_x/k_H)$ was plotted against the sigma Hammett parameter, which provided a linear relationship between them with a positive slope of 1.70574 (**Figure 54**). Positive slope or the increasing order of reactivity from OMe, Me, H, Br, CF_3 substituted benzoyl bromide can be explained by the increasing order of electrophilicity of carbonyl carbon of the substituted benzoyl bromides. Strong electron-withdrawing groups such as Br and CF_3 pull the electron of the carbonyl centre which makes it more electrophilic. Increasing the electrophilicity of the carbonyl carbon makes it easier for the rhenium nitride for the nucleophilic attack to give a benzoyl adduct complex.

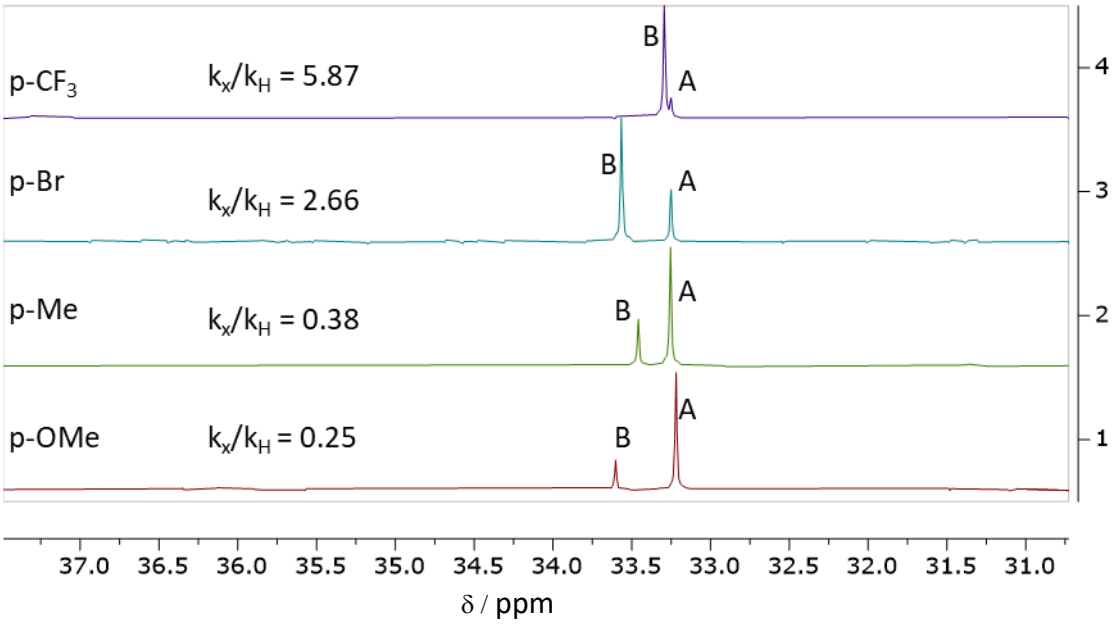

Figure 53: *$^{31}P\{^{1}H\}$ NMR spectrum, the reaction of complex **7** with substituted and non-substituted benzoyl bromide in DCM.*

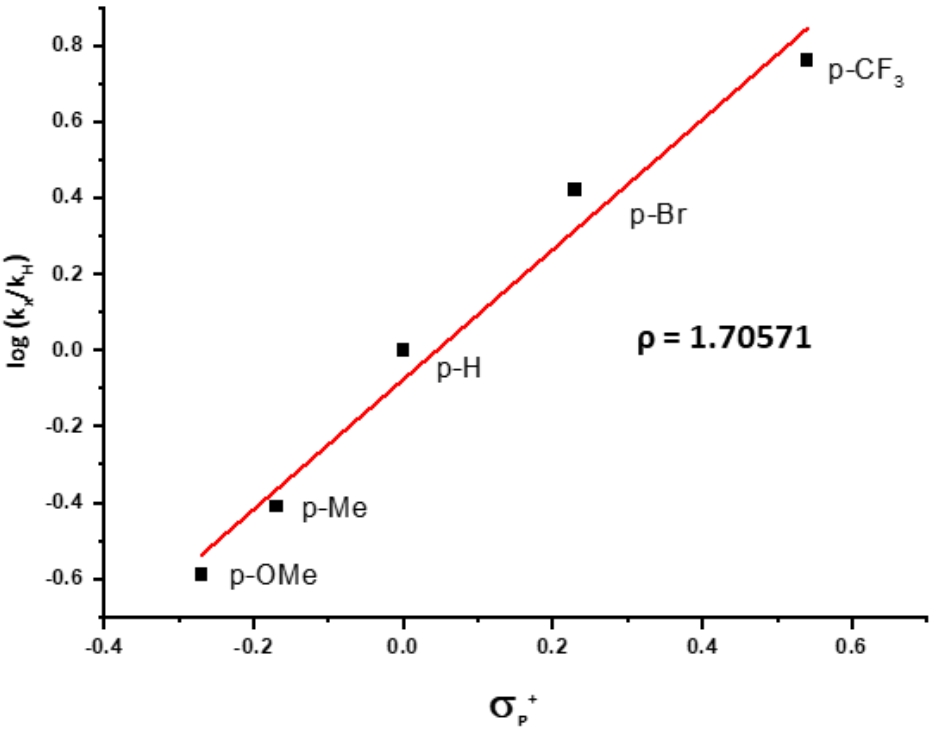

Figure 54: *Hammett plot in DCM.*

10.2 Hammett Plot (in THF)

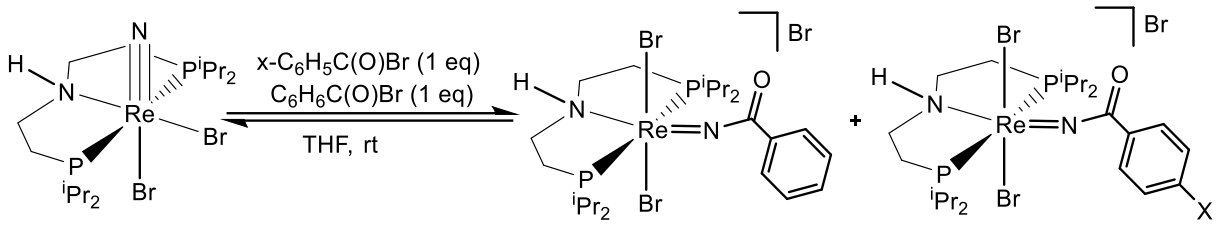

K_x/K_H= B/A x = OMe, Me, Br, CF_3 **A** **B**

Scheme 33: *Reaction of complex **7** with substituted and non-substituted benzoyl bromide in THF.*

Unlike in DCM, it is found to have a different reactivity with THF, so the Hammett plot is also drawn with it. There always exists an equilibrium when rhenium nitride complex **7** reacted with the substituted and the non-substituted benzoyl bromides to get **A** and **B**. Complex **7** is treated with equimolar of the substituted and the non-substituted benzoyl bromides simultaneously and the completive reaction is monitored by $^{31}P\{^1H\}$ NMR with an increased relaxation time to 15s, till the equilibrium established. Next, the equilibrium constant **K_x and K_H** are calculated. The ratio of the equilibrium constants **K_x/K_H** with p-OMe, p-Me, p-Br and p-CF_3 provides a gradual decreasing value i.e 2.15, 1.45, 0.80. 0.48 respectively.

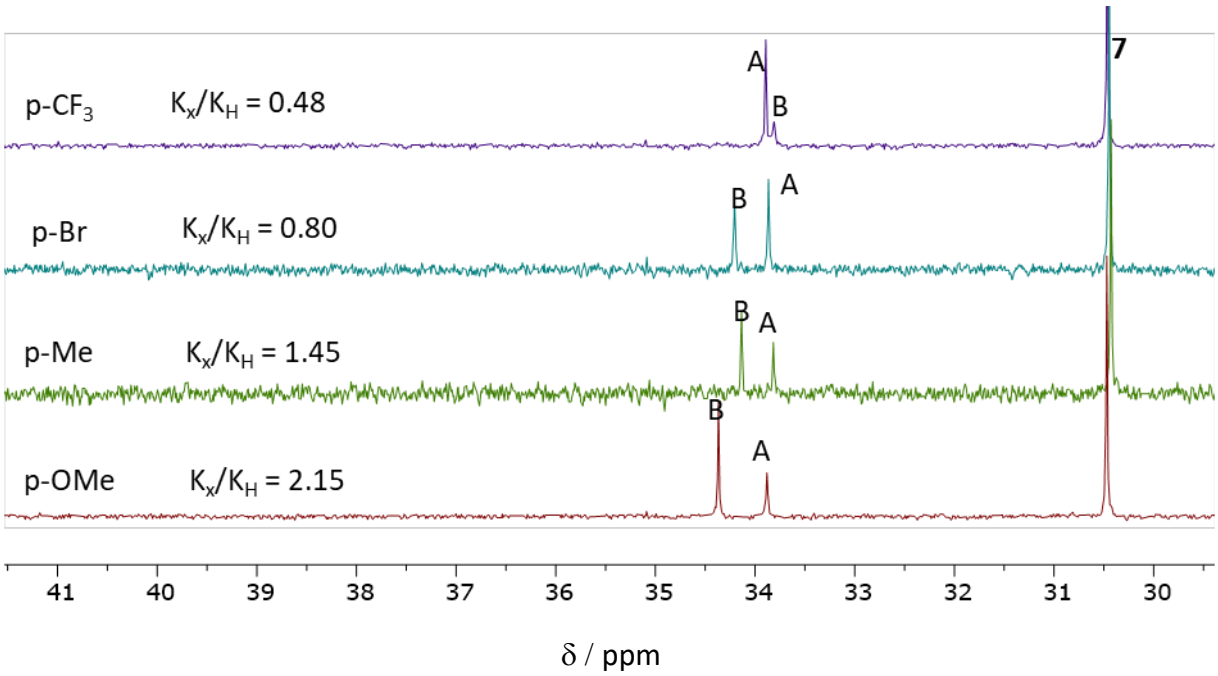

Figure 55: *$^{31}P\{^1H\}$ NMR spectrum, the reaction of complex **7** with substituted and non-substituted benzoyl bromide in THF.*

Hammett plot log (**K_x/K_H**) vs Hammett sigma parameter provides a linear relationship between them with a negative slope of -0.70093 (**Figure 56**).

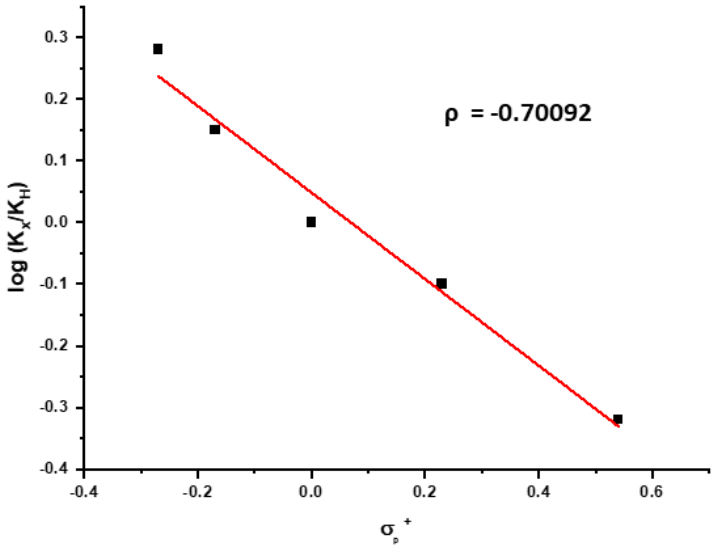

Figure 56: *Hammett plot in THF.*

To investigate further the competitive reaction of benzoyl bromide and 4-trifluoromethyl benzyl bromide (stronger electrophile than benzoyl bromide) with complex **7** is monitored (**Fig. 57. (a)**) and it is observed that the yield of complex **A** gradually increases when it reached to the equilibrium, on the other hand, strong electrophilic adduct complex **B**, the yield is gradually decreasing when it reached to equilibrium. To support the argument further, another pair is taken. Benzoyl bromide is stronger electrophilic than that of 4-methoxy benzoyl bromide (**Fig. 57. (b)**). When they are reacted with the complex **7** and monitored till there exists an equilibrium. It is observed that the yield of complex **A** decreases and the yield of complex **B** increases when it reaches equilibrium. Another competitive reaction is performed stepwise (**Fig.57. (c)**). Initially, complex **7** is reacted with the benzoyl bromide (stronger electrophile) and waits until the equilibrium reaches. Subsequently, an equimolar amount of 4-methylbenzoyl bromide (weaker electrophile) is added to it and monitored to equilibrium. it is found that the yield of complex **A** decreases from 27% to 8%. In this scenario, a completive reaction between strong and weak electrophiles provides a negative slope. The plausible explanation for this can be that the stronger the electrophile obtains an equilibrium faster than the weaker ones and the weaker electrophile takes a longer time to reach equilibrium. Meanwhile, a partial amount of the stronger electrophile that is in the equilibrium hydrolyses as stronger electrophile more sensitive towards light, air and moisture because of which equilibrium shifted backwards as per the *Le Chatelier's principle* and at some point hydrolysation ended to provide a new equilibrium constant which is less than that of the previous one. So basically, here first equilibrium constant (original) of the weaker electrophile and the second equilibrium constant (less than that of the first) of the stronger electrophile is considered, because of which it provides a negative slope. Hydrolysis of stronger electrophiles may be due to the formation of HBr as we found in **sec 5.2**. So, overall it can be concluded that due to hydrolysation of electrophiles in a competitive equilibrium reaction in THF, the equilibrium constants found are not equilibrium constants in reality, because of which we found a negative slope.

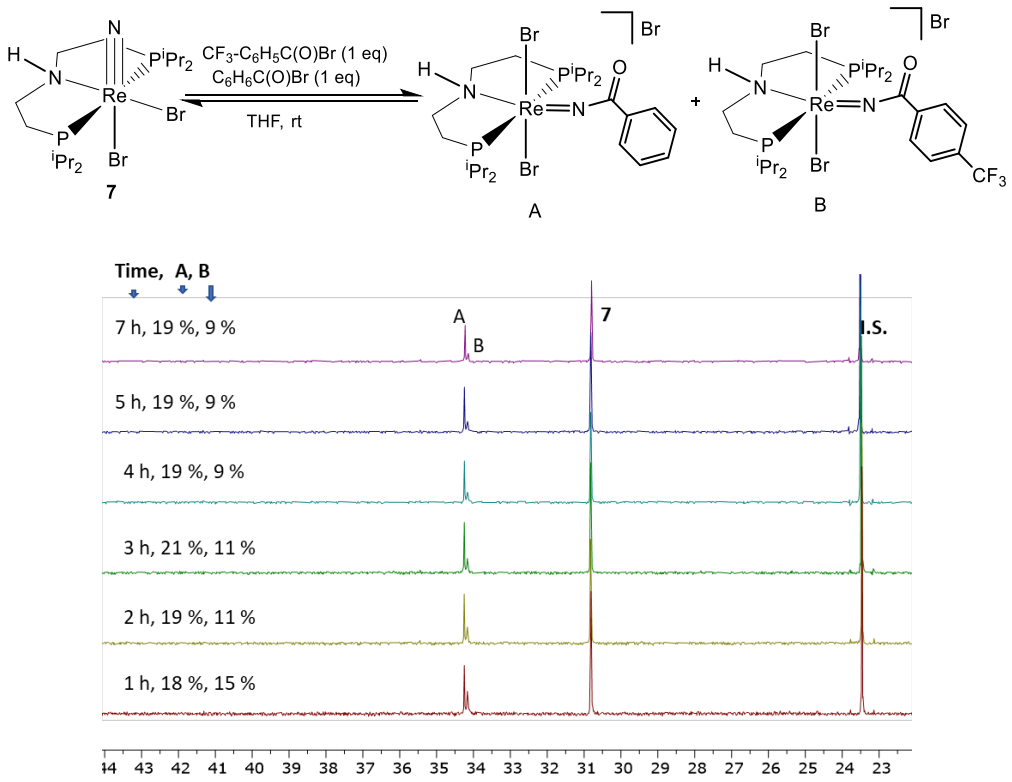

Figure 57 (a): *$^{31}P\{^{1}H\}$ NMR spectrum, the reaction of complex **7** with benzoyl bromide and 4-trifluoromethyl benzoyl bromide in THF.*

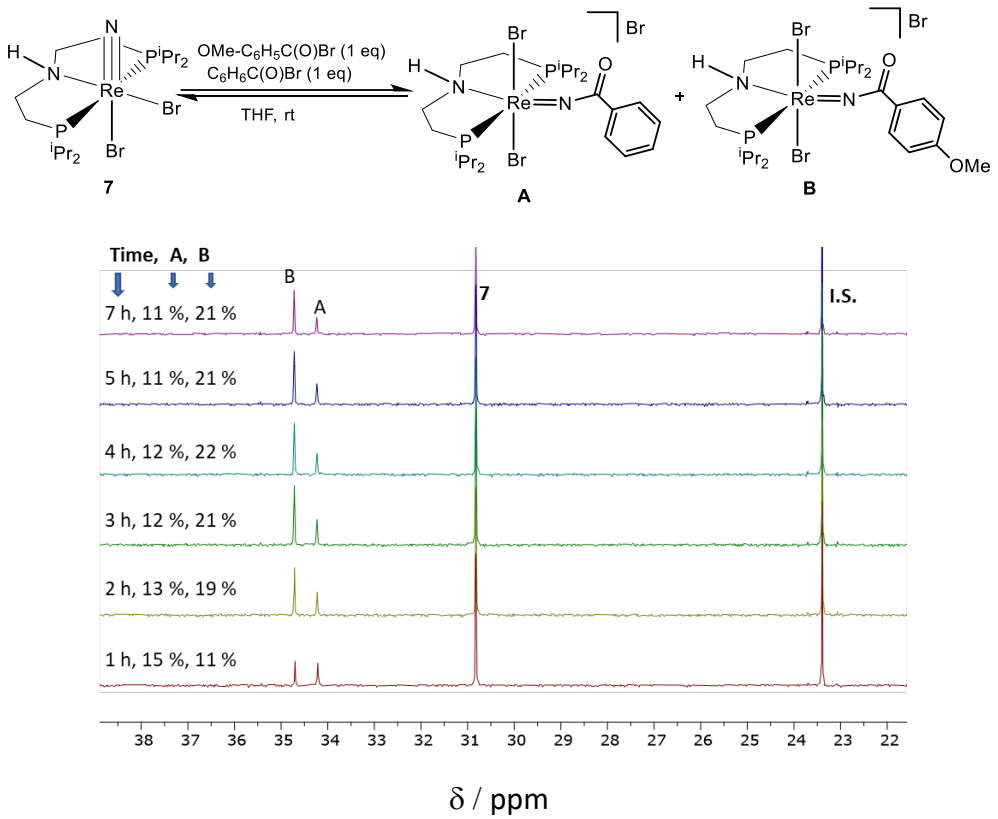

Figure 57(b): *$^{31}P\{^{1}H\}$ NMR spectrum, the reaction of complex **7** with benzoyl bromide and 4-methoxy benzoyl bromide in THF.*

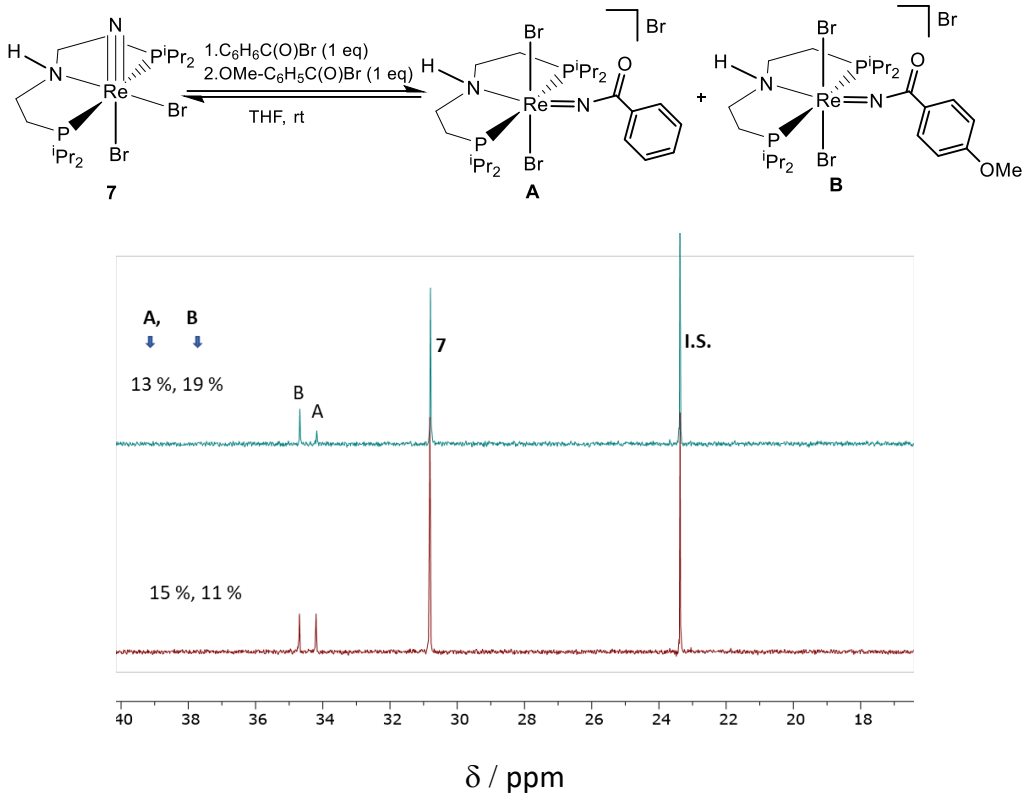

Figure 57 (c): *$^{31}P\{^{1}H\}$ NMR spectrum, step-wise addition of benzoyl bromide and 4-methoxy benzoyl bromide with complex **7** in THF.*

11. Reactivity of benzoylimido adduct complexes

11.1 Metal-Ligand cooperativity reactions

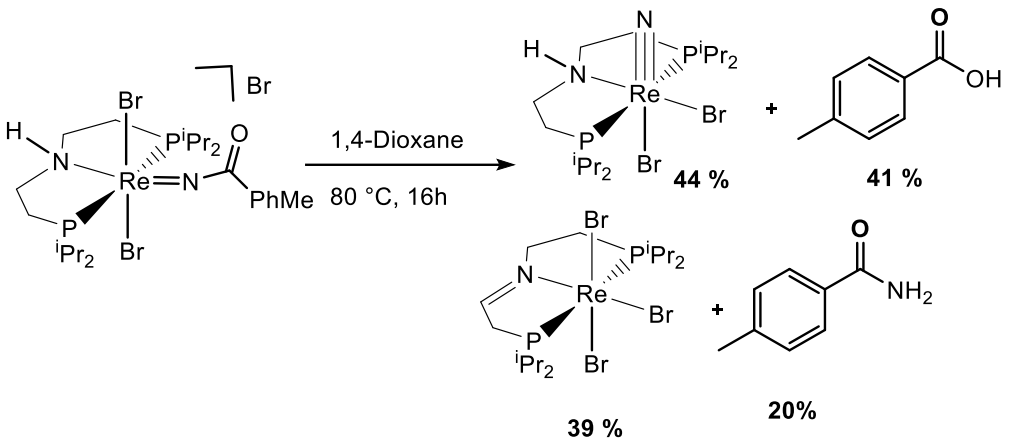

Scheme 35: *Metal-Ligand cooperative reaction by adduct complex **13.***

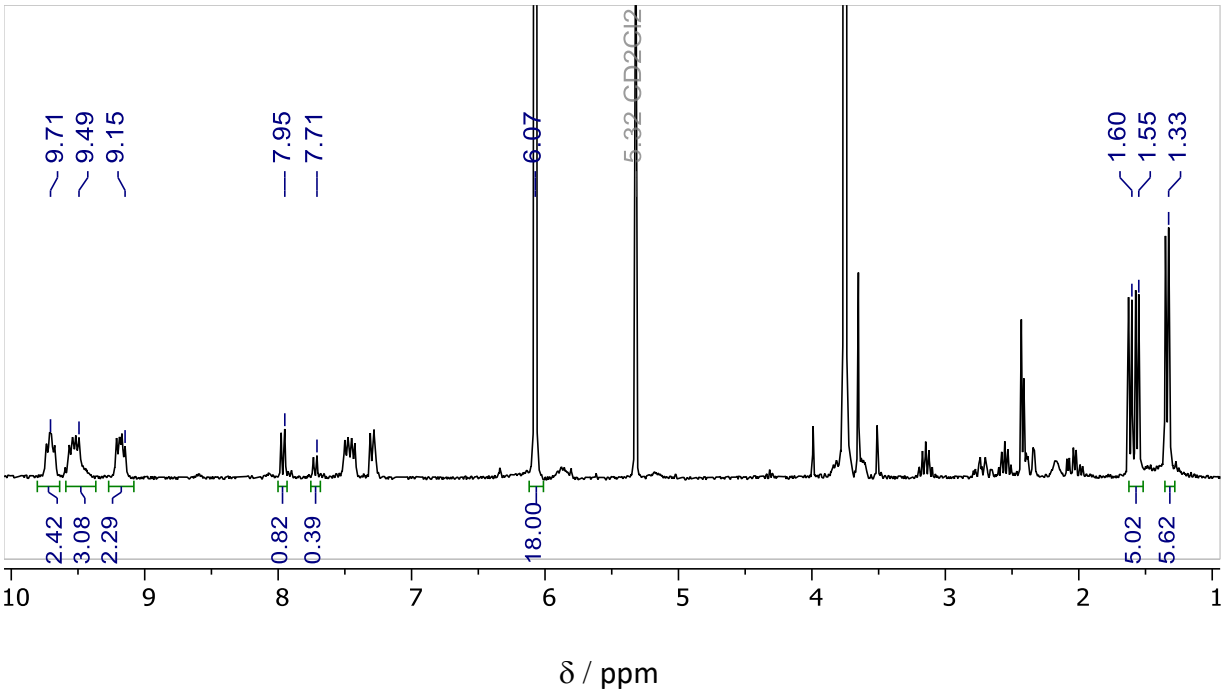

Figure 60. *^{1}H-NMR quantification of the reaction after heating complex **13** without benzoyl bromide to **7** and **5**. 1,3,5-trimethoxybenzene (6 eq) was added and the product was quantified by ^{1}H NMR spectroscopy. Integration of the methyl groups of 7.79 (δ_H = 9.74 / 9.53 / 9.19, 20H) indicates 39 % spectroscopic yield in **5** and Integration of the CH_3 proton of 10.64 (δ_H = 1.64/ 1.59/ 1.37, 24H) indicates 44 % spectroscopic yield in **7.** 4-methylbenzoic acid (δ_H = 7.95 ppm, 2H, H-ortho) and 4-methylbenzamide (δ_H = 7.71 ppm, 2H, H-ortho) are obtained in 41 % and 20% respectively.*

Metal-ligand cooperative reactions with substituted adduct complexes are tried with the different synthesised substituted adduct complexes. It was assumed that varying the electrophilicity of the carbonyl centre may give the selective rhenium imine complex **5** and 4-methylbenzamide. So, the adduct complexes are heated at 80 °C in dioxane overnight, which shows very similar reactivity to non-substituted benzoyl adduct complex **11.** The metal-ligand cooperative reaction of complex **13** provides 39% of rhenium imine complex **5** and 20 % of 4-methylbenzamide and 41 % of 4methylbenzoic acid. It also provided 44% rhenium nitride complex **7** (**Figure 60**). Therefore, the selectivity of the imine complex could not be achieved with substituted benzyl bromides.

11.2. Synthesis of benzamide with external reductant and acid

Previously the metal-ligand cooperative synthesis of benzamide and the benzonitrile is demonstrated with complex 11 which provided imine complex 5, benzamide, benzoic acid and benzonitrile upon heating with the extra equivalent of benzyl bromide at the elevated temperature of 80 °C. Here the 2e- and 2 H^+ are donated by the HPNP backbone of the complex. The selectivity could not be controlled by this method. So, here 2 eq reductant and acid each are added to get the benzamide selectively at room temperature.

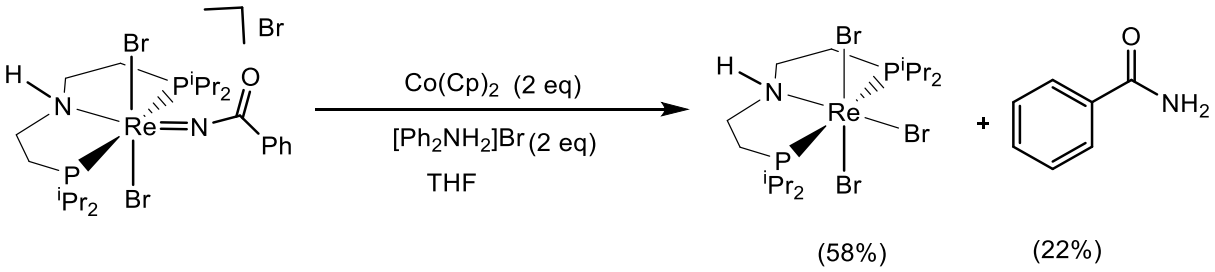

Scheme 36: *Synthesis of benzamide by PCET method with complex* ***11****.*

The reaction of **11** with 2 eq $Co(Cp)_2$ and 2 eq $[Ph_2NH_2]Br$ in THF, stirred at rt for 16h, 1 eq 1,3,5-trimethoxybenzene was added as internal standard and products were quantified by ^1H NMR, which provided complex **3,** 58% in yield and benzamide 22 % in yield (**Figure 61**). Further, the organic reaction mixture is extracted in Et_2O and compared with the ^1H -NMR spectrum of an authenticated sample of benzamide, which indicates the presence of benzamide in it. ^1H- COSY NMR spectrum of the organic mixture shows the ortho protons which couple meta protons. Next, the GC-MS of the organic mixture provided a peak at 121.05 (m/z) indicating the benzamide (**Figure 62**).

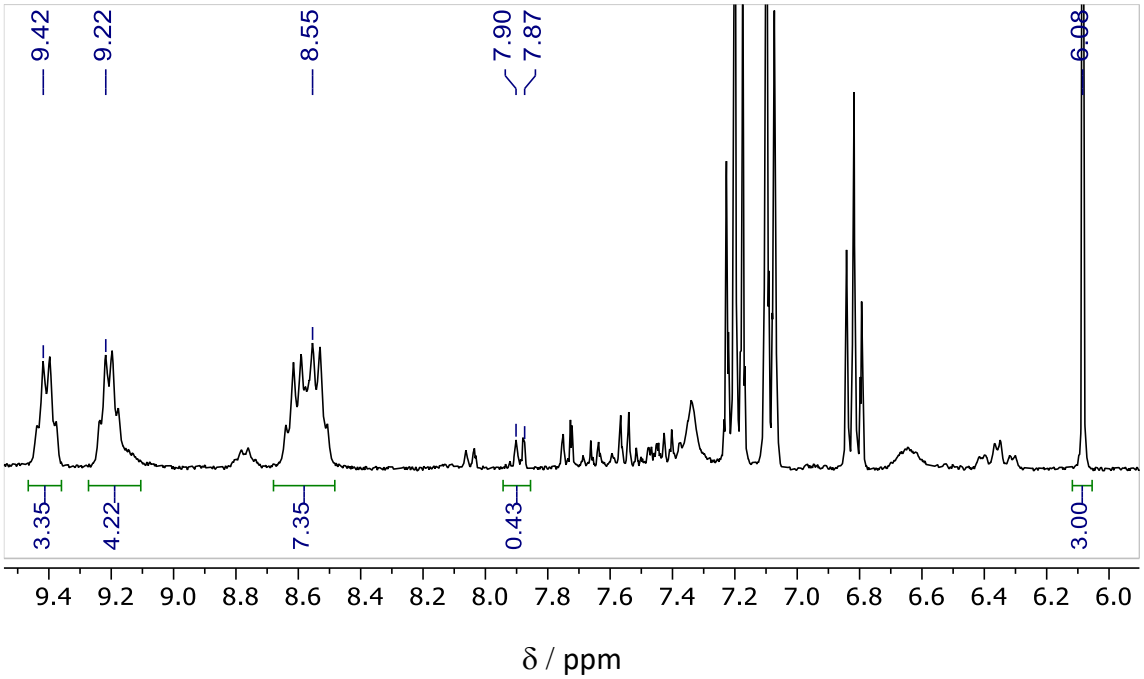

Figure 61. *^1H-NMR quantification of the reaction of* ***11*** *with 2 eq $Co(Cp)_2$ and 2 eq $[Ph_2NH_2]Br$ to* ***3****. 1,3,5-trimethoxybenzene (1 eq) was added and the product was quantified by ^1H NMR spectroscopy. Integration of the methyl groups of 14.92 (δ_H = 9.42 / 9.22 / 8.55, 26H) indicates 58 % spectroscopic yield in* ***3****. Benzamide (δ_H = 7.90 ppm, 2H, H-ortho) was obtained 22% in yield.*

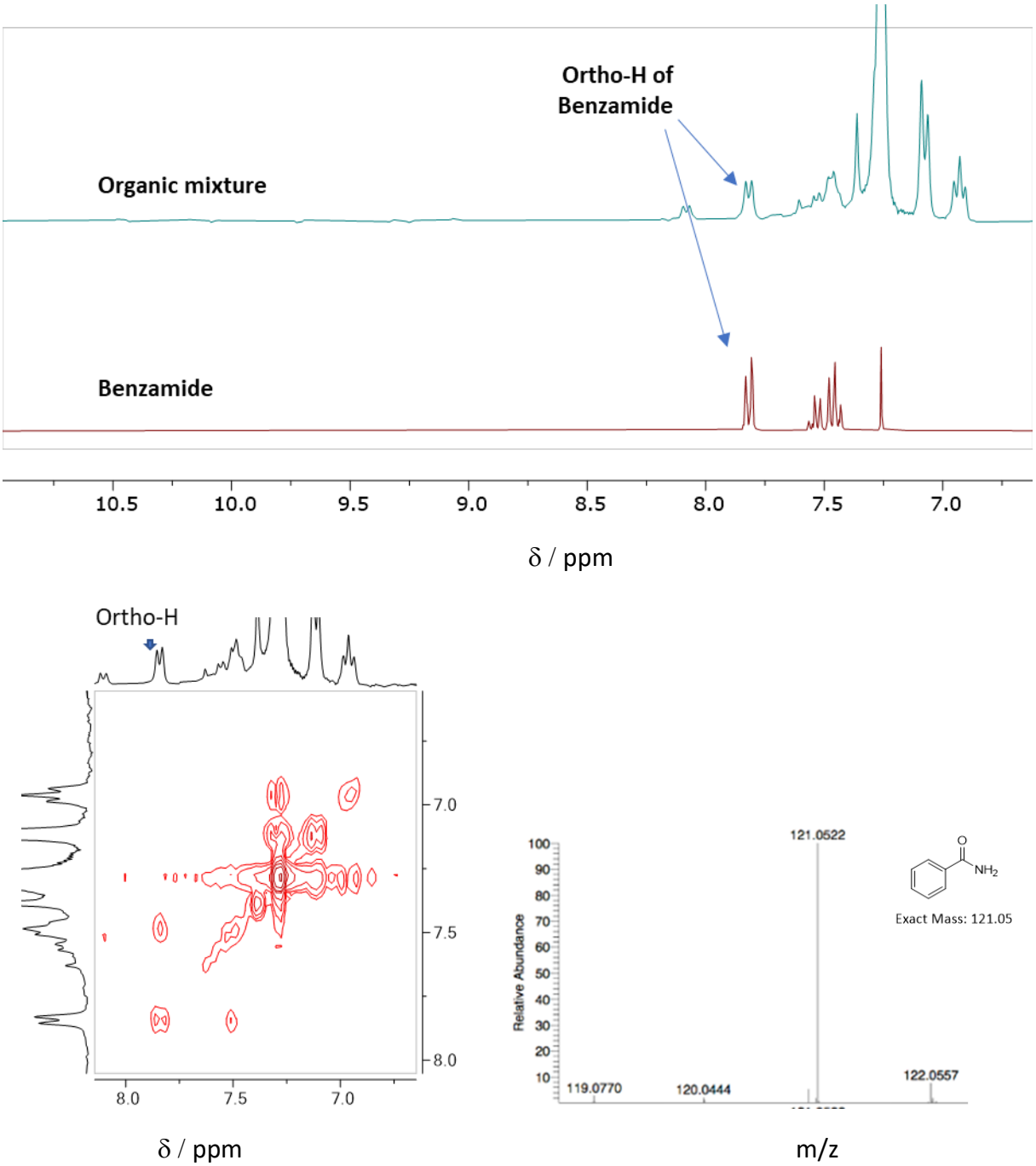

***Figure 62**. **a)** (top) ^{1}H -NMR spectra of the isolated organic mixture and authentic benzamide in $CDCl_3$. **b)** (bottom left) ^{1}H- COSY NMR spectrum showing cross-peaks between ortho-H and meta-H of benzamide. **c)** (bottom right) GC-MS indicates the presence of benzamide in the organic mixture.*

11.3. Synthesis of 4-trifluoromethylbenzonitrile with 12

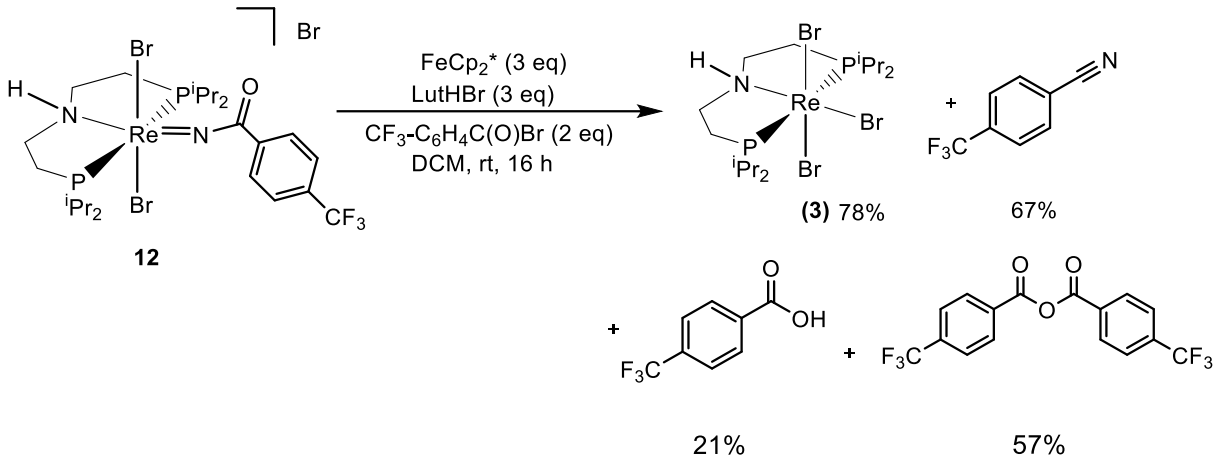

Scheme 37: *Selective synthesis of 4-trifluoromethylbenzonitrile from complex* ***12.***

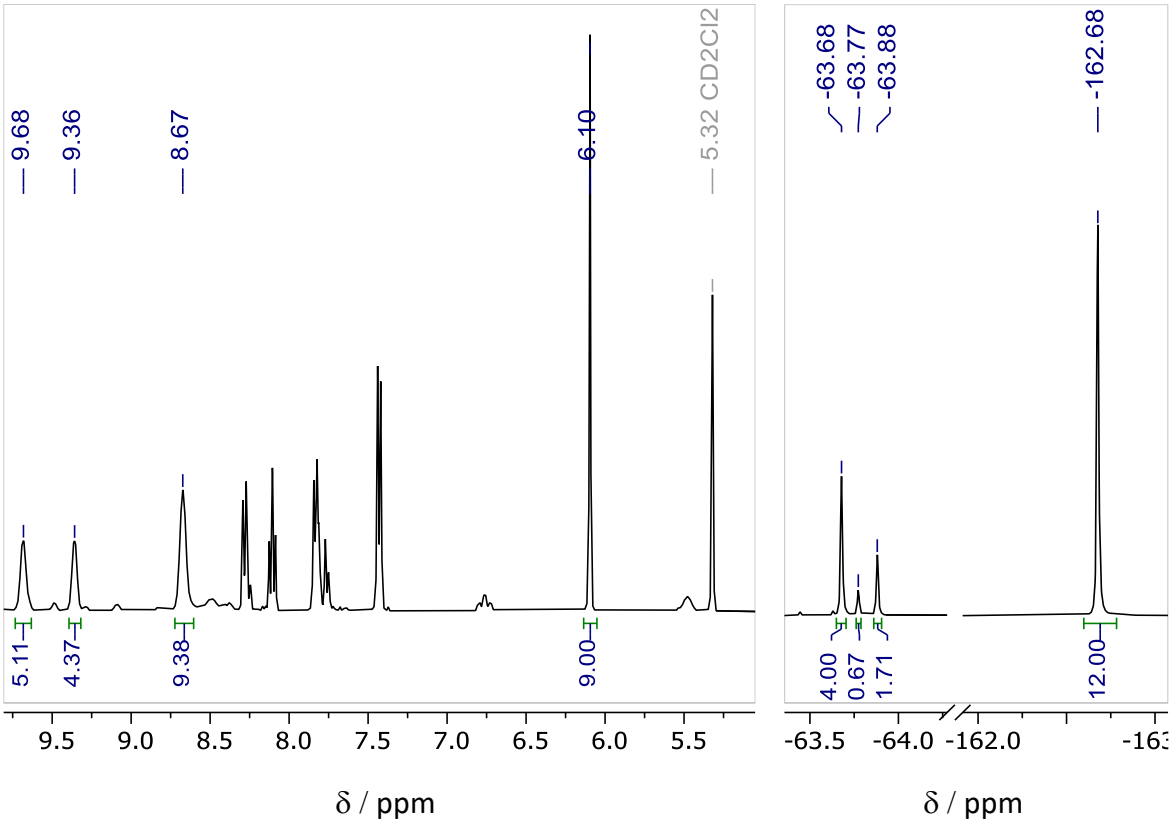

Figure 63.a) *(left) ^{1}H-NMR quantification of the reaction of* ***12*** *with $FeCp_2$* (3 eq), LutHBr (3 eq) and CF_3-$C_6H_4C(O)Br$ (2 eq) to* ***3****. 1,3,5-trimethoxybenzene (3 eq) was added and the product was quantified by ^{1}H NMR spectroscopy. Integration of the methyl groups of 18.86 (δ_H = 9.68 / 9.42 / 8.65, 24H) indicates 78 % spectroscopic yield in* ***3****.* ***b)*** *(right) ^{19}F-NMR quantification using hexafluoro benzene (2 eq) as internal standard, 4-trifluoromethylbenzonitrile (δ_H = -63.88 ppm, 3F, CF_3), 4-trifluoromethylbenzoic acid (δ_H = -63.77 ppm, 3F, CF_3), 4-trifluoromethylbenzoic anhydride (δ_H = -63.68 ppm, 3F, CF_3) obtained in 67%, 21%, 57% in yield respectively.*

Formation of the benzamide can be observed from complex **11** by the PCET method but the reaction was found unselective, which generated only 22% of the benzamide. As it has been observed in the case of metal-ligand cooperative reaction, in presence of benzoyl bromide some of the benzamides provide benzonitrile and the benzoic acids. A similar reaction is also occurring here, because of which benzamide yields get reduced. So, to convert all the benzamide to benzonitrile here little excess amount of reductant, acid and benzoyl bromide is used. When complex **12** is treated with 2eq 4-trifluoromethyl benzyl bromide, 3 eq $FeCp_2$* and 3 eq LutHBr in DCM and stirred at room temperature overnight provided 78% of complex **3**, 67% of 4-trifluoromethyl benzonitrile, 21% 4- trifluoromethyl benzoic acid and 57% of 4-trifluoromethyl benzoic anhydride (**Figure 63**). 2 eq of reductant and acid are needed for this reaction, extra eq is used to optimize the reaction. The formation of complex **3** and other organic compounds are confirmed by comparing the NMR spectra of the pure commercially available organic compounds. 4-trifluoromethyl benzoic anhydride is synthesised in the lab using 4-trifluoromethyl benzoic acid. Complex **3** was quantified by ^{1}H-NMR, adding 1,3,5-trimethoxybenzene (3eq) and the organic products are quantified by ^{19}F-NMR adding hexafluoro benzene (3eq) as they are perfectly distinguishable in it.

11.4 In-situ synthesis of [Re(p-$CF_3C_4H_4C(O)NH)Br_2(HPNP^{iPr})$] (15)

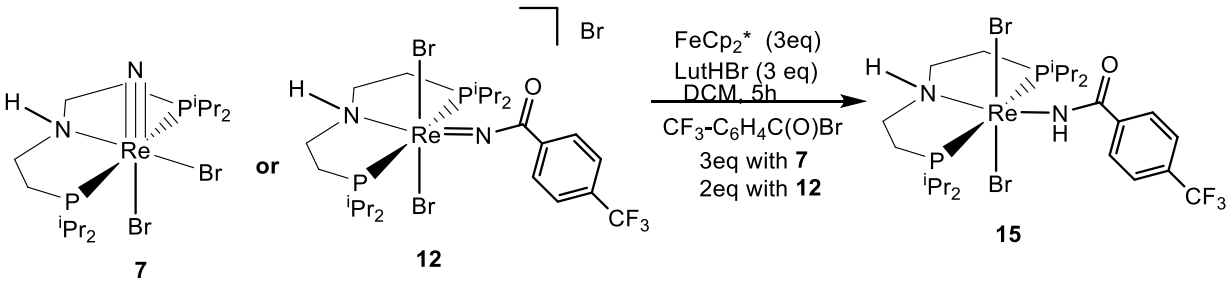

Scheme 38: *In-situ synthesis of complex* ***15.***

The last PCET reaction provided the benzonitrile selectively, so the reaction is monitored to investigate the intermediates involved in it. Complex **12** is treated with $FeCp_2$* (3 eq), LutHBr (3 eq) and CF_3-$C_6H_4C(O)Br$ (2 eq) in DCM and the reaction is monitored by $^{31}P\{^{1}H\}$ NMR. After stirring the reaction for 5h, there arises a prominent peak at 1270 ppm, which is because of the in-situ formation of complex **15**. To isolate it the reaction is stopped and the solvent was evaporated out by vaccuo. Next, the reaction mixture is washed with Et_2O and extracted the yellow complex **15** by benzene, providing a 90% in yield. A very similar result is obtained when rhenium nitride complex **7** is treated with $FeCp_2$* (3 eq), LutHBr (3 eq) and CF_3-$C_6H_4C(O)Br$ (3 eq). stirred the reaction mixture in DCM for 5h provided 90% of complex **15,** after sole isolation. ^{19}F NMR spectrum Complex **15** provides a prominent peak at δ_F = -61.82 ppm. At the same time, $^{31}P\{^{1}H\}$ NMR spectrum provided a signal at δ_P = 1270.04 ppm, which indicates the complex has a C_{2V} symmetry in the NMR time scale (**Figure 64**). ^{1}H -NMR spectrum provides sharp distinguishable signals from a range of δ_H = 214.49 ppm to -38.95 ppm. Six large and prominent peaks δ_H = 12.27 ppm to 6.48 ppm correspond to the isopropyl group. Two downfield shifted peaks δ_H = 18.23 ppm and 17.41 ppm are the aromatic signals of the benzoyl group. Signals at δ_H = 214.49 ppm and 2.28 ppm are denoted as the two signals of the N-H moiety. A peak at δ_H = 5.64 ppm and the remaining three signals in the negative region

indicates the 8-proton signal of the backbone. $^{13}C\{^{1}H\}$ NMR spectrum show 4 prominent methyl signals of the isopropyl group and three backbone and aromatic signals are there from δ_C = 223.65 ppm to 122.63 ppm.

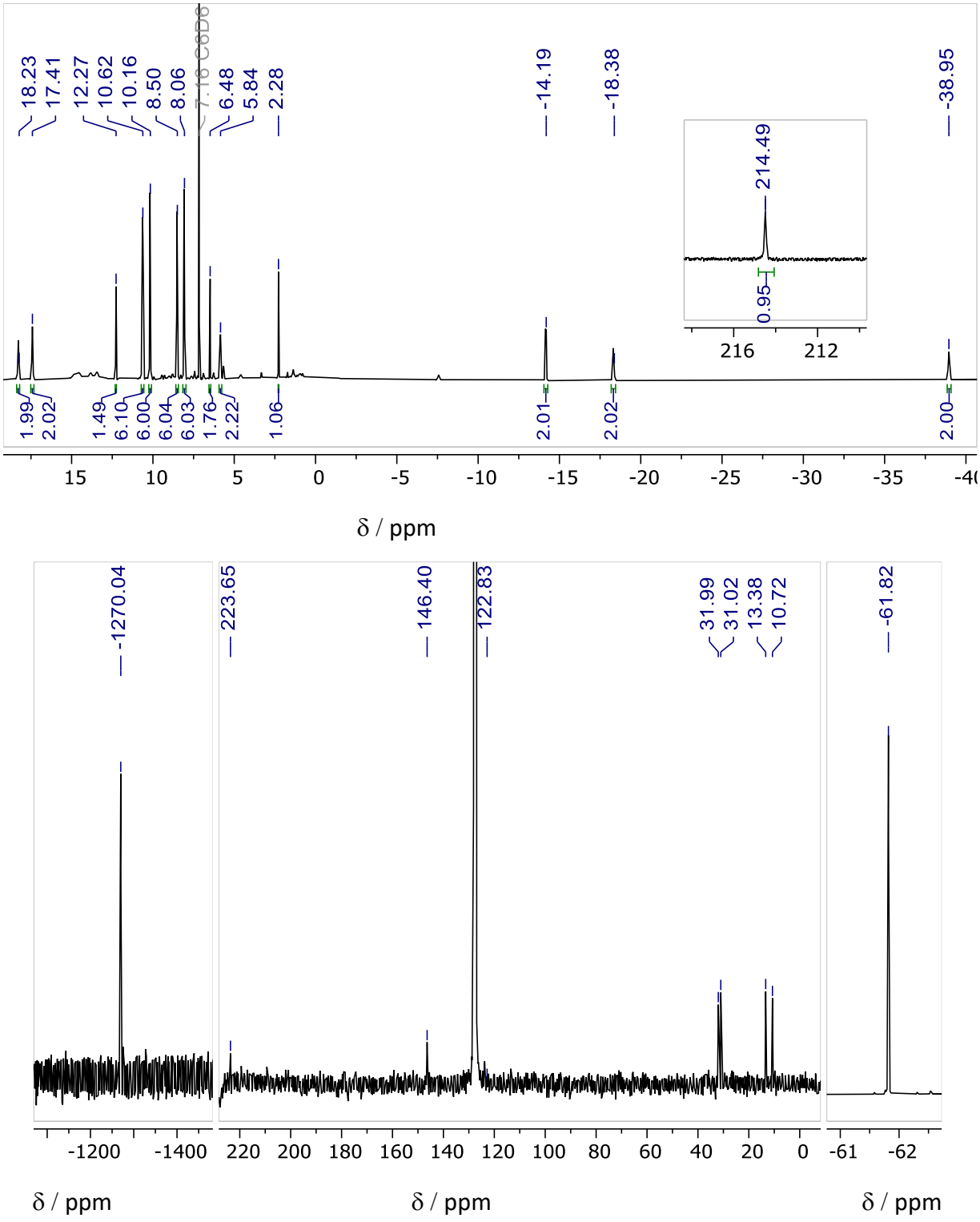

***Figure 64**. **a)** (top) ^{1}H -NMR spectrum of **15** in C_6D_6. **b)** (bottom left) $^{31}P\{^{1}H\}$ NMR spectrum. **c)** (bottom middle) $^{13}C\{^{1}H\}$ NMR spectrum. **d)** (bottom right) ^{19}F NMR spectrum.*

11.5 Selective synthesis of 4-trifluoromethylbenzamide from 15

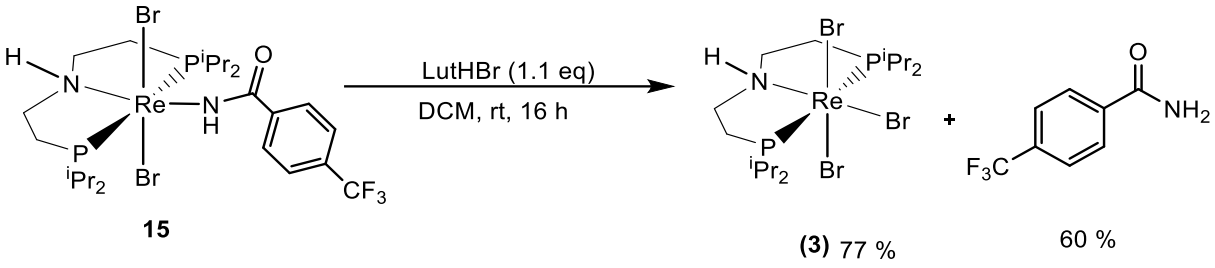

Scheme 39: *Selective synthesis of 4-trifluoromethyl benzamide from complex* ***15.***

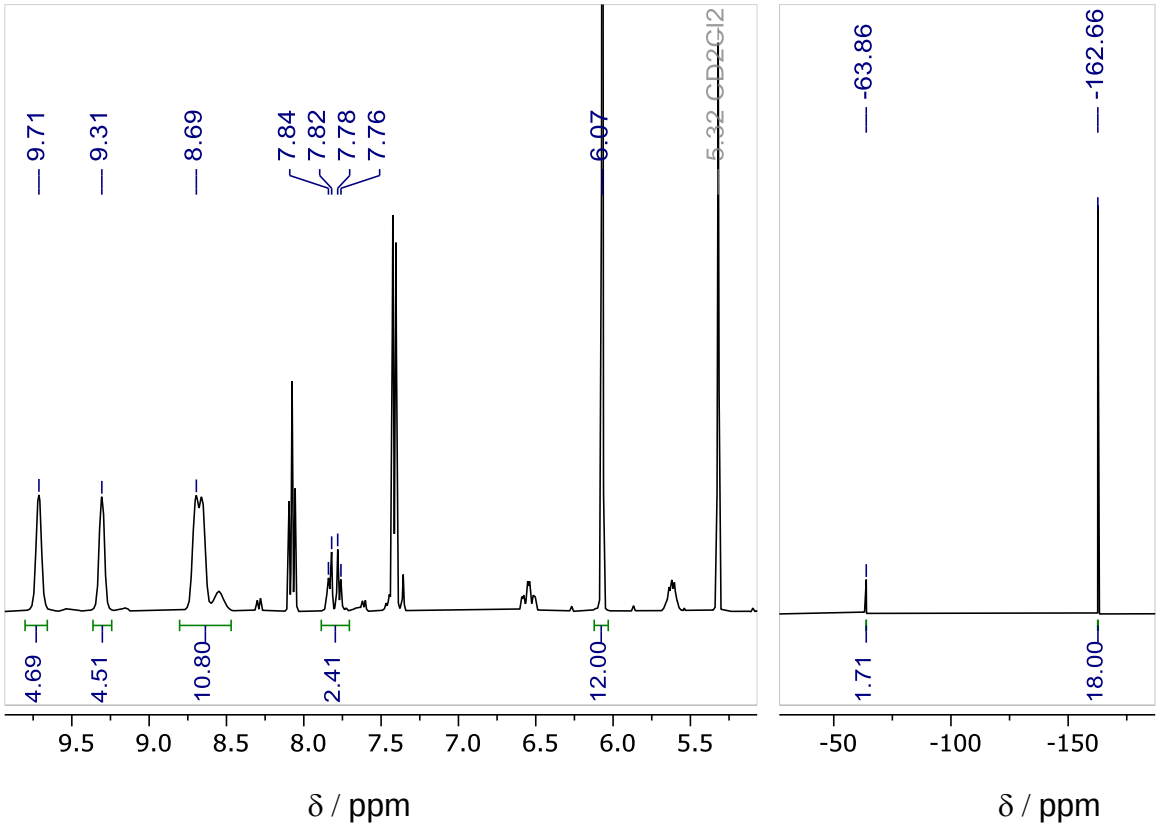

Figure 65. a) *(left)* ^{1}*H-NMR quantification of the reaction of* ***15*** *with 1 eq LutHBr to* ***3****. 1,3,5-trimethoxybenzene (2 eq) was added and the product was quantified by* ^{1}*H NMR spectroscopy. Integration of the methyl groups of 20 (*δ_H *= 9.71 / 9.31 / 8.69, 26H) indicates 77 % spectroscopic yield in* ***3****. 4-trifluoromethyl benzamide (*δ_H *= 7.84 ppm, 4H, H-ortho and H-meta) obtained in 60 % in yield.* ***b)*** *(right)* ^{19}*F-NMR quantification using hexafluoro benzene (3 eq) as internal standard, 4-trifluoromethylbenzamide (*δ_F *= -63.86 ppm, 3F,* CF_3*) obtained in 58 % in yield.*

Complex **15** is successfully trapped and isolated, which is further employed to regenerate complex **3** and synthesised 4-trifluoromethyl benzamide selectively. For that, complex **15** required an external proton. So, when the complex was treated with LutHBr (1.1 eq) in DCM and stirred overnight, it provided complex **3**, 77% in yield and 4-trifluoromethyl benzamide 60% in yield (**Figure 65**). These spectroscopic yields are calculated by ^{1}H-NMR using 1,3,5-

trimethoxybenzene (2 eq) as the internal standard and the formation of 4-trifluoromethyl benzamide is confirmed by comparing the NMR spectra of authenticating and commercially available 4- trifluoromethyl benzamide. Also, 4-trifluoromethyl benzamide is quantified by ^{19}F-NMR, using hexafluoro benzene (3 eq) as the internal standard, which provided 58% in yield. Here the complex **15** undergoing nucleophilic attack subsequently abstracts a proton. Further elimination of 4-trifluoromethyl benzamide and coordination of bromide ion at inner sphere regenerates rhenium tribromide complex **3**.

11.6 4-membered synthetic cycle for 4-trifluoromethylbenzamide

From all the above information 4-membered synthetic cycle for 4-trifluoromethyl benzyl bromide can be drawn (**Scheme 40**). Complex **3** is treated with TMS-N_3 to get rhenium nitride complex **7**, which is further treated with 1 eq of 4-trifluoromethyl benzoyl bromide to get complex **12,** 85% in yield. So here, DCM is used to avoid equilibrium. Complex **12** is treated with external reductant and acids with extra 2 eq if 4-trifluoromethylbenzoyl bromide to get back complex **3** and corresponding benzonitrile selectively, where no 4-trifluoromethyl benzamide is detected. It says all benzamide reacted with extra substituted benzyl bromide to get the 4-trifluoro benzonitrile. During this process, the in-situ formation of complex **15** is observed and the complex is further isolated and characterized. Alternatively, complex **15** also can be synthesized with complex **7** and 3 eq 4-trifluoro methylbenzoyl bromide in presence of reductant and acid. Reduction of complex **12** in absence of extra 4-trifluoromethyl benzyl bromide can be observed as a minor intermediate but it could not be isolated. The isolated complex **15**, further treated with LutHBr provided 4-trifluoromethyl benzamide selectively and complex **3** is regenerated. The selective synthesis of 4-trifluoromethyl benzamide and 4-trifluoromethyl benzonitrile is explained by the selective control PCET method.

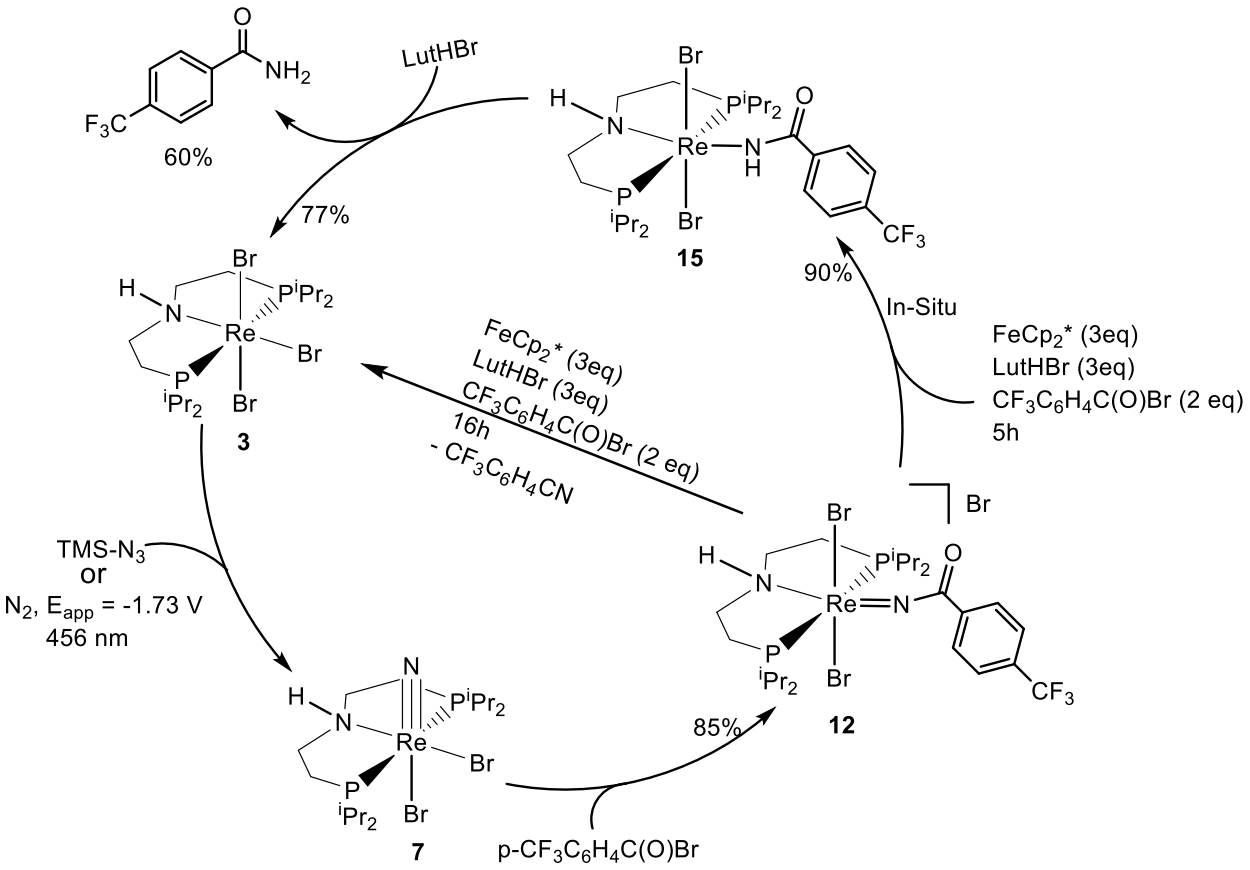

Scheme 40: *4-membered synthetic cycle for 4-trifluoromethylbenzamide.*

12. Synthesis of para-substituted benzonitriles with 7

12.1 Synthesis of 4-trifluoromethyl benzonitrile

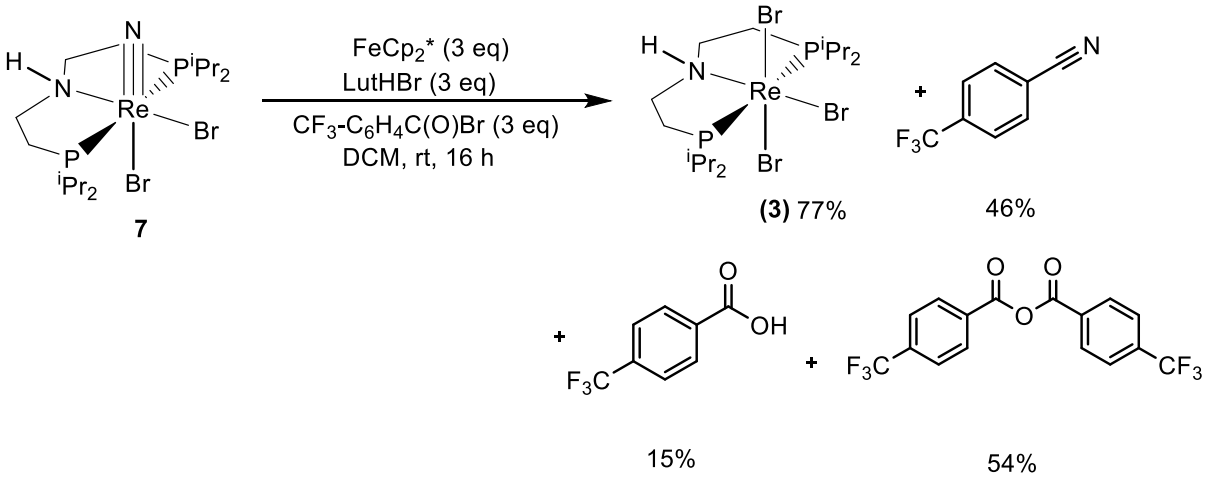

Scheme 41: *Selective synthesis of 4-trifluoromethylbenzonitrile from complex* ***7*** *by PCET.*

The selective formation of 4 trifluoromethyl benzonitrile with complex **12** is explained previously where all the 4-trifluoromethyl benzamide converted to 4-trifluoromethyl benzonitrile in presence of another 2 equivalents of 4-trifluoromethyl benzoyl bromide. As complex **12** is one of the key intermediates in the process. So, the same reaction is tried with complex **7** using 4-trifluoromethylbeznoyl bromide (3eq). When complex **7** is added with $FeCp_2$* (3 eq), LutHBr (3 eq) and CF_3-$C_6H_4C(O)Br$ (3 eq) in DCM and stirred the reaction mixture overnight obtained 77 % spectroscopic yield in **3,** 46% 4-trifluoromethyl benzonitrile, 15% 4-trifluoromethyl benzoic acid and 54% of 4-trifluoromethyl benzoic anhydride (**Figure 66**). The spectroscopic yield of complex **3** is calculated by ^{1}H-NMR using 1,3,5-trimethoxybenzene (1 eq) as the internal standard. On the other hand, the spectroscopic yields of the organic compounds could not achieve this as their signals are overlapping and they are quantified by ^{19}F-NMR using hexafluoro benzene (2eq) as the internal standard.

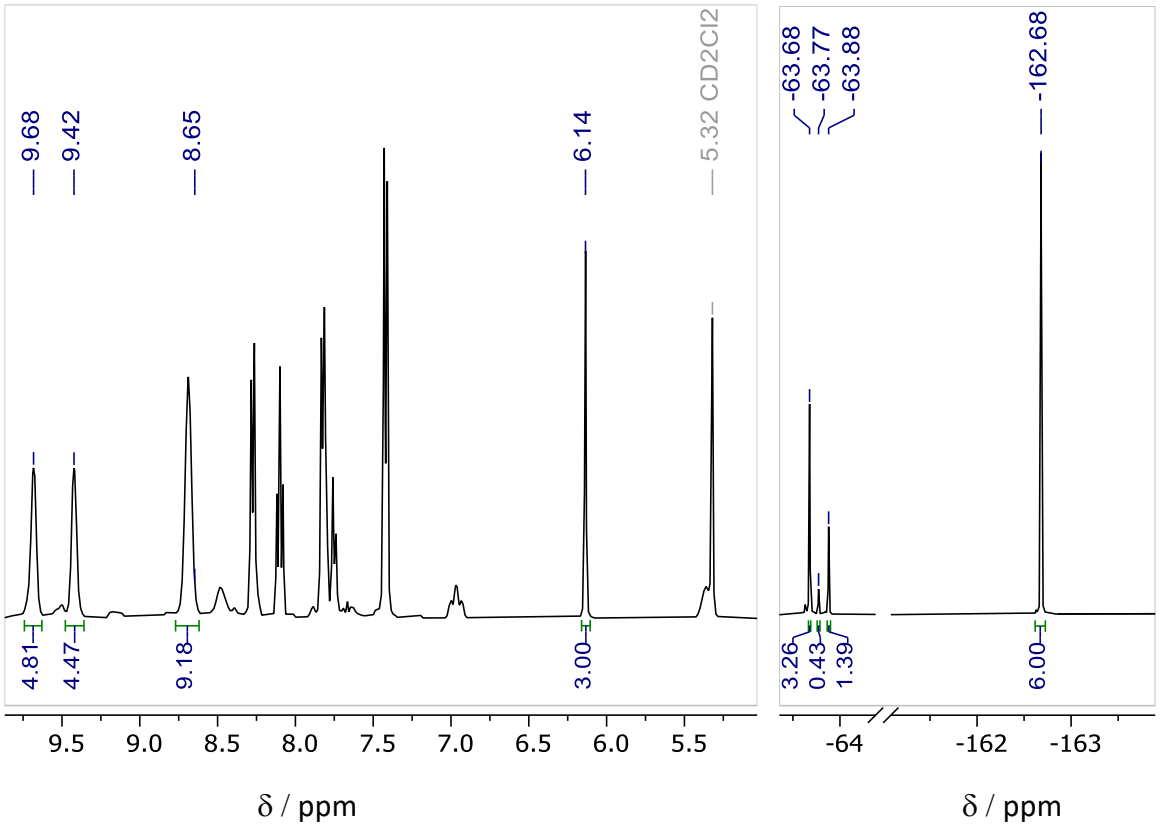

Figure 66.a) *(left) ^{1}H-NMR quantification of the reaction of **7** with $FeCp_2$* (3 eq), LutHBr (3 eq) and CF_3-$C_6H_4C(O)Br$ (3 eq) to **3**. 1,3,5-trimethoxybenzene (1 eq) was added and the product was quantified by ^{1}H NMR spectroscopy. Integration of the methyl groups of 18.46 (δ_H = 9.68 / 9.42 / 8.65, 24H) indicates 77 % spectroscopic yield in **3**.* ***b)*** *(right) ^{19}F-NMR quantification using hexafluoro benzene (1 eq) as internal standard, 4-trifluoromethylbenzonitrile (δ_F = -63.88 ppm, 3F, CF_3), 4-trifluoromethylbenzoic acid (δ_F = -63.77 ppm, 3F, CF_3), 4-trifluoromethylbenzoic anhydride (δ_F = -63.68 ppm, 3F, CF_3) obtained in 46%, 15%, 54% in yield respectively.*

12.2 Synthesis of 4-bromobenzonitrile

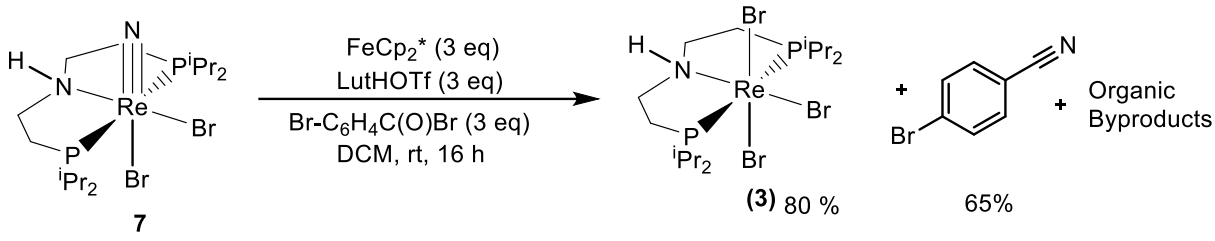

Scheme 42: *Selective synthesis of 4-bromolbenzonitrile.*

Synthesis of 4-trifluoromethyl benzonitrile was done by the one-pot reaction from **7**. So, here the selective synthesis of 4-bromobenzonitrile is tried using a similar procedure. Reaction complex 7 with $FeCp_2^*$ (3 eq), LutHOTf (3 eq) and Br-$C_6H_4C(O)Br$ (3 eq) in DCM and stirred at room temperature overnight, which provided 80% of complex **3** and 65 % of 4-bromobenzonitrile (**Figure 67**). Similar to the previous reaction other organic products such as 4-bromobenzoic acid and 4-bromobenzoic anhydride are also forming but as the signals are overlapping they could not be quantified. Complex **3** and the 4-bromobenzonitrile are quantified by ^{1}H-NMR using 1,3,5-trimethoxybenzene (2 eq) as the internal standard.

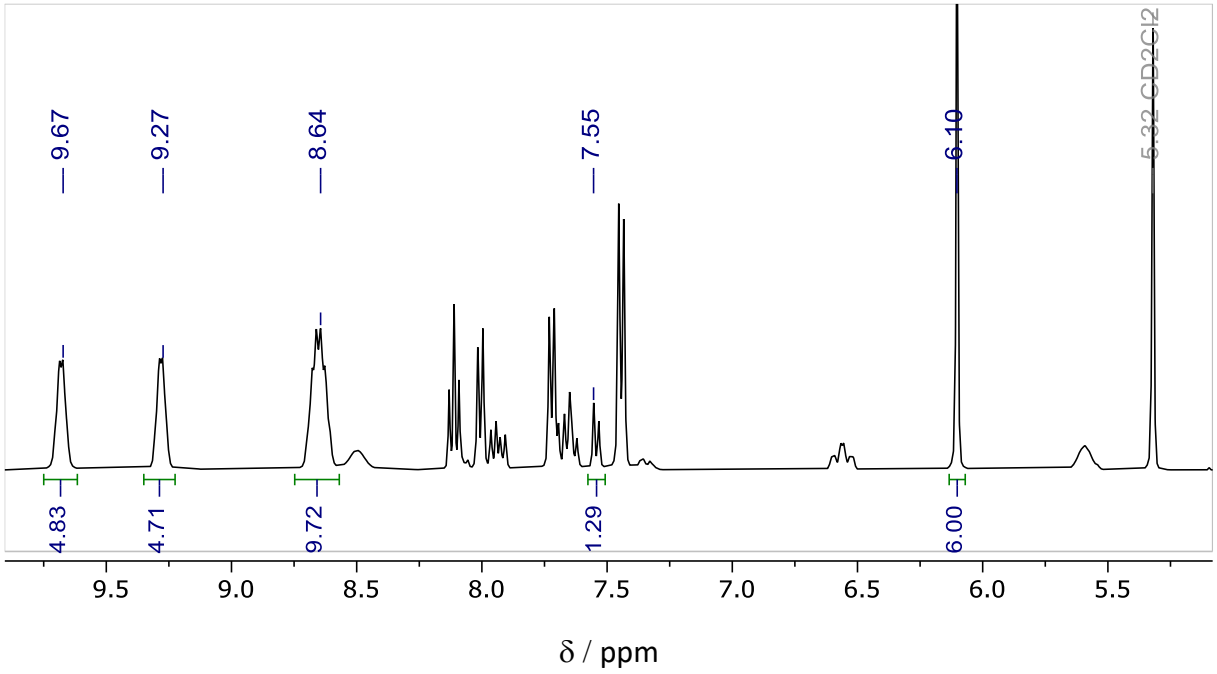

Figure 67. *^{1}H-NMR quantification of the reaction of **7** with $FeCp_2^*$ (3 eq), LutHOTf (3 eq) and Br-$C_6H_4C(O)Br$ (3 eq) to **3**. 1,3,5-trimethoxybenzene (2 eq) was added and the product was quantified by ^{1}H NMR spectroscopy. Integration of the methyl groups of 19.26 (δ_H = 9.67 / 9.27 / 8.64, 24H) indicates 80 % spectroscopic yield in **3** and 4-bromobenzonitrile (δ_H = 7.55 ppm, 2H, H-ortho), obtained 65% in yield.*

12.3 Synthesis of 4-methylbenzonitrile

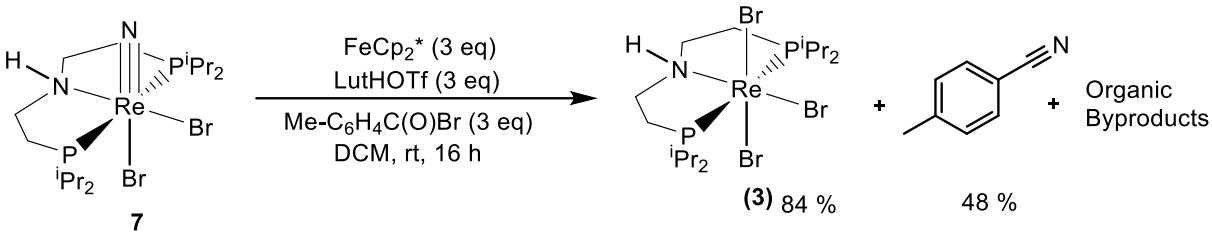

Scheme 43: *Selective synthesis of 4-methylbenzonitrile.*

Complex **7** and 4-methyl benzoyl bromide (3eq) are employed in similar conditions and stirred overnight provided the 84% of complex **3** and 48% of 4-methyl benzonitrile (**Figure 68**). The complex **3** and the 4-methylbenzonitrile are quantified by using 1,3,5-trimethoxybenzene (2.62 eq) as the internal standard. The internal standard is added from the beginning of the reaction which gives a normalised value of 7.87. Other organic by-products are also forming such as 4-methylbenzoic acid and 4-methylbenzoic anhydride but they could not be quantified as they have overlapping signals. The yield of 4-methylbenzonitrile is diminished than that of the 4-bromobenzonitrile, it can be explained because the electron donor nature of the methyl group makes it less electrophile, which does not help the nucleophilic attack of rhenium nitride **7** very much.

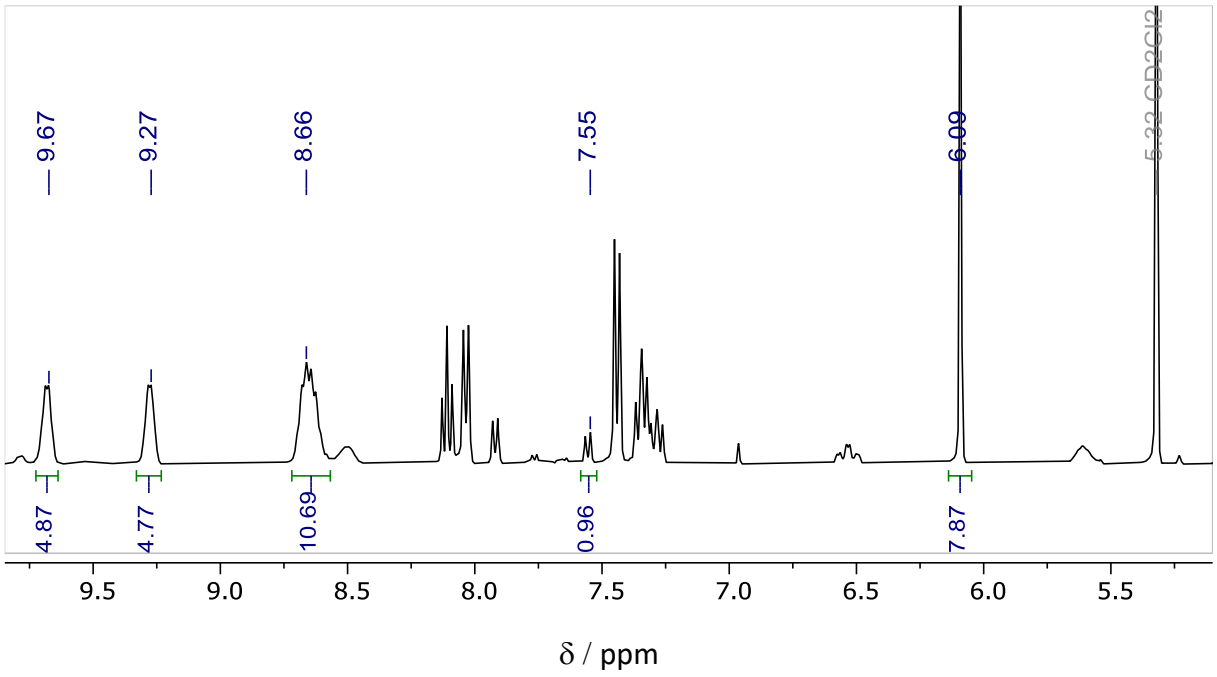

Figure 68. *^{1}H-NMR quantification of the reaction of **7** with $FeCp_2$* (3 eq), LutHOTf (3 eq) and Me-C_6H_4C(O)Br (3 eq) to **3**. 1,3,5-trimethoxybenzene (2.62 eq) was added and the product was quantified by ^{1}H NMR spectroscopy. Integration of the methyl groups of 20.33 (δ_H = 9.67 / 9.27 / 8.66, 24H) indicates 84 % spectroscopic yield in **3** and 4-methylbenzonitrile (δ_H = 7.55 ppm, 2H, H-ortho), obtained 48 % in yield.*

12.4 Synthesis of 4-methoxy benzonitrile

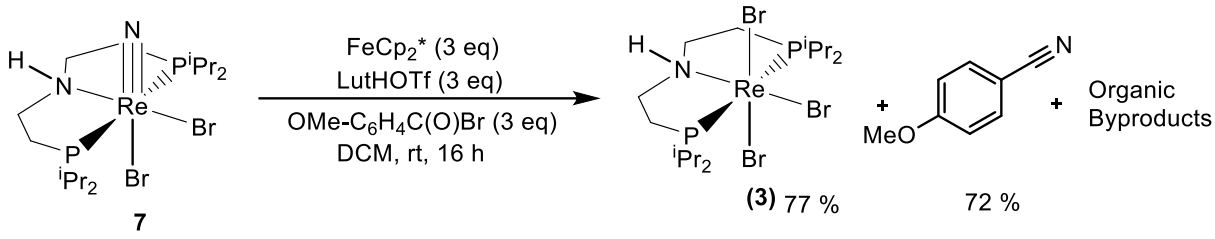

Scheme 44: *Selective synthesis of 4-methoxylbenzonitrile.*

Another electron releasing group substituted benzoyl bromide i.e. 4-methoxybenzoyl bromide (3eq) is treated with complex **7**. Upon adding $FeCp_2^*$ (3 eq), LutHOTf (3 eq) and stirred overnight obtained 77% of complex **3** and 72 % of 4-methoxy benzonitrile (**Figure 69**). 1,3,5-trimethoxybenzene (3.13 eq) is used as the internal standard and it is used from the beginning of the reaction to get a normalised value of 9.39 by which complex **3** and 4-methoxy benzonitrile are quantified. Unexpectedly the yield of 4-methoxy benzonitrile was higher than that of 4-bromobenzonitrile and 4-methylbenzonitrile which may explain because of its steric hindrance. Other organic bioproducts such as 4-methoxy benzonitrile and 4-methoxy benzoic anhydride are also forming but they have identical signals because of which they count to be quantified.

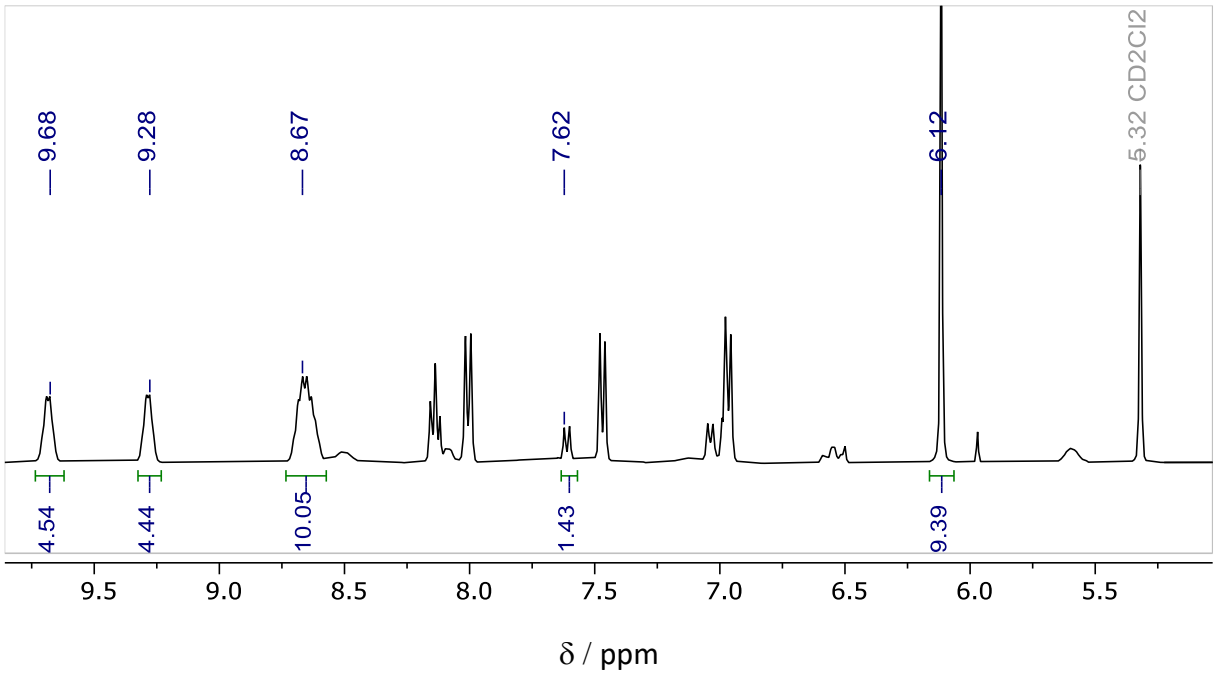

Figure 69. *^{1}H-NMR quantification of the reaction of **7** with $FeCp_2^*$ (3 eq), LutHOTf (3 eq) and OMe-$C_6H_4C(O)Br$ (3 eq) to **3**. 1,3,5-trimethoxybenzene (3.13 eq) was added and the product was quantified by ^{1}H NMR spectroscopy. Integration of the methyl groups of 19.03 (δ_H = 9.68 / 9.28 / 8.67, 24H) indicates 79 % spectroscopic yield in **3** and 4-methoxylbenzonitrile (δ_H = 7.62 ppm, 2H, H-ortho), obtained 72% in yield.*

III. Summary

In summary, the synthesis of rhenium nitride **7** and synthesis of nitrogen-containing organic compounds is demonstrated with a [$ReBr_3$ (PNP)] platform. Two main synthetic cycles are depicted here (**Scheme 45**). The starting complex is treated with TMS-N_3 to get the rhenium terminal nitride which is further employed in the metal-ligand cooperative reaction to get the benzamide and benzonitrile. Moreover, the key intermediate is synthesized and characterized. Also, the generation of benzamide, benzonitrile and complex **5** is explained with **11**. Subsequently, complex **3** is regenerated from complex **5** adding 2 electron and 2 proton sources. So, 4- membered metal-ligand cooperative synthetics of benzamide and benzonitrile are demonstrated successfully by isolating the key intermediate **11**. Unfortunately, the selectivity of benzamide and benzonitrile could not be achieved by this method.

To enhance the selectivity, here the bromide counter anion of complex **11** is changed to the $BArF_{24}$ complex and employed in the metal-ligand cooperative reaction which provided a very similar result. So, different para-substituted benzoyl bromides are synthesized with the help of DBI and oxalyl bromide reagents to play with the electrophilicity of the carbonyl carbon of the benzoyl bromide. They are further employed in the nitride functionalization to get the substituted benzoylimido complex which provided similar results in the metal-ligand cooperative reactions. Therefore, external reductant acids are used to get the benzamide and benzonitrile selectively. Upon reaction of complex **11** with 2 eq of reductant and acid, it regenerates complex **3** and minor amounts of benzamide. So, extra 2 eq of 4-trifluoromethyl benzoyl bromide with **12** in presence of reductant and acid to get the 4-trifluoromethyl benzonitrile selectively. In the process, the complex **15** can be trapped and the substituted benzamide is selectively synthesized by using a LutHBr. Hence, selective synthesis of 4-trifluoromethyl benzamide and 4-trifluoromethylbenzonitrile are demonstrated successfully by the PCET method.

A kinetic study is conducted to investigate the mechanistic pathway of metal-ligand cooperative reactions, but unfortunately, the mechanistic pathway could not depict it as it provided a rate of zero order. Hammett plot for the synthesis of substituted benzoyl imido complexes is plotted which indicates the electron-withdrawing group substituted benzoyl bromide gives better reactivity due to increasing the electrophilicity of the carbonyl carbon, which makes a nucleophilic attack of nitride easier.

A substrate scope for the synthesis of substituted benzonitrile is created where the formation of para-substituted benzonitrile is demonstrated using terminal rhenium nitride complex **7** and substituted benzoyl bromide in presence of reductant and acids.

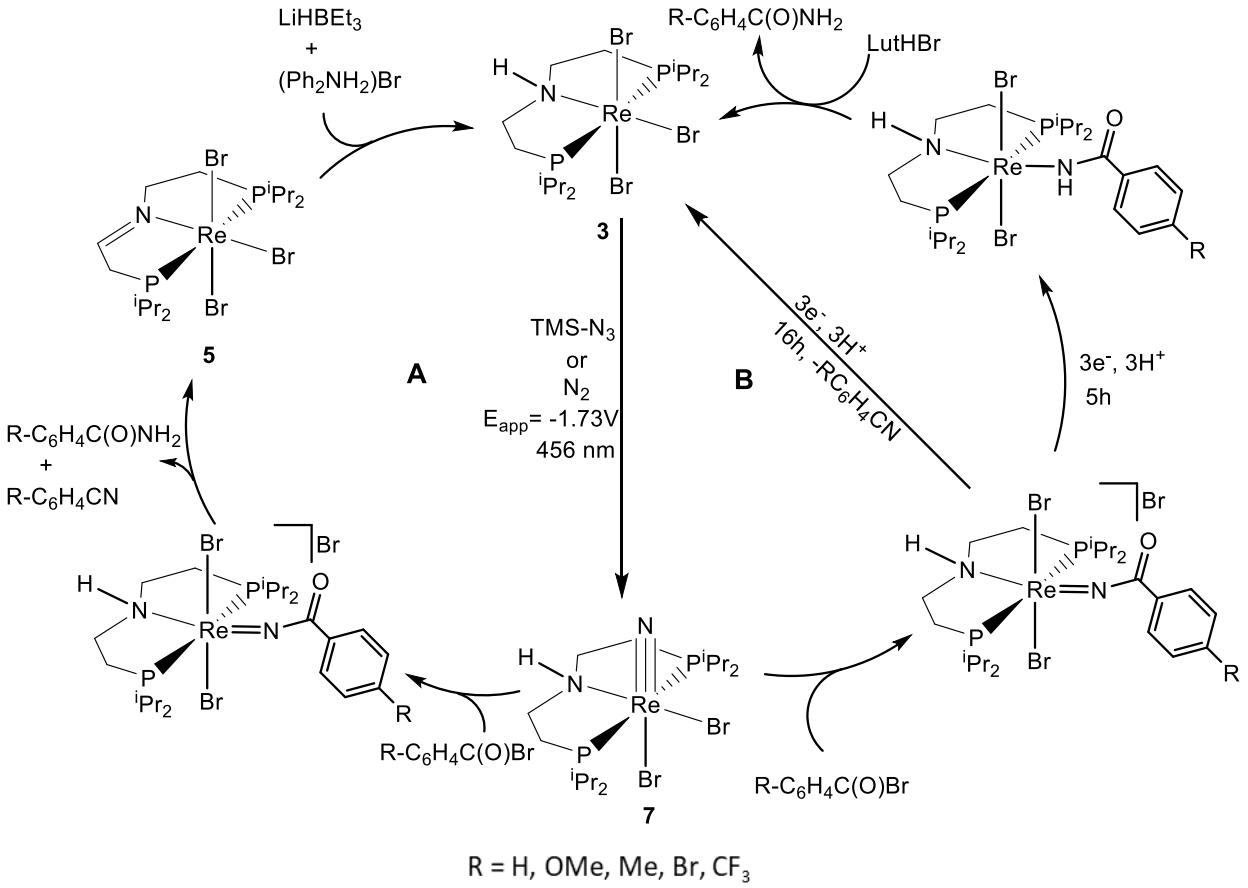

Scheme 45: *Summary- Different routes for the synthesis of organic compounds.*

IV. Experimental details

1. Experimental methods

1.1 Materials and synthetic methods

All experiments were carried out under inert conditions using standard Schlenk and glove-box techniques (argon and nitrogen as an inert gas). All solvents were purchased in HPLC quality (MERCK) and purified using an MBRAUN Solvent Purification System. THF and toluene were additionally dried over Na/K alloy. NMR solvents (THF-d8, toluene-d8, CD_2Cl_2) were obtained from EURISO-TOP GMBH and dried over Na/K alloy (THF-d8, toluene-d8) or CaH_2 (CD_2Cl_2). [$ReBr_3(PPh_3)_2(NCMe)$], Trimethylsilyl azide (TMS-N_3), 2,4,6-tri-tert-butylphenoxy radical were synthesized according established protocols. The employed pincer ligand $HN(CH_2CH_2P^{iPr})_2$ ($HPNP^{iPr}$) was synthesized according to the previously published procedure where tBu_2PCl was replaced with iPr_2PCl. All other chemicals were obtained from commercial sources and used without further purification.

1.2 Analytical methods

NMR data were recorded on machines from BRUKER (Avance III 300, Avance III 400 and Avance 500 with a Prodigy broadband cryoprobe). Spectra were referenced to the residual solvent signals (THF-d8: δ ^1H = 3.58 ppm, δ ^{13}C = 67.2 ppm; toluene-d8: δ ^1H = 2.08 ppm, δ ^{13}C = 20.4 ppm; CD_2Cl_2: δ ^1H = 5.32 ppm, δ ^{13}C = 53.8 ppm). ^{31}P and ^{15}N NMR spectra are reported relative to external standards (phosphoric acid and nitromethane respectively, both defined as δ = 0.0 ppm). Signal multiplicities are abbreviated as: s (singlet), d (doublet), t (triplet), q (quartet), qui (quintet), m (multiplet), br (broad). In all quantitative NMR experiments, the relaxation delay was set to 15 s to allow for full relaxation of all compounds. LIFDI (LINDEN CMS) mass spectra were measured by the Zentrale Massenabteilung, Fakultät für Chemie, Georg-August Universität Göttingen. Elemental analyses were measured on anElementar Vario EL 3 in the Analytisches Labor, Fakultät für Chemie, Gerog-August University Göttingen. UV/Vis spectra were recorded on an AGILENT Cary 300 spectrometer. IR spectra were measured in the solid-state using a BRUKER ALPHA FT-IR spectrometer with a Platinum ATR module. Resonance Raman (rR) spectra were measured using a Horiba Scientific LabRAM HR 800 spectrometer with an open-electrode CCD detector in combination with a free-space optical microscope and a He: Ne-laser (632.8nm). All electrochemical experiments were measured with a GAMRY 600 reference potentiostat or a METROHM Autolab PGSTAT101 potentiostat using GAMRY or NOVA software, respectively. A 0.1 M solution of [^nBu4N][PF_6] in THF was used as an electrolyte and an appropriate iR compensation was applied. Cyclic voltammetry (CV) was measured with a Glassy Carbon disk electrode (⌀ = 3 mm) as a working electrode, a Pt wire as a counter electrode and an Ag wire as a pseudo-reference electrode. Referencing was performed by addition of $FeCp_2$ as internal standard ($E_{1/2}(FeCp_2^+/FeCp_2)$ = 0.0 V). Controlled potential electrolysis (CPE) was carried out with a glass carbon rod as the working electrode. The pseudo-reference electrode and the counter electrode were placed in a fritted sample holder separate compartment. $FeCp^*_2$ was used as a sacrificial reductant.

2. Synthetic procedures

2.1 Re(III) platform

2.1.1 [$ReBr_3(HPNP^{iPr})$](3)

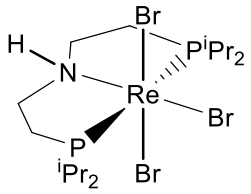

[$ReBr_3(PPh_3)_2$(NCMe)] (800 mg, 0.806 mmol, 1.00 eq) and $HPNP^{iPr}$ (270 mg, 0.884 mmol, 1.1 eq) were suspended in THF (15 mL) and the reaction mixture was stirred overnight at 60 ^{0}C. After 16 h, the solution is cooled to rt and the THF was evaporated out in vacuo. The residue was scratched and washed with Et_2O (3 * 5 mL). The solvent is removed in vacuo and the product of the above light green rhenium complex was obtained (650 mg, 0.888 mmol, 89 %).

^{1}H NMR (500 MHz, CD_2Cl_2): δ (ppm) = 151.3 (s, N*H*), 9.6 (m, 6H, CH(CH_3)$_2$), 9.2 (m, 6H, CH(CH_3)$_2$), 8.6 (m, 6H, CH(CH_3)$_2$), 8.6 (m, 6H, CH(CH_3)$_2$), 8.5 (m, 2H, C*H*(CH$_3$)$_2$), 6.4 (m, 2H, P-C*H*H-CH$_2$), 5.6 (m, 2H, C*H*(CH$_3$)$_2$), -1.0 (m, 2H, P-CH*H*-CH$_2$), -7.0 (m, 2H, N-C*H*H-CH$_2$), -13.3 (m, 2H, N-CH*H*-CH$_2$). **^{13}C{^{1}H} NMR** (125.7 MHz, CD_2Cl_2): δ (ppm) = 176.18 (s, N-*C*H$_2$), 141.26 (s, *C*HMe$_2$), 122.27 (s, *C*HMe$_2$), 65.63 (s, P-*C*H$_2$), 23.22 (s, *C*H$_3$), 20.46 (s, *C*H3), 17.30 (s, *C*H$_3$), 16.63 (s, *C*H$_3$). **^{15}N{^{1}H} NMR** (50.7 MHz, CD_2C_{l2}): δ (ppm) = -1250 (s, *N*H). **^{31}P{^{1}H} NMR** (202.6 MHz, $CD_2C\underline{l}_2$): δ (ppm) = -1491.06 (s). **LIFDI**: m/z (%) = 731.0 (100). **CV**: $E_{1/2}$ vs Fc/Fc^+ (V) = -1.70 ($Re^{II/III}$), -0.19 ($Re^{III/IV}$). **IR** (ATR, cm^{-1}): 3158 (N-H).

2.1.2 [$ReBr_3(PNP^{iPr})$] (4)

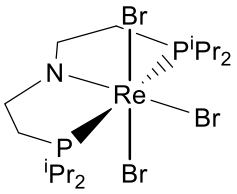

Complex **3** (30.0 mg, 41 µmol, 1.0 eq) and 2,4,6-tri-tert-butylphenoxy radical (10 mg, 41 µmol, 1 eq) are suspended in benzene (5 mL) and stirred at RT for 1 h, resulting in a deep red solution. All volatiles are removed in vacuo. The crude product is washed with pentane (3 * 5 mL) and extracted with benzene. Lyophilization gives **4** as a violate solid (19.0 mg, 26 µmol, 63 %).

^{1}H NMR (400 MHz, CD2Cl2): δ (ppm) = 21.06 (b, 2H), 18.53 (br, 12H), 16.22 (br, 12H), 2.41 (br, 4H). CV: $E_{1/2}$ vs Fc0/+ (V) = -0.93 (Re^{III}/Re^{IV}). **Elem. Anal.** Calcd. for $C_{16}H_{36}Br_3NP_2Re$ (729.94): C, 26.31; H, 4.97; N, 1.92. Found: C, 26.20; H, 4.74; N, 1.89. LIFDI: m/z (%) = 729.9 (100).

2.1.3 $[ReBr_3\{N(CHCH_2P^{iPr})(CH_2CH_2P^{iPr})\}]$(5)

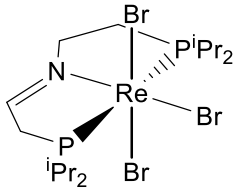

Route A – oxidation of **1**: Complex **3** (50 mg, 68 µmol, 1.0 eq) and 2,4,6-tri-tert-butylphenoxy radical (37.35 mg, 136 µmol, 2.0 eq) are mixed in benzene (0.5 mL) and stirred at 60 °C overnight. After 16 h the solvent is removed in vacuo. The product is washed with Et_2O and benzene and subsequently extracted with DCM. The product complex **4** was obtained as a grey powder (42 mg, 57 µmol, 84 %).

^{1}H NMR (500 MHz, CD_2Cl_2): δ (ppm) = 59.56 (s, 2H, P-CH_2-CH), 9.71 (dd, $^3J_{HH}$ = 6.8 Hz, $^3J_{HP}$ = 10.0 Hz, 6H, CH(CH_3)$_2$), 9.53 (dd, $^3J_{HH}$ = 7.2 Hz, $^3J_{HP}$ = 13.3 Hz, 6H, CH(CH_3)$_2$), 9.46 (m, $^3J_{HH}$ = 7.3 Hz, 2H, CH(CH$_3$)$_2$), 9.18 (dd, $^3J_{HH}$ = 6.8 Hz, $^3J_{HP}$ = 12.7 Hz, 6H, CH(CH_3)$_2$), 7.46 (dd, $^3J_{HH}$ = 7.2 Hz, $^3J_{HP}$ = 15.1 Hz, 6H, CH(CH_3)$_2$), 5.84 (m, $^3J_{HH}$ = 7.1 Hz, 2H, CH(CH$_3$)$_2$), 2.18 (m, $^3J_{HH}$ = 6.2 Hz, 2H, P-CH_2-CH$_2$), -18.13 (m, $^3J_{HH}$ = 6.2 Hz, 2H, N-CH_2-CH$_2$), -71.42 (d, $^3J_{HP}$ = 14.6 Hz, 1H, N-CH-CH$_2$). $^3J_{HH}$ coupling constants were assigned by ^{1}H{^{31}P} spectroscopy. **^{13}C{^{1}H} NMR** (125.7 MHz, CD2Cl2): δ (ppm) 358 (s, N-CH-CH$_2$), 276.89 (s, P-CH$_2$-CH$_2$), 156.18 (s, CH(CH$_3$)$_2$), 153.36 (s, N-CH$_2$-CH$_2$), 131.68 (s, CH(CH$_3$)$_2$), 54.43 (s, P-CH$_2$-CH$_2$), 24.44 (s, CH(CH_3)$_2$), 21.07 (s, CH(CH_3)$_2$), 19.63 (s, CH(CH_3)$_2$), 18.67 (s, CH(CH$_3$)$_2$). **^{31}P{^{1}H} NMR** (202.6 MHz, CD_2Cl_2): δ (ppm) = -1501.19 (d, $^2J_{PP}$ = 247.6 Hz), - 1512.76 (d, $^2J_{PP}$ = 248.1 Hz). **CV:** $E_{1/2}$ vs Fc/Fc^+ (V) = -1.53 (Re^{II}/Re^{III}), -0.14 (Re^{III}/Re^{IV}). **Elem. Anal**. Calcd. for $C_{16}H_{35}Br_3NP_2Re$ (728.93): C, 26.35; H, 4.84; N, 1.92. Found: C, 26.02; H, 4.52; N, 1.83. **LIFDI**: m/z (%) = 728.9 (100). **IR** (ATR, cm^{-1}): 1603 (N=C).

Route B – reaction of **2** with benzoyl bromide: Rhenium nitride complex 2 (10 mg, 15 µmol, 1.0 eq) and benzoyl chloride (3.5 µL, 30 µmol, 2.0 eq) are mixed in 1,4-dioxane and heated to 60 °C for 15 h. All volatiles are subsequently removed in vacuo and 1,3,5-trimethoxybenzene (2.5 mg, 15 µmol, 1 eq) is added as an internal standard. NMR spectroscopic examination in CD_2Cl_2 reveals the formation of 4 in 60.0 % yield. NMR spectroscopic features as well as the LIFDI mass spectrum are identical to those of 4 obtained from route A.

The reaction is accompanied by the formation of benzamide (28 % spectroscopic yield) and equimolar amounts of benzoic acid and a benzonitrile (64 % spectroscopic yield each), respectively. Benzonitrile can be detected when the reaction is carried out in toluene-d8. Use of 1 eq benzoyl chloride results in incomplete conversion of 2.

Route C – reaction of **3** with benzoyl bromide: Rhenium complex 3 (10 mg, 11.7 µmol, 1.0 eq) and benzoyl chloride (1.4 µL, 11.7 µmol, 1.0 eq) are mixed in 1,4-dioxane and heated to 60 °C for 12 h. All volatiles are subsequently removed in vacuo and 1,3,5-trimethoxybenzene (2 mg, 11.7 µmol, 1 eq) is added as an internal standard. NMR spectroscopic examination in CD_2Cl_2 reveals the formation of 4 in 54.0 % yield. NMR spectroscopic features as well as the LIFDI mass spectrum are identical to those of 4 obtained from route A. The reaction is accompanied by the formation of benzamide (24 % spectroscopic yield) and equimolar amounts of benzoic acid and benzonitrile (60 % spectroscopic yield each), respectively.

2.1.4 $[ReBr_3\{N(CHCHP^{iPr})_2]$ (6)

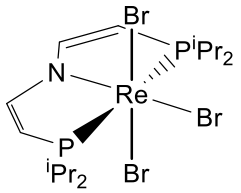

Route A-Complex **3** (30.0 mg, 50.2 µmol, 1.0 eq) and 2,4,6-tri-tert-butylphenoxy radical (14.4 mg, 55.2 µmol, 6.1 eq) are suspended in benzene (5 mL) and stirred at RT for 1.5 h, resulting in a deep red solution. All volatiles are removed in vacuo. The crude product is washed with pentane and extracted with benzene. Lyophilization gives 8 as a red powder (19.0 mg, 31.8 µmol, 70 %).

Route B-Complex 1 (30.0 mg, 50.2 µmol, 1.0 eq) and 2,4,6-tri-tert-butylphenoxy radical (14.4 mg, 55.2 µmol, 6.1 eq) are suspended in benzene (5 mL) and stirred at RT for 1.5 h, resulting in a deep red solution. All volatiles are removed in vacuo. The crude product is washed with pentane and extracted with benzene. Lyophilization gives 8 as a red powder (19.0 mg, 31.8 µmol, 63 %).

^{1}H NMR (400 MHz, CD_2Cl_2): δ (ppm) = 13.03 (br, 6H), 12.59 (br, 6H), 11.26 (br, 6H), 11.11 (br, 6H) 7.82 (br, 2H), 6.40 (br, 6H), -13.80 (br, 2H), -51.36 (br, 2H). CV: E1/2 vs Fc0/+ (V) = (Re^{III}/Re^{IV}). Elem. Anal. Calcd. for C16H36Cl3NP2Re (725.9): C, 26.31; H, 4.97; N, 1.92. Found: C, 26.82; H, 5.02; N, 1.90. **LIFDI**: m/z (%) = 725.9 (100)

2.2 Nitride synthesis and functionalization

2.2.1 [Re(N)Br$_2$(HPNP^{iPr})](7)

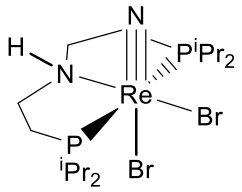

Azide as nitrogen source: Complex **3** (200 mg, 270 µmol, 1.0 eq) and [TMS]N_3 (40 µl, 300 µmol, 1 eq) are mixed in THF (3 mL) and stirred at 60 °C for 6 h. After that, the solvent was removed in vacuo and the product was washed with ether. Then the solvent was dried completely to obtain an orange brown product (170 mg, 250 µmol, 93%).

^{1}H NMR (500 MHz, CD_2Cl_2): δ (ppm) = 5.18 (t, $^1J_{NH}$ = 12.5 Hz, 1H, N*H*), 3.64 (m, 2H, N-C*H*H-CH2), 3.14 (m, $^3J_{HH}$ = 7.3 Hz, 2H, C*H*Me$_2$), 2.55 (m, 2H, N-CH*H*-CH2), 2.36 (m, $^3J_{HH}$ = 6.9 Hz, 2H, C*H*Me$_2$), 2.03 (m, 2H, P-C*H*H-CH2), 1.61 (m, 2H, P-CH*H*-CH2), 1.61 (m, $^3J_{HH}$ = 7.4 Hz, 6H, CH(C*H*$_3$)$_2$), 1.56 (m, $^3J_{HH}$ = 6.9 Hz, 6H, CH(C*H*$_3$)$_2$), 1.34 (m, $^3J_{HH}$ = 7.1 Hz, 6H, CH(C*H*$_3$)$_2$), 1.33 (m, $^3J_{HH}$ = 7.2 Hz, 6H, CH(C*H*$_3$)$_2$). For the assignment of J_{HH} coupling constants, a ^{1}H{^{31}P} spectrum was measured. **^{13}C{^{1}H} NMR** (125.7 MHz, CD_2Cl_2): δ (ppm) = 62.78 (s, N-*C*H$_2$), 31.50 (AXY, N = |$^1J_{AX}$ + $^3J_{AY}$| = 24.6 Hz, P-*C*H2), 28.59 (AXY, N = |= |$^1J_{AX}$ + $^3J_{AY}$| = 27.2 Hz, *C*HMe$_2$), 25.33 (AXY, N = |$^1J_{AX}$ + $^3J_{AY}$| = 20.2 Hz, *C*HMe$_2$), 21.58 (s, *C*H$_3$), 19.2 (s, *C*H$_3$), 18.34 (s, *C*H$_3$), 18.22 (s, *C*H$_3$). **^{15}N{1H} NMR** (50.7 MHz, CD_2Cl_2): δ (ppm) = -331.75 (s, *N*H). **^{31}P{^{1}H} NMR** (202.6 MHz, CD_2Cl_2): δ (ppm) = 31.37 (s). **CV**: $E_{1/2}$ vs Fc/Fc+ (V) = +0.06 (Re^V/Re^{VI}). **LIFDI**: m/z (%) = 665.90 (100). **IR** (ATR, cm^{-1}): 3140 (N-H), 1450 (Re=N).

2.2.2 [Re(N)Br$_2${N(CHCH$_2$P^{iPr})(CH$_2$CH$_2$P^{iPr})}] (9)

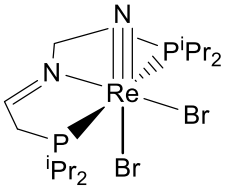

Complex **5** (50 mg, 6.8 µmol, 1.0 eq) and [TMS]N_3 (10 µl, 68 µmol, 1 eq) are mixed in THF (5 mL) and stirred at 60 °C for 2 days. The volatiles was removed in vacuo and the crude product was purified by column chromatography in benzene over silanized silica gel. The solvent was removed in vacuo to obtain **9** as a reddish-brown product (31 mg, µmol, 70%).

^{1}H NMR (400 MHz, CD_2Cl_2): δ (ppm) = 4.30 (m, 1H), 3.60 (m, 2H), 3.24 (m, 2H), 2.62 (m, 2H), 2.30 (m, 2H), 2.18 (m, 2H), 1.46 (m, 24 H). **^{31}P{^{1}H} NMR** (202.6 MHz, CD_2Cl_2): δ (ppm) = 48.13 (d, $^{2}J_{PP}$ = 247.6 Hz), 32.10 (d, $^{2}J_{PP}$ = 248.1 Hz). **CV**: $E_{1/2}$ vs $Fc^{0/+}$ (V) = 0.06 (Re^{V}/Re^{VI}). **LIFDI**: m/z (%) = 662.02 (100)

2.2.3 [Re(PhC(O)N)Br$_2$(PNP^{iPr})](10)

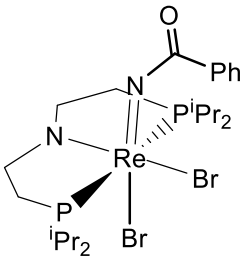

Addition benzoyl bromide (3.2 µl, 27 µmol, 1 eq) to the THF (2mL) solution of [Re(N)Br(PNP^{iPr})] (16 mg, 27 µmol, 1 eq), stirring at rt gives the purple coloured solution within no time. Subsequently, the solvent is evaporated out and washed with minimal amount of pentane and further, it was extracted with Et_2O. The solvent was evaporated out in vaccuo and the green complex **10** is obtained (18 mg, 23 µmol, 87 %).

^{1}H{^{31}P} NMR (400 MHz, THF-d8): δ (ppm) = 8.14 (d, $^{3}J_{HH}$ = 8 Hz, 2H, ArC*H*), 7.41 (m, 3H, ArC*H*), 4.64 (m, 2H, N-CH*H*-CH_2-P), 4.08 (m, 2H, C*H*Me_2), 3.29 (m, 2H, C*H*Me_2), 2.46 (m, 2H, N-CH*H*-CH_2-P), 2.23 (m, 2H, N-CH_2-C*H*H-P), 1.92 (m, 2H, N-CH_2-CH*H*-P), 1.67 (m, 6H, CH_3), 1.43 (m, 12H, CH_3), 1.04 (m, 6H, CH_3). **^{31}P{^{1}H} NMR** (202.6 MHz, THF-d8): δ (ppm) = 28.09 (s). **LIFDI**: m/z (%) = 768.06 (100). **IR** (ATR, cm^{-1}): 1607 (C=O).

2.2.4 [Re(PhC(O)N)Br$_2$(HPNP^{iPr})]Br(11)

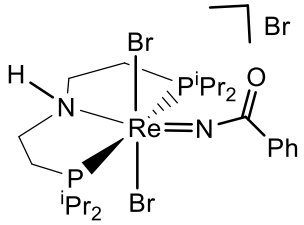

Route A (in DCM): [Re(N)Br$_2$(HPNP^{iPr})] (30 mg, 45 µmol, 1.0 eq) and benzoyl bromide (5.8 µl, 45 µmol, 1 eq) are mixed in DCM (2 mL) and stirred at rt for 2h. Subsequently, solvent is evaporated out and washed with minimal amount of THF and further, it was extracted with DCM. The solvent was evaporated out in vaccuo and the green complex **11** is obtained (33 mg, 38 µmol, 86 %).

Route B (in THF): [Re(N)Br$_2$(*H*PNP^{iPr})] (20 mg, 30 µmol, 1.0 eq) and benzoyl bromide (3.9 µl, 33 µmol, 1.1 eq) are mixed in THF (2 mL) and stirred at rt for 5h. Later the green precipitated product is filtered out and washed with minimal amount of THF and further it was extracted with DCM. The solvent was evaporated out in vaccuo and the green complex **11** is obtained

(18 mg, 21 µmol, 72 %). Absolute dissolving rhenium nitride before adding benzoyl bromide may not give precipitation of product due to equilibrium.

Route C: To the complex [Re(N)Br(PNP^{iPr})] (16 mg, 27 µmol, 1.0 eq), step wise addition of benzoyl bromide (3.22 µl, 27 µmol, 1 eq) and diphenyl ammonium bromide (6.8 mg, 27 µmol, 1 eq), stirring for 2h at room temperature provided complex **11** (18 mg, 22 µmol), 80% in yield after evaporating the solvent and extracted with DCM.

^{1}H{^{31}P} NMR (500 MHz, CD_2Cl_2): δ (ppm) = 8.02 (d, $^{3}J_{HH}$ = 7.9 Hz, 2H, ArC*H*), 7.69 (t, $^{3}J_{HH}$ = 7.4 Hz, 1H, ArC*H*), 7.55 (t, $^{3}J_{HH}$ = 7.9Hz, 2H, ArC*H*), 5.53 (t, $^{1}J_{NH}$ = 9.7 Hz, 1H, N*H*), 3.67 (m, 4H, N-CH*H*-CH_2-P, C*H*Me_2, signals superimposed), 3.49 (h, $^{3}J_{HH}$ = 7.3 Hz, 2H, C*H*Me_2), 2.70 (m, $^{3}J_{HH}$ = 7.3 Hz, 2H, N-CH*H*-CH_2-P), 2.53 (dt, $^{3}J_{HH}$ = 5.5 Hz, $^{3}J_{HH}$ = 13.8 Hz, 4 H, N-CH_2-C*H*H-P and N-CH_2-CH*H*-P), 1.53 (d, $^{3}J_{HH}$ = 6.8 Hz, $^{3}J_{HP}$ = 10.0 Hz, 6H, CH_3), 1.48 (d, $^{3}J_{HH}$ = 7.2 Hz, $^{3}J_{HP}$ = 13.3 Hz, 12H, CH_3), 1.25 (d, $^{3}J_{HH}$ = 6.8 Hz, $^{3}J_{HP}$ = 12.7 Hz, 6H, CH_3). **^{13}C{^{1}H}** NMR (125.7 MHz, CD_2Cl_2): δ (ppm) = 177.04 (s, Ar*C*O), 136.67 (s, Ar*C*), 131.33 (s, Ar*C*H), 129.94 (s, Ar*C*H), 129.2 (s, Ar*C*), 51.8 (s, N-*C*H_2-CH_2-P), 27.2 (m, N-*C*H_2-*C*H_2-P, *C*HMe_2, signals superimposed), 25.6 (AXY, N = $|^{1}J_{AX} + {}^{3}J_{AY}|$ = 24.5 Hz, *C*HMe_2), 19.9 (s, *C*H_3), 19.83 (s, *C*H_3), 19.34 (s, *C*H_3), 19.16 (s, *C*H_3). **^{31}P{^{1}H} NMR** (202.6 MHz, CD_2Cl_2): δ (ppm) = 33.26 (s). **CV**: $E_{1/2}$ vs $Fc^{0/+}$ (V) = -0.5 (Re^{V}/Re^{VI}). **Elem. Anal.** Calcd. For $C_{23}H_{42}Br_3N_2OP_2Re$: C, 32.48; H, 4.98; N, 3.29. Found: C, 32.58; H, 5.07; N, 3.23. **LIFDI**: m/z (%) = 770.00 (100). **IR** (ATR, cm^{-1}): 2963 (N-H), 1693 (C=O).

2.2.5 [Re{p-CF_3(C_6H_4)C(O)N}Br_2(HPNP^{iPr})]Br(12)

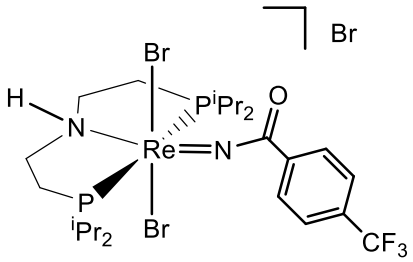

[Re(N)Br_2(HPNP^{iPr})] (30 mg, 45 µmol, 1.0 eq) and 4-trifluoromethylbenzoyl bromide (6.84 µl, 45 µmol, 1 eq) are mixed in DCM (2 mL) and stirred at rt for 2h. Subsequently, solvent is evaporated out and washed with minimal amount of THF and further, it was extracted with DCM. The solvent was evaporated out in vacuo and the green complex **12** is obtained (36 mg, 39 µmol, 88 %).

^{1}H{^{31}P} NMR (500 MHz, CD_2Cl_2): δ (ppm) = 8.15 (d, $^{3}J_{HH}$ = 7.9 Hz, 2H, ArC*H*), 7.82 (d, $^{3}J_{HH}$ = 7.4 Hz, 2H, ArC*H*), 5.68 (t, $^{1}J_{NH}$ = 9.7 Hz, 1H, N*H*), 3.63 (m, 4H, N-CH*H*-CH_2-P, C*H*Me_2, signals superimposed), 3.46 (h, $^{3}J_{HH}$ = 7.3 Hz, 2H, C*H*Me_2), 2.71 (m, $^{3}J_{HH}$ = 7.3 Hz, 2H, N-CH*H*-CH_2-P), 2.55 (dt, $^{3}J_{HH}$ = 5.5 Hz, $^{3}J_{HH}$ = 13.8 Hz, 2H, N-CH_2-C*H*H-P), 2.46 (m, 2H, N-CH_2-CH*H*-P), 1.55 (d, $^{3}J_{HH}$ = 6.8 Hz, $^{3}J_{HP}$ = 10.0 Hz, 6H, CH_3), 1.5 (d, $^{3}J_{HH}$ = 7.2 Hz, $^{3}J_{HP}$ = 13.3 Hz, 12H, CH_3), 1.24 (d, $^{3}J_{HH}$ = 6.8 Hz, $^{3}J_{HP}$ = 12.7 Hz, 6H, CH_3). **^{13}C{^{1}H}** NMR (125.7 MHz, CD_2Cl_2): δ (ppm) = 176.03 (s,

Ar*C*O), 136.40 (s, Ar*C*H), 131.70 (q, Ar*C*H), 131.11 (s, Ar*C*H), 126.37 (s, Ar*C*), 120.79 (s, *C*F_3), 51.55 (s, N-*C*H_2-CH_2-P), 27.00 (q, N-*C*H_2-*C*H_2-P), 26.67 (q, *C*HMe_2), 19.36 (s, *C*H_3), 18.79 (s, *C*H_3), 18.59 (s, *C*H_3), 17.67 (s, *C*H_3). **^{31}P{^{1}H} NMR** (202.6 MHz, CD_2Cl_2): δ (ppm) = 33.29 (s). **^{19}F{^{1}H} NMR** (470.38 MHz, CD_2Cl_2): δ (ppm) = -63.83 (s). **CV**: $E_{1/2}$ vs $Fc^{0/+}$ (V) = -0.44 (Re^{V}/Re^{VI}). **Elem. Anal.** Calcd. For $C_{24}H_{41}Br_3N_2OP_2F_3Re$: C, 32.17; H, 4.75; N, 3.0. Found: C, 32.50; H, 5.12; N, 3.0. **LIFDI**: m/z (%) = 839.06 (100). **IR** (ATR, cm^{-1}): 2963 (N-H), 1680 (C=O).

2.2.6[Re{p-CH_3(C_6H_4)C(O)N}Br_2(HPNP^{iPr})]Br(13)

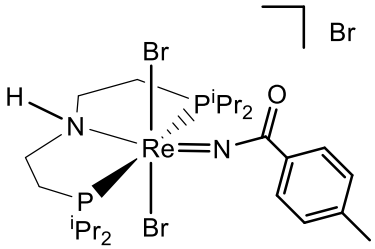

[Re(N)Br_2(HPNP^{iPr})] (40 mg, 60 µmol, 1.0 eq) and 4-methylbenzoyl bromide (8 µl, 60 µmol, 1 eq) are mixed in DCM (2 mL) and stirred at rt for 2h. Subsequently, the solvent is evaporated out and washed with minimal amount of THF and further, it was extracted with DCM. The solvent was evaporated out in vacuo and the green complex **13** is obtained (45 mg, 52 µmol, 87 %).

^{1}H{^{31}P} NMR (500 MHz, CD_2Cl_2): δ (ppm) = 7.93 (d, $^{3}J_{HH}$ = 7.9 Hz, 2H, Ar*CH*), 7.35 (d, $^{3}J_{HH}$ = 7.4 Hz, 2H, Ar*CH*), 5.50 (t, $^{1}J_{NH}$ = 9.7 Hz, 1H, N*H*), 3.68 (m, 4H, N-CH*H*-CH_2-P, C*H*Me_2, signals superimposed), 3.49 (h, $^{3}J_{HH}$ = 7.3 Hz, 2H, C*H*Me_2), 2.70 (m, $^{3}J_{HH}$ = 7.3 Hz, 2H, N-CH*H*-CH_2-P), 2.46 (m, $^{3}J_{HH}$ = 5.5 Hz, $^{3}J_{HH}$ = 13.8 Hz, 7H, N-CH_2-C*H*H-P, N-CH_2-CH*H*-P and CH_3 signal superimposed), 1.54 (d, $^{3}J_{HH}$ = 6.8 Hz, $^{3}J_{HP}$ = 10.0 Hz, 6H, CH_3), 1.48 (d, $^{3}J_{HH}$ = 7.2 Hz, $^{3}J_{HP}$ = 13.3 Hz, 12H, CH_3), 1.25 (d, $^{3}J_{HH}$ = 6.8 Hz, $^{3}J_{HP}$ = 12.7 Hz, 6H, CH_3). **^{13}C{^{1}H}** NMR (125.7 MHz, CD_2Cl_2): δ (ppm) = 176.07 (s, Ar*C*O), 148.21 (s, Ar*C*H), 130.92 (s, Ar*C*H), 130.17 (s, Ar*C*H), 126.00 (s, Ar*C*), 67.74 (s, *C*H_3), 51.20 (s, N-*C*H_2-CH_2-P), 26.68 (s, N-*C*H_2-*C*H_2-P), 24.96 (s, *C*HMe_2), 21.83 (s, *C*H_3), 19.35 (s, *C*H_3), 19.29 (s, *C*H_3), 18.61 (s, *C*H_3). **^{31}P{^{1}H} NMR** (202.6 MHz, CD_2Cl_2): δ (ppm) = 33.45 (s). **CV**: $E_{1/2}$ vs $Fc^{0/+}$ (V) = -0.56 (Re^{V}/Re^{VI}).

2.2.7 [Re{p-OCH_3(C_6H_4)C(O)N}Br_2(HPNP^{iPr})]Br(14)

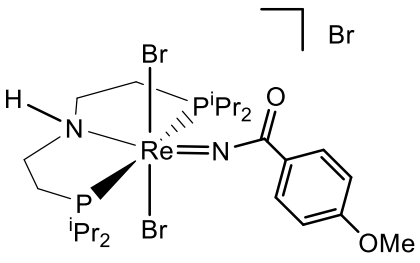

[Re(N)Br_2(*H*PNP^{iPr})] (40 mg, 60 µmol, 1.0 eq) and 4-methoxylbenzoyl bromide (8.6 µl, 60 µmol, 1 eq) are mixed in DCM (3 mL) and stirred at rt for 2h. Subsequently, the solvent is evaporated out and washed with minimal amount of THF and further, it was extracted with DCM. The solvent was evaporated out in vacuo and the green complex **14** is obtained (45 mg, 51 µmol, 85 %).

^{1}H{^{31}P} NMR (500 MHz, CD_2Cl_2): δ (ppm) = 8.04 (d, $^3J_{HH}$ = 7.9 Hz, 2H, ArC*H*), 7.05 (d, $^3J_{HH}$ = 7.4 Hz, 2H, ArC*H*), 5.50 (t, $^1J_{NH}$ = 9.7 Hz, 1H, N*H*), 3.94 (s, O*C*H_3), 3.70 (m, 4H, N-CH*H*-CH_2-P, C*H*Me_2, signals superimposed), 3.51 (h, $^3J_{HH}$ = 7.3 Hz, 2H, C*H*Me_2), 2.74 (m, $^3J_{HH}$ = 7.3 Hz, 2H, N-CH*H*-CH_2-P), 2.53 (m, $^3J_{HH}$ = 5.5 Hz, $^3J_{HH}$ = 13.8 Hz, 4H, N-CH_2-C*H*H-P, N-CH_2-CH*H*-P), 1.56 (d, $^3J_{HH}$ = 6.8 Hz, $^3J_{HP}$ = 10.0 Hz, 6H, C*H*$_3$), 1.50 (d, $^3J_{HH}$ = 7.2 Hz, $^3J_{HP}$ = 13.3 Hz, 12H, C*H*$_3$), 1.29 (d, $^3J_{HH}$ = 6.8 Hz, $^3J_{HP}$ = 12.7 Hz, 6H, C*H*$_3$). **^{13}C{^{1}H}** NMR (125.7 MHz, CD_2Cl_2): δ (ppm) = 175.11 (s, Ar*C*O), 166.14 (s, Ar*C*), 133.52 (s, Ar*C*H), 121.00 (s, Ar*C*), 114.93 (s, Ar*C*H), 67.74 (s, O*C*H_3), 55.98 (s, N-*C*H_2-CH_2-P), 51.09 (s, N-CH_2-*C*H_2-P), 26.56 (s, *C*HMe_2), 19.37 (s, *C*H_3), 19.29 (s, *C*H_3), 18.78 (s, *C*H_3), 18.62 (s, *C*H_3). **^{31}P{^{1}H} NMR** (202.6 MHz, CD_2Cl_2): δ (ppm) = 33.63 (s). **Elem. Anal.** Calcd. For $C_{24}H_{44}Br_3N_2O_2P_2Re$: C, 32.74; H, 5.04; N, 3.14. Found: C, 32.21; H, 5.19; N, 3.14.

2.2.8 [Re{p-Br(C_6H_4)C(O)N}Br_2(HPNP^{iPr})]Br(16)

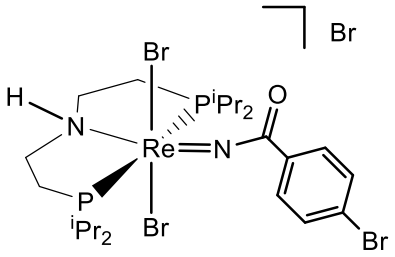

[Re(N)Br_2(HPNP^{iPr})] (50 mg, 75 µmol, 1.0 eq) and 4-bromobenzoyl bromide (9.8 µl, 75 µmol, 1 eq) are mixed in DCM (3 mL) and stirred at rt for 2h. Subsequently, the solvent is evaporated out and washed with minimal amount of THF and further, it was extracted with DCM. The solvent was evaporated out in vacuo and the green complex **16** is obtained (57 mg, 61 µmol, 82 %).

^{1}H{^{31}P} NMR (500 MHz, CD_2Cl_2): δ (ppm) = 7.90 (d, $^3J_{HH}$ = 7.9 Hz, 2H, ArC*H*), 7.72 (d, $^3J_{HH}$ = 7.4 Hz, 2H, ArC*H*), 5.61 (t, $^1J_{NH}$ = 9.7 Hz, 1H, N*H*), 3.67 (m, 4H, N-CH*H*-CH_2-P, C*H*Me_2, signals superimposed), 3.49 (h, $^3J_{HH}$ = 7.3 Hz, 2H, C*H*Me_2), 2.70 (m, $^3J_{HH}$ = 7.3 Hz, 2H, N-CH*H*-CH_2-P), 2.55 (m, $^3J_{HH}$ = 5.5 Hz, $^3J_{HH}$ = 13.8 Hz, 4H, N-CH_2-C*H*H-P, N-CH_2-CH*H*-P), 1.55 (d, $^3J_{HH}$ = 6.8 Hz, $^3J_{HP}$ = 10.0 Hz, 6H, C*H*$_3$), 1.49 (d, $^3J_{HH}$ = 7.2 Hz, $^3J_{HP}$ = 13.3 Hz, 12H, C*H*$_3$), 1.25 (d, $^3J_{HH}$ = 6.8 Hz, $^3J_{HP}$ = 12.7 Hz, 6H, C*H*$_3$). **^{13}C{^{1}H}** NMR (125.7 MHz, CD_2Cl_2): δ (ppm) = 176.03 (s, Ar*C*O), 132.89 (s, Ar*C*H), 132.00 (s, Ar*C*H), 127.53 (s, Ar*C*), 67.74 (s, Ar*C*), 51.50 (s, N-*C*H_2-CH_2-P), 26.72 (q, N-CH_2-*C*H_2-P), 25.20 (s, *C*HMe_2), 19.37 (s, *C*H_3), 19.32 (s, *C*H_3), 18.79 (s, *C*H_3), 18.60 (s, *C*H_3). **^{31}P{^{1}H} NMR** (202.6 MHz, CD_2Cl_2): δ (ppm) = 33.56 (s). **Elem. Anal.** Calcd. For $C_{24}H_{44}Br_3N_2O_2P_2Re$: C, 32.74; H, 5.04; N, 3.14. Found: C, 32.21; H, 5.19; N, 3.14.

2.2.9 [Re{p-$CF_3(C_6H_4)$C(O)NH}Br_2(HPNP^{iPr})](15)

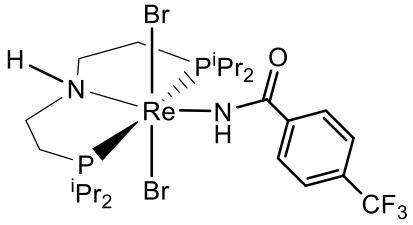

Route A: [Re(N)Br_2(HPNP^{iPr})] (15 mg, 22 µmol, 1.0 eq) reacted with 4-trifluoromethylbenzoyl bromide (10 µl, 66 µmol, 3 eq) are mixed in DCM (2 mL) in presence of decamethylferrocene (22 mg, 66 µmol, 3.0 eq) and LutHBr (13 mg, 66 µmol, 3.0 eq). The reaction mixture is stirred at rt for 5h. Subsequently, the solvent is evaporated out and washed with minimal amount of Et_2O and further, it was extracted with benzene. The solvent was evaporated out in vaccuo and the green complex **15** is obtained (17 mg, 20 µmol, 90 %).

Route B: [Re{p-$CF_3(C_6H_4)$(CO)N}Br_2(HPNP^{iPr})]Br (30 mg, 32 µmol, 1.0 eq) reacted with 4-trifluoromethylbenzoyl bromide (9.8 µl, 64 µmol, 2 eq) are mixed in DCM (3 mL) in presence of decamethylferrocene (32 mg, 98 µmol, 3.0 eq) and LutHBr (18.5 mg, 98 µmol, 3.0 eq). The reaction mixture is stirred at rt for 5h. Subsequently, the solvent is evaporated out and washed with minimal amount of Et_2O and further, it was extracted with benzene. The solvent was evaporated out in vacuo and the green complex **15** is obtained (24 mg, 29 µmol, 90 %).

^{1}H{^{31}P} NMR (500 MHz, CD_2Cl_2): δ (ppm) = 214.4 (s, 1H, N*H*, *H*PNP), 18.2 (d, $^3J_{HH}$ = 7.9 Hz, 2H, ArC*H*), 17.4 (d, $^3J_{HH}$ = 7.4 Hz, 2H, ArC*H*), 12.2 (d, $^3J_{HH}$ = 7.3 Hz, 2H, C*H*Me$_2$), 10.6 (d, $^3J_{HH}$ = 6.8 Hz, $^3J_{HP}$ = 7.9 Hz, 6H, C*H*$_3$), 10.1 (d, $^3J_{HH}$ = 6.8 Hz, $^3J_{HP}$ = 7.9 Hz, 6H, C*H*$_3$), 8.5 (d, $^3J_{HH}$ = 6.8 Hz, $^3J_{HP}$ = 7.9 Hz, 6H, C*H*$_3$), 8.0 (d, $^3J_{HH}$ = 6.8 Hz, $^3J_{HP}$ = 7.9 Hz, 6H, C*H*$_3$), 6.4 (d, $^3J_{HH}$ = 7.3 Hz, 2H, C*H*Me$_2$), 5.84 (m, $^3J_{HH}$ = 7.3 Hz, 2H, N-CH*H*-CH$_2$-P), 2.28 (s, 1H, N*H*), -14.1 (d, $^3J_{HH}$ = 25 Hz, 2H, N-CH$_2$-C*H*H-P), -18.3 (m, $^3J_{HH}$ = 20 Hz, 2H, N-CH$_2$-CH*H*-P), -38.9 (s, 2H, N-C*H*H-CH$_2$-P).**^{13}C{^{1}H}** NMR (125.7 MHz, CD_2Cl_2): δ (ppm) = 223.6 (s, Ar*C*O), 146.40 (s, Ar*C*H), 122.8 (s, Ar*C*H), 31.9 (s, *C*H$_3$), 31.0 (s, *C*H$_3$), 13.3 (s, *C*H$_3$), 10.7 (s, *C*H$_3$). **^{31}P{^{1}H} NMR** (202.6 MHz, CD_2Cl_2): δ (ppm) = -1270 (s). **Elem. Anal.** Calcd. For $C_{24}H_{42}Br_2N_2OP_2F_3Re$: C, 34.33; H, 5.04; N, 3.34. Found: C, 34.41; H, 4.81; N, 2.91. **LIFDI**: m/z (%) = 842.0 (100).

2.3 Synthesis of para-substituted benzoyl bromides

2.3.1 p-$CF_3(C_6H_4)C(O)Br$

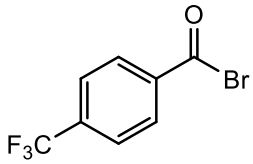

4-triflouromethylbenzaldehide (156.86 µl, 1.148 mmol, 1.0 eq) is treated with dibromoisocyanuric acid (DBI)(197.10 mg, 0.68 mmol, 0.6 eq) in dry DCM (4 mL) and stirred at room temperature for 24 h. Evaporating the solvent and after a vacuum distillation at 60 °C/ 0.1 mbar provided 4-triflouromethylbenzoylbromide (121.8 µl, 0.80 mmol) 70% in yield.

^{1}H NMR (400 MHz, CD_2Cl_3): δ (ppm) = 8.21 (d, $^3J_{HH}$ = 8 Hz, 2H, ortho-ArC*H*), 7.8 (d, $^3J_{HH}$ = 8 Hz, 2H, meta-ArC*H*). **^{13}C{^{1}H}** NMR (125.7 MHz, CD_2Cl_3): δ (ppm) = 164.79 (s, Ar*C*O), 138.04 (s, quat-*C*-CO, Ar*C*H), 136.46 (q, $^2J_{CF}$ = 41.48 Hz, quat-*C*-CF_3, Ar*C*H), 132.06 (s, ortho-Ar*C*H), 126.04 (q, $^3J_{CF}$ = 5 Hz, meta-Ar*C*H), 121.79 (q, $^1J_{CF}$ = 378 Hz, *C*F_3). **^{19}F{^{1}H} NMR** (CD_2Cl_3): δ (ppm) = -63.43 (s). **Mass (M+)**: m/z = 173.02. ATR-IR ($\upsilon_{C\text{-}O}$) = 1769 cm^{-1}.

2.3.2 p-$CH_3(C_6H_4)C(O)Br$

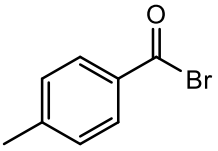

Oxalyl bromide $(COBr)_2$ (700 µl, 4.74 mmol, 1.5 eq) is dissolved in 3 mL of dried benzene. Then p-$CH_3(C_6H_4)COONa$ (500 mg, 3.16 mmol, 1.0 eq) is added slowly to the solution with vigorous stirring. The emission of CO_2 can be observed. Once the addition is finished, the reaction mixture is refluxed at 90 °C for 2h. The reaction mixture is cooled down to room temperature. Subsequently, the solid NaBr is filtered out. Evaporating the solvent and upon a vacuum distillation at 90 °C/ 26 mbar provided 4-methylbenzoyl bromide (340 µl, 2.52 mmol) 80% in yield.

^{1}H NMR (400 MHz, C_6D_6): δ (ppm) = 7.73 (d, $^3J_{HH}$ = 8 Hz, 2H, ortho-ArC*H*), 6.60 (d, $^3J_{HH}$ = 8 Hz, 2H, meta-ArC*H*), 1.78 (s, 3H, CH_3). **^{13}C{^{1}H}** NMR (125.7 MHz, C_6D_6): δ (ppm) = 164.86 (s, Ar*C*O), 146.38 (s, quat-*C*-CH_3, Ar*C*H), 132.21 (s, quat-*C*-CO, ArCH), 131.95 (s, ortho-Ar*C*H), 129.29 (s, meta-Ar*C*H), 20.91 (s, *C*H_3).

2.3.3 p-$OCH_3(C_6H_4)C(O)Br$

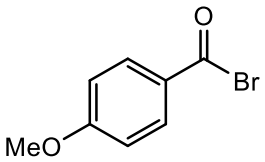

Oxalyl bromide $(COBr)_2$ (632.7 µl, 4.3 mmol, 1.5 eq) is dissolved in 3 mL of dried benzene. Then p-$OCH_3(C_6H_4)COONa$ (500 mg, 2.87 mmol, 1.0 eq) is added slowly to the solution with vigorous stirring. The emission of CO_2 can be observed. Once the addition is finished, the reaction mixture is refluxed at 90 °C for 2h. The reaction mixture is cooled down to room temperature. Subsequently, the solid NaBr is filtered out. Evaporating the solvent and upon a vacuum distillation at 70 °C/ 0.001 mbar provided 4-methoxylbenzoyl bromide (376.4 µl, 2.64 mmol) 92% in yield.

^{1}H NMR (400 MHz, C_6D_6): δ (ppm) = 7.80 (d, $^3J_{HH}$ = 8 Hz, 2H, ortho-ArC*H*), 6.33(d, $^3J_{HH}$ = 8 Hz, 2H, meta-ArC*H*). **^{13}C{^{1}H}** NMR (125.7 MHz, C_6D_6): δ (ppm) = 165.26 (s, quat-*C*-OCH_3, Ar*C*H), 163.72 (s, Ar*C*O), 134.46 (s, ortho-Ar*C*H), 120.04 (s, quat-*C*-CO, Ar*C*H), 113.88 (s, meta-Ar*C*H), 54.69 (s, O*C*H_3).

2.3.4 p-$Br(C_6H_4)C(O)Br$

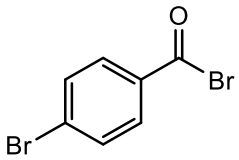

Oxalyl bromide $(COBr)_2$ (493.7 µl, 3.36 mmol, 1.5 eq) is dissolved in 3 mL of dried benzene. Then p-$Br(C_6H_4)COONa$ (500 mg, 2.24 mmol, 1.0 eq) is added slowly to the solution with vigorous stirring. The emission of CO_2 can be observed. Once the addition is finished, the reaction mixture is refluxed at 90 °C for 2h. The reaction mixture is cooled down to room temperature. Subsequently, the solid NaBr is filtered out. Evaporating the solvent and upon a vacuum distillation at 100 °C/ 0.021 mbar provided 4-bromobenzoyl bromide (276.4 µl, 2 mmol) 90% in yield.

^{1}H NMR (400 MHz, C_6D_6): δ (ppm) = 7.30 (d, $^3J_{HH}$ = 8 Hz, 2H, ortho-ArC*H*), 6.68 (d, $^3J_{HH}$ = 8 Hz, 2H, meta-ArC*H*). **^{13}C{^{1}H}** NMR (125.7 MHz, C_6D_6): δ (ppm) = 164.53 (s, Ar*C*O), 133.81 (s, quat-*C*-CO, Ar*C*H), 133.06 (s, ortho-Ar*C*H), 132.12 (s, meta-Ar*C*H), 131.12(s, quat-*C*-CH_3, Ar*C*H).

V. References

[1] B. S. Patil, V. Hessel, L. C. Seefeldt, D. R. Dean, B. M. Hoffman, B. J. Cook, L. J. Murray, Nitrogen *Fixation, In Ullmann's Encyclopedia of Industrial Chemistry*; Wiley: **2017**.
[2] Q. Cheng, *J. Integr. Plant Biol.* **2008**, *50*, 786–798.
[3] T. Spatzal, M. Aksoyoglu, L. Zhang, S. L. A. Andrade, E. Schleicher, S. Weber, D. C. Rees, O. Einsl, *Science* **2011**, *334*,940–940.
[4] K. M. Lancaster, M. Roemelt, P. Ettenhuber, Y. Hu, M. W. Ribbe, F. Neese, U. Bergmann, S. DeBeer, *Science* **2011**, *334*, 974–977.
[5] R. R. Eady, *Chem. Rev.* **1996**, *96*, 3013–3030.
[6] B. M. Hoffman, D. Lukoyanov, Z.-Y. Yang, D. R. Dean, L. C. Seefeldt, *Chem. Rev.* **2014**, *114*, 4041–4062.
[7] Haber, F, *Die Naturwissenschaften* **1922**, *10*, 1041–1049.
[8] Ertl, G, *Angew. Chem. Int. Ed.* **2008**, *47*, 3524–3535.
[9] a) R. R. Schrock, *Angew. Chem. Int. Ed.* **2008**, *47*, 5512;
b) A. Eizawa, Y. Nishibayashi, *Top. Organomet. Chem.* **2017**, *60*, 153;
c) S. Kuriyama, Y. Nishibayashi, *Top. Organomet. Chem.* **2017**, *60*, 215.
[10] D. V. Yandulov, R. R. Schrock, *Science* **2003**, *301*, 76.
[11] a) K. Arashiba, Y. Miyake, Y. Nishibayashi, *Nat. Chem.* **2011**, *3*, 120;
b) K. Arashiba, E. Kinoshita, S. Kuriyama, A. Eizawa, K. Nakajima, H. Tanaka, K. Yoshizawa, Y. Nishibayashi, *J. Am. Chem. Soc.* **2015**, *137*, 5666.
[12] a) J. S. Anderson, J. Rittle, J. C. Peters, *Nature* **2013**, *501*, 84;
b) G. Ung, J. C. Peters, *Angew. Chem. Int. Ed.* **2015**, *54*, 532. *Z. Anorg. Allg. Chem.* **2018**, 916–919.
[13] A. Eizawa, K. Arashiba, H. Tanaka, S. Kuriyama, Y. Matsuo, K. Nakajima, K. Yoshizawa, Y. Nishibayashi, *Nat. Commun.* **2017**, *8*, 14874.
[13] Nitrogen Statistics and Information, https://www.usgs.gov/centers/nmic/nitrogen statistics-and-information (visited on May 6, 2019).
[14] I. J. McPherson, T. Sudmeier, J. Fellowes, S. C. E. Tsang, *Dalton Trans.* **2019**, 48, 1562–1568.
[15] A. J. Martín, T. Shinagawa, J. Pérez-Ramírez, *Chem* **2019**, *5*, 263–283.
[16] J. M. Smith in Progress in Inorganic Chemistry Volume 58, (Ed.: K. D. Karlin), John Wiley & Sons, Inc., **2014**, pp. 417–470.
[17] I. Klopsch, E. Y. Yuzik-Klimova, S. Schneider in, Topics in Organometallic Chemistry, Springer Berlin Heidelberg, **2017**, pp. 1–42.
[18] A. D. Allen, C. V. Senoff, *Chem. Commun.*(London) **1965**, *0*, 621–622.
[19] M. D. Fryzuk, S. A. Johnson, *Coord. Chem. Rev* **2000**, 200-202, 379–409.
[20] B. A. MacKay, M. D. Fryzuk, *Chem. Rev.* **2004**, *104*, 385–402.
[21] R. M. Badger, *J. Chem. Phys.* **1934**, *2*, 128–131.
[22] A. Poveda, I. C. Perilla, C. R. Pérez, *J. Coord. Chem.* **2001**, *54*, 427–440.
[23] (a) J. S. Figueroa, N. A. Piro, C. R. Clough, C. C. Cummins, *J. Am. Chem. Soc.* **2006**, *128*, 940. (b) J. J. Curley, E. L. Sceats, C. C. Cummins, *J. Am. Chem. Soc.* **2006**, *128*, 14036.
[24] (a) I.Klopsch, M. Kinauer, M. Finger, C. Würtele, S. Schneider, *Angew. Chem. Int. Ed.* **2016**, *55*, 4786. (b) I. Klopsch, F. Schendzielorz, C. Volkmann, C. Würtele, S.Schneider, *Z. Anorg. Allg. Chem.* **2018**, *644*, 916.
[25] M. M. Guru, T. Shima, Z. Hou, *Angew. Chem. Int. Ed.* **2016**, *128*, 12504.
[26] Y. Tanabe, Y. Nishibayashi, *Coord. Chem. Rev*. **2013**, *257*, 2551.
[27] A. J. Keane, W. S. Farrell, B. L. Yonke, P. Y. Zavalij, L. R. Sita, *Angew. Chem. Int. Ed*. **2015**, *54*, 10220.

[28] Q. Liao, A. Cavaillé, N. Saffon-Merceron, N. Mézailles, *Angew. Chem. Int. Ed.* **2016**, *128*, 11378.
[29] L. M. Duman, L. R. Sita*, J. Am. Chem. Soc*. **2017**, *139*, 17241.
[30] M. F. Espada, S. Bennaamane, Q. Liao, N. Saffon-Merceron, S. Massou, E. Clot, N. Nebra, M. Fustier-Boutignon, N. Mézailles, *Angew. Chem. Int. Ed.* **2018**, *130*, 13047.
[31] J. Fritzsche, H. Struve, *J. Für Prakt. Chem.* **1847**, *41*, 97–113.
[32] R. A. Eikey, M. M. Abu-Omar, *Coord. Chem. Rev.* **2003**, 243, 83–124.
[33] C. E. Laplaza, M. J. A. Johnson, J. C. Peters, A. L. Odom, E. Kim, C. C. Cummins, G. N.George, I. J. Pickering, *J. Am. Chem. Soc.* **1996**, *118*, 8623–8638.
[34] J. J. Curley, T. R. Cook, S. Y. Reece, P. Müller, C. C. Cummins, *J. Am. Chem. Soc.* **2008**, *130*, 9394–9405.
[35] C. E. Laplaza, C. C. Cummins, *Science* **1995,** *268*, 861–863.
[36] R. J. Burford, M. D. Fryzuk, *Nat. Rev. Chem.* **2017**, *1*, 0026.
[37] K. Arashiba, Y. Miyake, Y. Nishibayashi, *Nat. Chem.* **2011**, *3*, 120–125.
[38] T. Miyazaki, H. Tanaka, Y. Tanabe, M. Yuki, K. Nakajima, K. Yoshizawa, Y. Nishibayashi, *Angew. Chem. Int. Ed.* **2014**, *53*, 11488–11492.
[39] T. J. Hebden, R. R. Schrock, M. K. Takase, P. Müller, *Chem. Commun.* **2012**, *48*, 1851.
[40] I. Klopsch, M. Finger, C. Würtele, B. Milde, D. B. Wertz, S.Schneider, *J. Am. Chem. Soc.* **2014**, *136*, 6881.
[41] Q. Liao, A. Cavaille, N. Saffon-Merceron, N. Meźailles, *Angew.Chem. Int. Ed.* **2016**, *55*, 11212−11216.
[42] T. Godemeyer, K. Dehnicke, E. Fluck, *Z. Anorg. Allg. Chem*. **1988**,*565*, 41-46.
[43] T. Godemeyer, K. Dehnicke, *Z. Anorg. Allg. Chem*. **1988**,*566*, 77-82.
[44] M. M. B. Holl, M. Kersting, B. D. Pendley. P. T. Wolczanski, *Inorg. Chem.* **1990**, *29*, 1518-1526.
[45] R. A. Wheeler, R. Hoffmann. J. Strihle, *J. Am. Chem. Soc.***1986**, *108*, 5381-5387.
[46] L. Maya, *Inorg. Chem.* **1987**, *26*, 1459-1462.
[47] M. Homer. K.-P. Frank, J. Strlhle, *Z. Naturfbrsch. B* **1986**,*41*, 423-428.
[48] H. W. Roesky, Y. Bai, M. Noltemeyer, *Angew. Chem.* **1989**, *101*, 788-789.
[49] A Frankenau. K. Dehnicke, *Z. Naturjorsch. B* **1989**, *44*, 493-494.
[50] A . Gorge, K. Dehnicke, D. Fenske, *Z . Naturforsch. B* **1988**, *43*, 677-681.
[51] A. Gorge, U. Patt-Siebel, U. Miller, K. Dehnicke, *Z. Naturforsch. B.* **1988**, *43*, 1633-1638.
[52] J. R. Dilworth, P. L. Dahlstrom, J. R. Hyde, J. Zubieta*, Inorg. Chem. Acta* **1983**, *71*, 11-28.
[53] P. C. Bevan, J. Chatt, J. R. Dilworth, R. A. Henderson, G. J. Leigh, *J. Chem. Soc. Dalton Trans.* **1982**, 821-824.
[54] D. L. Hughes. M. Y. Mohammed. C. J. Pickett, *J. Chem. Soc Dalton Trons.* **1990**, 2013.
[55] E. Schweda, J. Strihle. *Z. Nuturforsch. B* **1981**. *36*, 662-665.
[56] J. Beck. E. Schweda, J. Striihle, *Z . Naturforsch. B* **1985**, *40*, 1073-1076.
[57] L. G. Hubert-Pfalzgraf, G. Aharonian, *Inorg. Chem. Acta* **1985**, *100*, L21 - L22.
[58] C. J. Barner, T. J. Collins, B. E. Mapes, B. D. Santarsiero, *Inorg. Chem*. **1986**, *25*, 4322.
[59] M E. Noble, K. Folting, J. C. Huffman, R. A. D. Wentworth, *Inorg. Chem*. **1982**. *21*, 3772.
[60] S. 1. Arshankow, A. L. Poznjak, *Z. Anorg. Allg. Chem*. **1981**, *481*,201- 106.
[61] J. W. Buchler, C. Dreher. *Z. Nuturforsch.B* 1984, 39, 222-230.
[62] C. M. Che. J. X. Ma, W. T. Wong, T. F. Lai, C. K. Poon, *Inorg. Chem*. **1988**. *27*, 2547-2548.

[63] K. Dehnicke. U. Miiller, *Comments Inorg. Chem.* **1985**, *4,* 213-228.
[64] U. Kynast. U. Miiller, K. Dehnicke, *Z. Anorg. Allg. Chem.* **1984**, *508*, 26-32.
[65] U. Kynast, K. Dehnicke, *Z. Anorg. Allg. Chem.* **1983**, *502*, 29-34.
[66] U. Muller. W. Kafitz. K. Dehnicke, *Z. Anorg. Allg. Chem.* **1983**. *501, 69--78.*
[67] H. G. Hauck. P. Klingelhofer, U. Muller, K. Dehnicke, *Z. Anorg. Anorg. Chrm.* **1984***. 510,* 180-188.
[68] J. Chatt, C. D. Falk. G. J. Leigh, R. J. Paske, *J. Chem. Soc. A* **1969**, 2288- 2293.
[69] R J. Doedens, J. A. Ibers, *Inorg. Chem.* **1967**, *6,* 204-210.
[70] E. Forselhni, U. Casellato, R. Graziani, L. Magon. *Acta Crystullogr. Sect. B* **1982***, 38,* 3081-3083.
[71] K. Hosler, K. Dehnicke. *Z. Anorg. Allg. Chem.* **1987**, *554,* 108-112.
[72] K Volp. K. Dehnicke. D. Fenske. *Z. Anorg. Allg. Chem.* **1989**, *572*, 26- 32.
[73] W. A. Nugent, J. M. Mayer, Metal-Ligand Multiple Bonds: The Chemistry of Transition Metal Complexes Containing Oxo, Nitrido, Imido, Alkylidene, or Alkylidyne Ligands, Wiley-Interscience, **1988**.
[74] E. D. Hedegård, J. Bendix, S. P. A. Sauer, *J. Mol. Str*: THEOCHEM, **2009**, *913*, 1–7.
[75] T. J. Crevier, J. M. Mayer, *J. Am. Chem. Soc.* **1998**, *120*, 5595–5596.
[76] T. J. Crevier, B. K. Bennett, J. D. Soper, J. A. Bowman, A. Dehestani, D. A. Hrovat, S. Lovell, W. Kaminsky, J. M. Mayer, *J. Am. Chem. Soc.* **2001**, *123*, 1059–1071.
[77] T. J. Crevier, J. M. Mayer, *Angew. Chem. Int. Ed.* **1998**, *37*, 1891–1893.
[78] H. Henderickx, G. Kwakkenbos, A. Peters, J. van der Spoel, K. de Vries, Chem. Commun. **2003**, 2050–2051.
[79] Q. Liao, N. Saffon-Merceron, N. Mézailles, *ACS Catal.* **2015**, *5*, 6902–6906.
[80] M. F. Espada, S. Bennaamane, Q. Liao, N. Saffon-Merceron, S. Massou, E. Clot, N. Nebra, M. Fustier-Boutignon, N. Mézailles, *Angew. Chem.* **2018**, *130*, 13047–13050.
[81] J. J. Curley, E. L. Sceats, C. C. Cummins, *J. Am. Chem. Soc.* **2006**, *128*, 14036–14037.
[82] F. Schendzielorz, M. Finger, J. Abbenseth, C. Würtele, V. Krewald, S. Schneider, *Angew. Chem. Int. Ed.* **2019**, *58*, 830–834.
[83] S. Kang, M. T. La and H. K. Kim, *Tetrahedron Lett.* **2018**, *59*, 3541- 3546.
[84] R. Adams and L. H. Ulich. *J. Am. Chem. Soc.* **1920**, *42*, 3, 599–611.
[85] F. Wätjen, "Rhenium and Osmium PNP Pincer Complexes for Nitrogen Fixation and Nitride Transfer", Georg-August Universität Göttingen, **2019**.
[86] M. Fritz, "N_2 Fixation by Chromium and Rhenium PNP Pincer Complexes" Georg-August Universität Göttingen, **2021**.

VI. Appendix

1. List of complexes

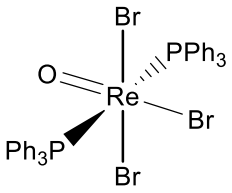

1

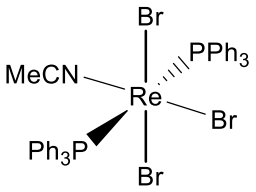

2

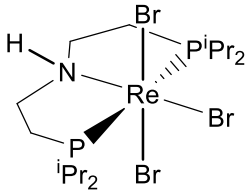

3

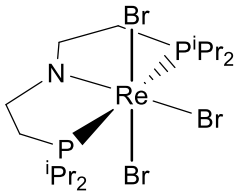

4

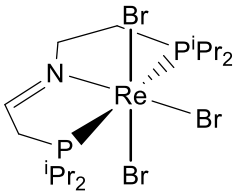

5

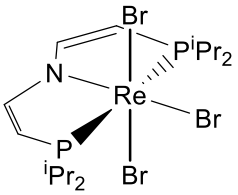

6

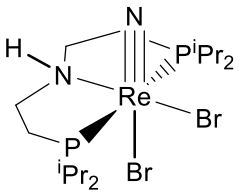

7

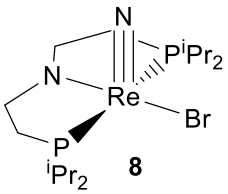

8

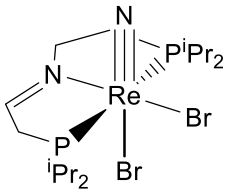

9

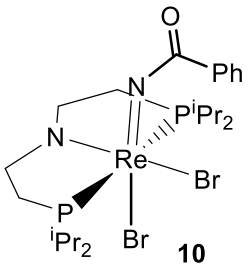

10

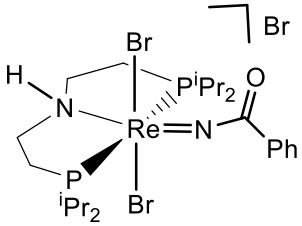

11

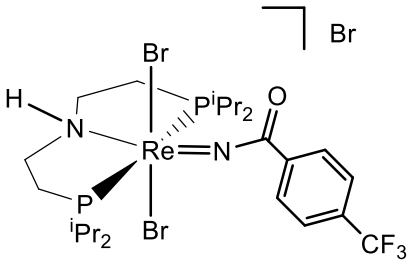
Br
Br
H
N
Re
N
P
iPr2
Br
PiPr2
O
CF3

12

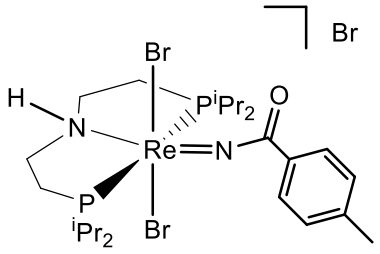
Br
Br
H
N
Re
N
P
iPr2
Br
PiPr2
O

13

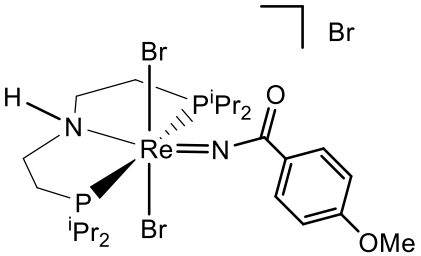
Br
Br
H
N
Re
N
P
iPr2
Br
PiPr2
O
OMe

14

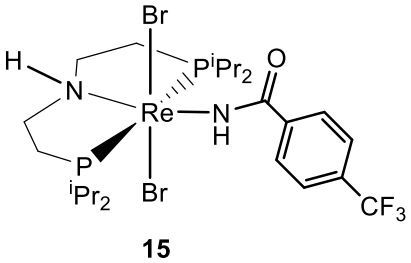
Br
H
N
Re
N
H
P
iPr2
Br
PiPr2
O
CF3

15

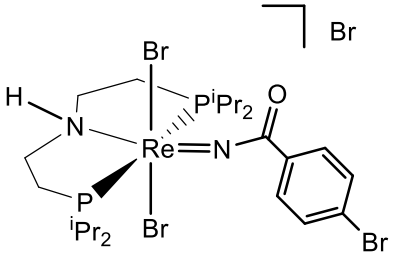
Br
Br
H
N
Re
N
P
iPr2
Br
PiPr2
O
Br

16

2. List of abbreviations

δ	chemical shift [ppm]
υ	wave number [cm-1]
µmol	micromolar
atm	standard atmosphere
ATR-IR	attenuated total reflection infrared
$BArF_{24}$	$[B\{C_6H_3(CF_3)_2\}_4]^-$
br	broad
^tBu	tert–butyl
calcd.	calculated
Cp	cyclopentadienyl
Cp*	(penta-methyl)cyclopentadienyl
CV	cyclic voltammetry
d	doublet
DCM	dichloromethane
DFT	density functional theory
Et	ethyl
eq.	equivalents
Fc	ferrocene
Fc+	ferrocenium cation
h	hour
HSQC	heteronuclear single quantum coherence
HOMO	highest occupied molecular orbital
^iPr	Iso-propyl
IR	Infrared
KHMDS	potassium bis(trimethylsilyl)amide
LUMO	lowest unoccupied molecular orbital
LIFDI	liquid injection field desorption ionization

m	multiplet
Me	methyl
MO	molecular orbital
NMR	nuclear magnetic resonance
OTf	trifluoromethanesulfonate
Ph	phenyl
PhO·	2,4,6-tri-tert-butylphenoxyl radical
$HPNP^{iPr}$	bis(di-iso-propylphosphinoethylene)amine
PCET	roton coupled electron transfer
ppm	parts per million
q	quartet
RT	room temperature
s	singlet
t	triplet
THF	tetrahydrofuran
TMS	trimethylsilyl
vs	versus
V	Volt

3. Crystallographic details

General details:

Suitable single crystals for X-ray structure determination were selected from the mother liquor under an inert gas atmosphere and transferred in protective perfluoro polyether oil on a microscope slide. The selected and mounted crystals were transferred to the cold gas stream on the diffractometer. The diffraction data were obtained at 100 K on a Bruker D8 three-circle diffractometer, equipped with a PHOTON 100 CMOS detector and an INCOATEC microfocus source with Quazar mirror optics (Mo-Kα radiation, λ= 0.71073 Å).

The data obtained were integrated with SAINT and a semi-empirical absorption correction from equivalents with SADABS was applied. The structure was solved and refined using the Bruker SHELX 2014 software package. All non-hydrogen atoms were refined with anisotropic displacement parameters. All C-H hydrogen atoms were refined isotropically on calculated positions by using a riding model with their Uiso values constrained to 1.5 Ueq of their pivot atoms for terminal sp^3 carbon atoms and 1.2 times for all other atoms.

3.1 [PNP^{iPr}ReBr$_3$]

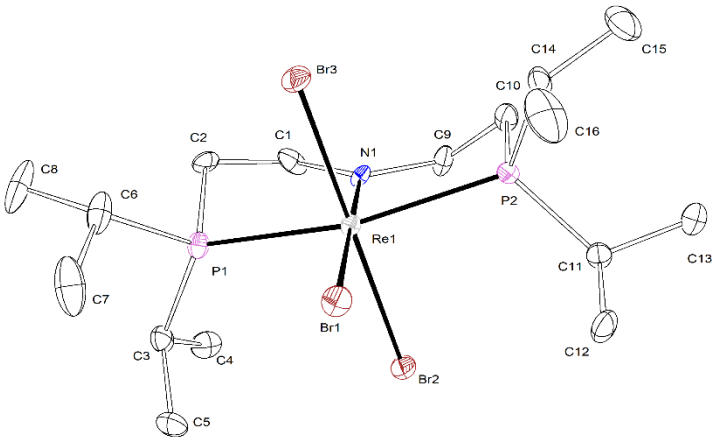

Fig. 70. *Thermal ellipsoid plot of **4** with the anisotropic displacement parameters drawn at the 50% probability level. The asymmetric unit contains one complex molecule*.

Crystal data and structure refinement for **4**.

Identification code	**4**
Empirical formula	$C_{16}H_{36}Br_3NP_2Re$
Formula weight	730.33
Temperature	101(2) K
Wavelength	0.71073 Å

Crystal system	Orthorhombic	
Space group	$P2_12_12_1$	
Unit cell dimensions	a = 7.3749(6) Å	α= 90°
	b = 12.9207(11) Å	β= 90°
	c = 24.549(2) Å	γ = 90°
Volume	2339.3(3) $Å^3$	
Z	4	
Density (calculated)	2.074 Mg/m^3	
Absorption coefficient	10.456 mm^{-1}	
F(000)	1396	
Crystal size	0.085 x 0.085 x 0.044 mm^3	
Crystal shape and color	Block,	dark violet
Theta range for data collection	2.289 to 26.446°	
Index ranges	-9<=h<=9, -16<=k<=16, -30<=l<=30	
Reflections collected	52024	
Independent reflections	4814 [R(int) = 0.0552]	
Completeness to theta = 25.242°	99.9 %	
Refinement method	Full-matrix least-squares on F^2	
Data / restraints / parameters	4814 / 0 / 216	
Goodness-of-fit on F^2	1.116	
Final R indices [I>2sigma(I)]	R1 = 0.0243,	wR2 = 0.0449
R indices (all data)	R1 = 0.0278,	wR2 = 0.0457
Absolute structure parameter	0.012(5)	
Largest diff. peak and hole	1.014 and -1.708 $eÅ^{-3}$	

3.2 [(P=N-P)ReBr$_3$]

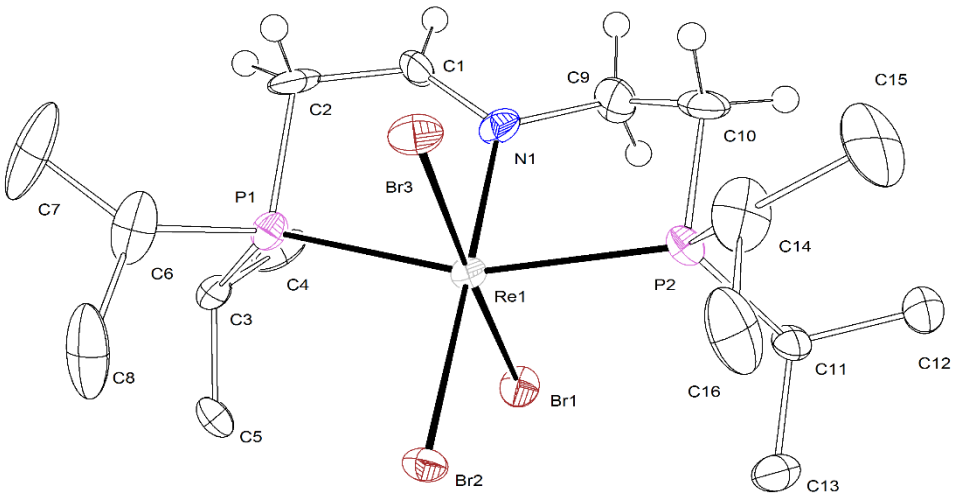

Fig. 71. *Thermal ellipsoid plot of* ***5*** *with the anisotropic displacement parameters drawn at the 50% probability level. The asymmetric unit contains one complex molecule.*

Crystal data and structure refinement for **5**.

Identification code	**5**	
Empirical formula	$C_{16}H_{35}Br_3NP_2Re$	
Formula weight	729.32	
Temperature	100(2) K	
Wavelength	0.71073 Å	
Crystal system	Orthorhombic	
Space group	$P2_12_12_1$	
Unit cell dimensions	a = 7.3522(5) Å	α= 90°
	b = 13.0043(8) Å	β= 90°
	c = 24.2618(16) Å	γ = 90°
Volume	2319.7(3) $Å^3$	
Z	4	
Density (calculated)	2.088 Mg/m^3	
Absorption coefficient	10.544 mm^{-1}	
F(000)	1392	
Crystal size	0.242 x 0.133 x 0.056 mm^3	
Crystal shape and color	Plate,	clear intense brown
Theta range for data collection	2.296 to 26.402°	
Index ranges	-9<=h<=9, -16<=k<=16, -28<=l<=30	
Reflections collected	52736	
Independent reflections	4762 [R(int) = 0.1700]	
Completeness to theta = 25.242°	99.9 %	
Refinement method	Full-matrix least-squares on F^2	
Data / restraints / parameters	4762 / 0 / 216	
Goodness-of-fit on F^2	1.049	
Final R indices [I>2sigma(I)]	R1 = 0.0384,	wR2 = 0.0687
R indices (all data)	R1 = 0.0616,	wR2 = 0.0762
Absolute structure parameter	-0.007(11)	
Largest diff. peak and hole	1.417 and -1.067 $eÅ^{-3}$	

3.3 [(HPNP)Re(N)Br_2]

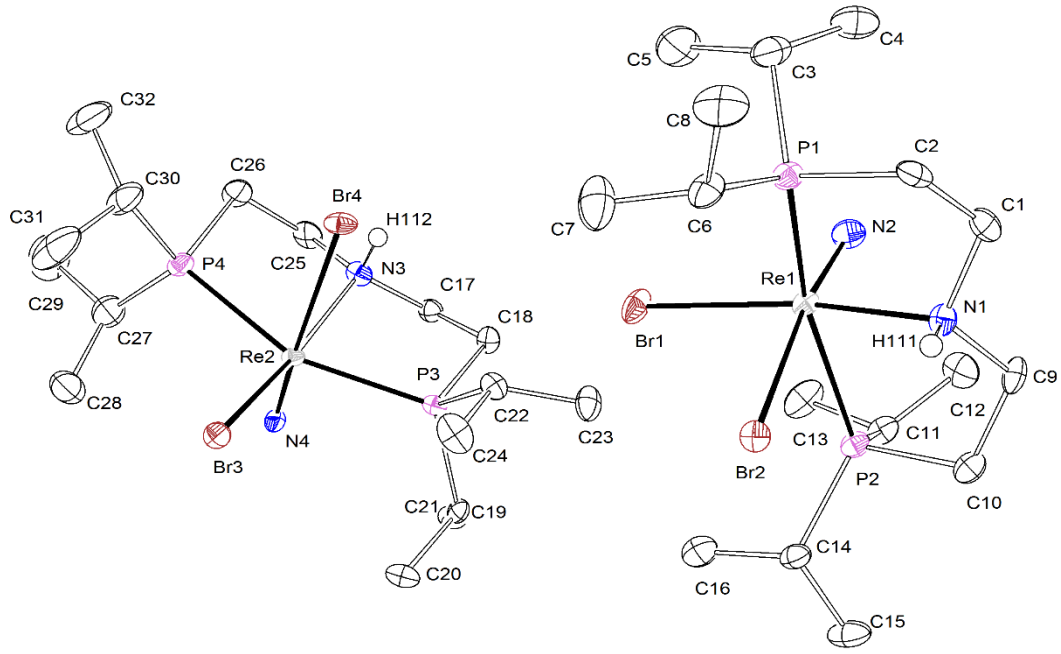

Fig. 72. *Thermal ellipsoid plot of **5** with the anisotropic displacement parameters drawn at the 50% probability level. The asymmetric unit contains two complex molecules. The N-H hydrogen atoms were found from the residual density map and isotropically refined using SADI restraints.*

Crystal data and structure refinement for **7**.

Identification code	**7**	
Empirical formula	$C_{16}H_{37}Br_2N_2P_2Re$	
Formula weight	665.43	
Temperature	100(2) K	
Wavelength	0.71073 Å	
Crystal system	Monoclinic	
Space group	$P2_1/c$	
Unit cell dimensions	a = 16.1189(11) Å	α= 90°
	b = 17.1834(12) Å	β= 100.543(3)°
	c = 16.7454(11) Å	γ = 90°
Volume	4559.8(5) $Å^3$	
Z	8	
Density (calculated)	1.939 Mg/m^3	
Absorption coefficient	8.977 mm^{-1}	
F(000)	2576	
Crystal size	0.157 x 0.114 x 0.099 mm^3	
Crystal shape and color	Plate,	clear intense yellow
Theta range for data collection	2.273 to 26.481°	
Index ranges	-20<=h<=20, -21<=k<=21, -20<=l<=20	

Reflections collected	162245	
Independent reflections	9389 [R(int) = 0.0927]	
Completeness to theta = 25.242°	100.0 %	
Refinement method	Full-matrix least-squares on F^2	
Data / restraints / parameters	9389 / 1 / 439	
Goodness-of-fit on F^2	1.100	
Final R indices [I>2sigma(I)]	R1 = 0.0291,	wR2 = 0.0588
R indices (all data)	R1 = 0.0458,	wR2 = 0.0664
Largest diff. peak and hole	2.454 and -1.599 eÅ^{-3}	

3.4 [Re(PhC$_4$H$_4$C(O)N)Br$_2$(PNP^{iPr})]

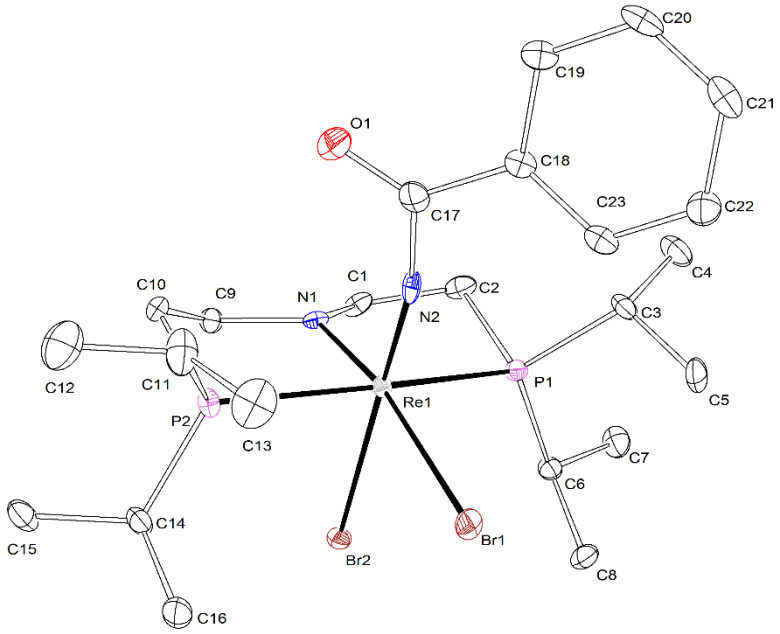

Fig. 73. *Thermal ellipsoid plot of **10** with the anisotropic displacement parameters drawn at the 50% probability level. The asymmetric unit contains one complex molecule.*

Crystal data and structure refinement for **10**.

Identification code	**10**	
Empirical formula	$C_{23}H_{41}Br_2N_2OP_2Re$	
Formula weight	769.54	
Temperature	100(2) K	
Wavelength	0.71073 Å	
Crystal system	Monoclinic	
Space group	$P2_1/c$	
Unit cell dimensions	a = 10.8135(4) Å	α= 90°
	b = 15.3626(5) Å	β= 95.493(2)°
	c = 16.6587(6) Å	γ = 90°
Volume	2754.69(17) Å^3	

Z	4
Density (calculated)	1.856 Mg/m^3
Absorption coefficient	7.446 mm^{-1}
F(000)	1504
Crystal size	0.068 x 0.049 x 0.026 mm^3
Theta range for data collection	2.310 to 28.356°
Crystal shape and color	Plate, clear intense brown
Index ranges	-14<=h<=14, -20<=k<=20, -22<=l<=22
Reflections collected	64474
Independent reflections	6884 [R(int) = 0.0825]
Completeness to theta = 25.242°	100.0 %
Refinement method	Full-matrix least-squares on F^2
Data / restraints / parameters	6884 / 0 / 288
Goodness-of-fit on F^2	1.035
Final R indices [I>2sigma(I)]	R1 = 0.0282, wR2 = 0.0420
R indices (all data)	R1 = 0.0432, wR2 = 0.0449
Largest diff. peak and hole	0.611 and -1.179 $eÅ^{-3}$

Curriculum Vitae

Personal Data

Name:	Sesha Kisan
Nationality:	Indian
Date of birth:	04/03 /1994
Place of birth:	Bhubaneswar, India
Email:	sesha.kisan@uni-goettingen.de

Education

Since Oct 2018	Ph.D. student in the GAUSS program Chemistry at the Georg-August-Universität Göttingen (Germany) Research group of Prof. Dr. Sven Schneider PhD Thesis: "Rhenium Mediated Formation of *N*-Containing Organic Compounds by Nitride Transfer"
06/2013–06/2018	Integrated Master of Science (B.Sc. & M.Sc.) in Chemistry at the National Institute of Science Education and Research (NISER), Bhubaneswar, India Research group of Prof. Dr. Chidambaram Gunanathan Int. M.Sc. Thesis: "*Ruthenium-Catalysed Sustainable Organic Transformations*"

Publications

1 *"Ruthenium Catalyzed Anti-Markovnikov Selective Hydroboration of Olefins"*, **Kisan, S;** Krishnakumar, V; and Gunanathan, C. *ACS Catal.* **2017**, *7*, 5950−5954.

2 *"Ruthenium Catalyzed Deoxygenative Hydroboration Carboxylic Acids"*, **Kisan, S;** Krishnakumar, V; and Gunanathan, C. *ACS Catal.* **2018**, *8*, 4772−4776.

3 *"Photoelectrochemical Conversion of Dinitrogen to Benzonitrile: Selectivity Control by Electrophile- vs. Proton-Coupled Electron Transfer",* Fritz, F; Rupp, S; Kiene, C; **Kisan, S**; Telser, J; Würtele, C; Krewald, V; and Schneider, S. *Angew. Chem. Int. Ed.* **2022.** (accepted manuscript, https://doi.org/10.1002/anie.202205922)